

Novel approaches for the investigation of sound localization in mammals

Dissertation
zur Erlangung des Grades eines Doktors
der Naturwissenschaften

der Fakultät für Biologie
der Ludwig-Maximilians-Universität München

vorgelegt von
Ida Siveke
München, September 2007



Erstgutachter: Prof. Dr. Benedikt Grothe
Zweitgutachter: apl. Prof. Dr. Mark Hübener
Tag der mündlichen Prüfung: 7. Dezember 2007

Table of contents

List of abbreviations	5
Zusammenfassung	6
Summary	9
1 Introduction	11
1.1 The first stages of the binaural auditory pathway in mammals	12
1.2 Processing of binaural differences	14
1.3 Processing of interaural time differences in the MSO	17
1.4 Issues with the investigation of processing interaural time differences	19
1.4.1 Processing of interaural time differences in higher stages of the binaural pathway	19
1.4.2 Localization of multiple sound sources.....	20
1.4.3 The phenomenon of binaural sluggishness	21
1.5 The animal model	22
1.6 Aims	23
2 Binaural response properties of low-frequency neurons in the gerbil dorsal nucleus of the lateral lemniscus	25
2.1 Abstract	25
2.2 Introduction	26
2.3 Methods	27
2.3.1 Experimental animals.....	27
2.3.2 Surgical procedures.....	28
2.3.3 Neuronal recordings.....	29
2.3.4 Stimulus presentation and recording protocols	29
2.3.5 Data analysis.....	32
2.3.6 Immunohistochemistry.....	34
2.4 Results	35
2.4.1 General response features of DNLL cells	35
2.4.2 Features of ITD-sensitive neurons.....	38
2.4.3 Distribution of ITDs across frequency.....	44
2.4.4 DNLL neurons are sensitive to ITDs evoked with brief chirps.....	45
2.4.5 IID-sensitive neurons in the DNLL	46
2.4.6 Anatomy	48

2.5	Discussion.....	50
2.5.1	Peak- and trough-type DNLL neurons inherit their ITD features from the SOC.....	51
2.5.2	ITD tuning of peak-type neurons in the DNLL.....	54
2.5.3	Intermediate-type ITD sensitivity.....	56
3	Spectral composition of concurrent noise affects neuronal sensitivity to interaural time differences of tones in the dorsal nucleus of the lateral lemniscus.....	58
3.1	Abstract.....	58
3.2	Introduction.....	59
3.3	Methods.....	60
3.3.1	Animal preparation, recording procedures.....	60
3.3.2	Stimuli.....	61
3.3.3	Data analysis.....	64
3.3.4	Binaural correlation and model.....	66
3.4	Results.....	68
3.4.1	Effects of binaural noise on tone delay functions.....	68
3.4.2	Monaural contributions to the noise-induced effects on tone delay functions.....	72
3.4.3	Effects of notched noise and tuned noise on TDFs.....	73
3.4.4	Simulated effect of the noise level on binaural correlations.....	76
3.5	Discussion.....	78
3.5.1	Comparison with previous monaural studies.....	80
3.5.2	Comparison with binaural studies on the detection of tones in noise.....	80
3.5.3	Comparison with binaural studies on the localization of tones in noise.....	81
3.5.4	Functional relevance.....	82
4	Perceptual and physiological characteristics of binaural sluggishness.....	83
4.1	Abstract.....	83
4.2	Introduction.....	84
4.3	Methods.....	85
4.3.1	Stimuli.....	85
4.3.2	Psychophysics.....	88
4.3.3	Neurophysiology.....	89
4.4	Results.....	90
4.4.1	Psychophysics.....	90
4.4.2	Electrophysiology.....	93
4.4.3	Comparison of psychophysical and electrophysiological performance.....	97
4.5	Discussion.....	100

5	General discussion and outlook	105
5.1	Sensitivity to interaural time differences in the dorsal nucleus of the lateral lemniscus	106
5.2	Processing of concurrent sounds by neurons sensitive to interaural time differences	108
5.2.1	Localization of concurrent sounds	108
5.2.2	Detection and grouping of concurrent sounds	111
5.2.3	Pitch detection of concurrent sounds	112
5.2.4	Adaptation to noisy background	113
5.3	Processing of binaurally modulated auditory signal	114
	References	116
	Contributions to the manuscripts.....	136
	Curriculum Vitae.....	137
	Acknowledgments	140
	Ehrenwörtliche Versicherung und Erklärung.....	141

List of abbreviations

CN	cochlear nucleus	Monaural nucleus in the brainstem
CP	characteristic phase	Characteristic of ITD-sensitive neurons
DNLL	dorsal nucleus of the lateral lemniscus	Binaural nucleus, receives strong inputs from binaural SOC neurons
IC	inferior colliculus	Nucleus in the midbrain, receives inputs from the DNLL and the SOC
IID	interaural intensity difference	Intensity difference between the ears
IPD	interaural phase difference	Arrival phase difference between the ears (the interaural time difference normalized to the phase of the stimulus frequency)
ITD	interaural time difference	Arrival time difference between the ears
LNTB	lateral nucleus of the trapezoid body	Monaural inhibitory nucleus of the SOC
LSO	lateral superior olive	Binaural nucleus of the SOC, receives excitation from the ipsilateral and inhibition from the contralateral side, IID and ITD processing
MNTB	medial nucleus of the trapezoid body	Monaural inhibitory nucleus of the SOC
MSO	medial superior olive	Binaural nucleus of the SOC, receives binaural excitation and inhibition, ITD processing
SOC	superior olivary complex	Nucleus in the brainstem, first major relay station of binaural processing
VCN	ventral cochlear nucleus	Ventral part of the CN, projects to the SOC

Zusammenfassung

Die Fähigkeit auditorische Signale im Raum lokalisieren zu können, ist für Säugetiere zum Verständnis ihrer Umwelt sowie zur intra- und interspezifischen Kommunikation eine wichtige Voraussetzung. Zur Lokalisation tieffrequenter auditorischer Signale nutzen Säugetiere vor allem interaurale Zeitunterschiede (interaural time differences, ITDs). Diese Zeitunterschiede entstehen dadurch, dass auditorische Signale, deren Schallquellen sich nicht direkt vor dem Hörer befinden, zeitversetzt die Ohren erreichen. Viele Säugetiere, insbesondere Menschen, können durch eine besondere Empfindlichkeit für sehr kleine ITDs sehr genau Töne lokalisieren. Diese Empfindlichkeit basiert auf einer sehr präzisen neuronalen Verarbeitung. Im auditorischen Hirnstamm, dem oberen Olivenkomplex (superior olivary complex, SOC), befinden sich binaurale Neurone, die auf Änderungen der ITD im Mikrosekundenbereich antworten. Trotz jahrelanger Forschung sind bis heute die Mechanismen, die der neuronalen Verarbeitung von ITDs zugrunde liegen, weiterhin Ausgangspunkt kontroverser Diskussionen. In der vorliegenden Arbeit wurden anhand von *in vivo* Einzelzell-Ableitungen drei neue Ansätze verwendet, um die neuronale Verarbeitung von ITDs zu untersuchen. Als Modellorganismus wurde die Wüstenrennmaus verwendet, ein bereits gut etabliertes Tiermodell zur Untersuchung der Schalllokalisierung.

Die erste Studie konzentriert sich auf die ITD-Verarbeitung von Reintönen im dorsalen Nukleus des lateralen Lemniskus (DNLL). Hier konnte gezeigt werden, dass tieffrequente Neurone im DNLL eine ähnliche Empfindlichkeit für ITDs besitzen, wie sie für Neurone im SOC beschrieben wurde. Außerdem bestätigten Tracer-Injektionsversuche direkte neuronale Verbindungen zwischen den untersuchten DNLL Neuronen und binauralen SOC Neuronen. Diese Ergebnisse zeigen, dass sich elektrophysiologische Ableitungen im DNLL gut dafür eignen, allgemeine Eigenschaften der Verarbeitung von ITDs zu untersuchen, unter anderem vor dem Hintergrund, dass elektrophysiologische Einzelzell-Ableitungen von Neuronen im SOC technisch sehr schwierig sind. Des Weiteren zeigte sich, dass DNLL Neurone im Allgemeinen ihre Antwort stark über den Bereich

physiologisch relevanter ITDs modulieren, wohingegen die maximale Antwort dieser Neurone in den meisten Fällen außerhalb dieses Bereiches liegt. Dieses Antwortverhalten widerspricht einer möglichen Kodierung physiologisch relevanter ITDs durch eine maximale Antwort einzelner Neurone. Stattdessen unterstützen diese Daten die kürzlich veröffentlichte Hypothese, dass eine bestimmte Antwortrate, die sich gemittelt über eine Population von ITD-empfindlichen Neuronen ergibt, die Position tieffrequenter Töne kodiert.

In der zweiten Studie wurde die zeitliche Verarbeitung von gleichzeitig präsentierten auditorischen Signalen mit unterschiedlichen ITDs untersucht. Dieser physiologischere Ansatz steht im Gegensatz zu klassischen Studien, in denen ausschließlich die Lokalisation einzelner Schallquellen untersucht wurde. Als gleichzeitige Signale wurden ein Reinton und ein Rauschen verwendet. Die Daten zeigen, dass die Antwort von DNLL Neuronen auf den Reinton stark durch gleichzeitig präsentiertes weißes Rauschen verändert wird und umgekehrt: Die Antwort auf das Rauschen wird verstärkt, wenn gleichzeitig ein Ton präsentiert wird, wohingegen in Abhängigkeit von der ITD des Tones die Antwort auf den Ton bei gleichzeitigem Rauschen entweder verstärkt oder gehemmt wird. Zusätzliche Untersuchungen der neuronalen Antworten auf monaurale Signale und auf Reintöne mit gleichzeitig präsentiertem spektral gefiltertem Rauschen ergaben, dass die ITD Empfindlichkeit der Neuronen stark vom spektralen Gehalt, der Position und der Lautstärke der gleichzeitig präsentierten Schallquellen abhängt. Aus diesen Ergebnissen kann geschlussfolgert werden, dass die Effekte, die konkurrierende Schallquellen aufeinander haben, grundsätzlich auf zwei unterschiedlichen Mechanismen basieren: Monaurale Integration über bestimmte Frequenzbereiche und zeitliche Interaktionen am Koinzidenz-Detektor im SOC. Simulationen mit einfachen Koinzidenz-Detektor-Modellen (in Kooperation mit Christian Leibold) bestätigten diese These.

In der dritten Studie der hier vorgestellten Arbeit, wurde die zeitliche Auflösung des binauralen Systems untersucht. Um zu ermitteln, wie schnell das neuronale System Änderungen der ITDs folgen kann, wurden mit identischer akustischer Stimulation psychophysikalische Experimente am Menschen und elektrophysiologische Aufnahmen im DNLL der Wüstenrennmaus durchgeführt. Obwohl das binaurale System in früheren Studien als träge beschrieben worden ist, konnte diese Studie zeigen, dass die binauralen Antworten der Neurone im DNLL schnellen Änderungen der ITDs durchaus folgen

können. Außerdem zeigten die psychophysikalischen Experimente, dass die menschliche Wahrnehmung binauralen Veränderungen folgen kann, wenn die präsentierten Signale akustisch plausibel sind. Daher weisen diese Daten darauf hin, dass das binaurale System den schnellen binauralen Veränderungen viel schneller als beschrieben und womöglich sogar so schnell wie das monaurale System monauralen Veränderungen folgen kann, wenn es physiologisch relevanten Reizen ausgesetzt ist.

Zusammenfassend zeigen die hier dargestellten Resultate, dass die Untersuchung von Neuronen im DNLL, die empfindlich auf ITDs reagieren, eine gute Methode für die Untersuchungen der prinzipiellen Verarbeitung von ITDs ist. Des Weiteren ist die Anwendung komplizierter und naturalistischer akustischer Stimulationen eine viel versprechende und notwendige Methode für zukünftige Studien, die zum Ziel haben, komplexe neuronale Prozesse der Schallverarbeitung zu analysieren.

Summary

The ability to localize sounds in space is important to mammals in terms of awareness of the environment and social contact with each other. In many mammals, and particularly in humans, localization of sound sources in the horizontal plane is achieved by an extraordinary sensitivity to interaural time differences (ITDs). Auditory signals from sound sources, which are not centrally located in front of the listener travel different distances to the ears and thereby generate ITDs. These ITDs are first processed by binaural sensitive neurons of the superior olivary complex (SOC) in the brainstem. Despite decades of research on this topic, the underlying mechanisms of ITD processing are still an issue of strong controversy and the processing of concurrent sounds for example is not well understood. Here I used *in vivo* extra-cellular single cell recordings in the dorsal nucleus of the lateral lemniscus (DNLL) to pursue three novel approaches for the investigation of ITD processing in gerbils, a well-established animal model for sound localization.

The first study focuses on the ITD processing of static pure tones in the DNLL. I found that the low frequency neurons of the DNLL express an ITD sensitivity that closely resembles the one seen in the SOC. Tracer injections into the DNLL confirmed the strong direct inputs of the SOC to the DNLL. These findings support the population of DNLL neurons as a suitable novel approach to study the general mechanism of ITD processing, especially given the technical difficulties in recording from neurons in the SOC. The discharge rate of the ITD-sensitive DNLL neurons was strongly modulated over the physiological relevant range of ITDs. However, for the majority of these neurons the maximal discharge rates were clearly outside this range. These findings contradict the possible encoding of physiological relevant ITDs by the maximal discharge of single neurons. In contrast, these data support the more recent hypothesis that the discharge rate averaged over a population of ITD-sensitive neurons encodes the location of low frequency sounds.

In the second study, I investigated the ITD processing of two concurrent sound sources, extending the classical approach of using only a single sound source. As concurrent sound sources a pure tone and background noise were chosen. The data show that concurrent white noise has a high impact on the response to tones and *vice versa*. The discharge rate to tones was mostly suppressed by the noise. The discharge rate to the noise was suppressed or enhanced by the tone depending on the ITD of the tone. Investigating the responses to monaural stimulation and to tone stimulation with concurrent spectrally filtered noise, I found that the ITD sensitivity of DNLL neurons strongly depends on the spectral compositions, the ITDs, and the levels of the concurrent sound sources. Two different mechanisms that mediate these findings were identified: monaural across-frequency interactions and temporal interactions at the level of the coincidence detector. Simulations of simple coincidence detector models (in cooperation with Christian Leibold) suggested this interpretation.

In the third study of my thesis, the temporal resolution of binaural motion was analyzed. Particularly, it was investigated how fast the neuronal system can follow changes of the ITD. Here, psychophysical experiments in humans and electrophysiological recordings in the gerbil DNLL were performed using identical acoustic stimulation. Although the binaural system has previously been described as sluggish, the binaural response of ITD-sensitive DNLL neurons was found to follow fast changes of ITDs. Furthermore, in psychophysical experiments in humans, the binaural performance was better than expected when using a novel plausible motion stimulus. These data suggest that the binaural system can follow changes of the binaural cues much faster than previously reported and almost as fast as the monaural system, given a physiological useful stimulus. In summary, the results presented here establish the ITD-sensitive DNLL neurons as a novel approach for the investigation of ITD processing. In addition, the usage of more complex and naturalistic stimuli is a promising and necessary approach for opening the field for further studies regarding a better understanding of the hearing process.

1 Introduction

The ability to localize sounds in space is vital to animals, both as predator and as prey, in terms of awareness of the environment and social contact with each other. For humans in a modern world, sound localization serves not only to alert us to a car approaching from behind but also allows us to enjoy the multi-layered and complex wealth of sounds when listening to Brahms "Deutsches Requiem" in the Opera House. Sounds are complex mixtures of auditory signals originating from multiple sources and localizations. Our auditory system is able to extract the relevant cues, the amplitude and the timing of the sound waves, representing the different sound sources. For humans and most other mammals, the ability to localize sounds is significantly based on the fact that they have two ears. The sound waveforms arriving at each ear differ in amplitude and time. Mammals use this interaural intensity and interaural time differences (IIDs and ITDs respectively) to localize sounds in the horizontal plane (Thompson 1882; Rayleigh 1907). IIDs are generated by an acoustic shadow of the head (figure 1.1A). If, for example, a sound originates from the right side, the sound is more intense on the right than on the left ear. IIDs are generated by an acoustic shadow of the head (figure 1.1A). If, for example, a sound originates from the right side, the sound is more intense on the right than on the left ear.

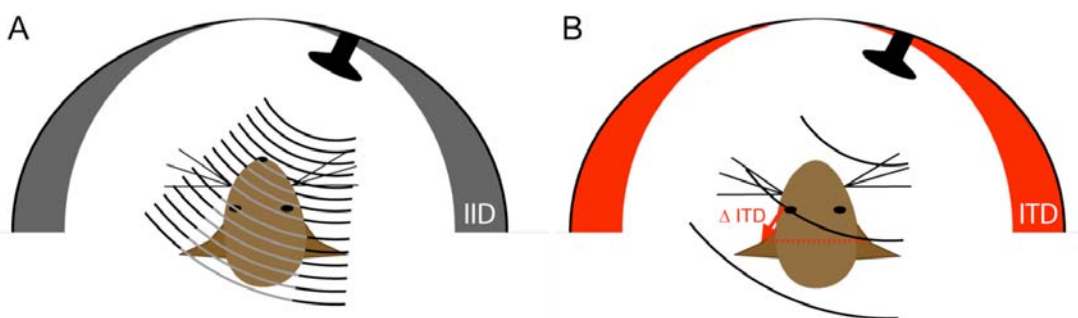


Figure 1.1 Schematic drawing of the generation of IIDs (A) and ITDs (B) by the head of the gerbil. IIDs and ITDs increase, if the sound source moves to the lateral side (indicated by the grey and red bar). High frequencies are attenuated by the head (A). The low frequency sound waves reach the close ear first and with a certain time delay (Δ ITD) the distant ear (B).

Low frequency sound waves, which have wavelengths longer than the distance between the ears, can orbit the head. Therefore, low frequency tones do not create significant IIDs except when arising from sound sources in close distances to the ears (Shinn-Cunningham et al. 2000). However, low frequency sounds generate ITDs (figure 1.1B). For example, a sound arriving from the right side reaches the right ear first and the left ear microseconds later. The resulting ITD depends on the distance between the ears and the position of the sound source. The head width of an adult gerbil creates ITDs ranging from 0 μ s for sound arriving from straight ahead to around 120 μ s for sounds from 90° laterally. Thus, in anechoic conditions, the maximal ITDs gerbils can experience range from -120 μ s to +120 μ s (= physiological relevant range; Heffner and Heffner 1988; Maki and Furukawa 2005). High frequency tones with wavelengths shorter than the width of the head generate ambiguous ITDs. Therefore, Rayleigh and Thompson postulated the duplex theory of sound localization: high frequency sounds are localized by IIDs and low frequency sounds by ITDs (Thompson 1882; Rayleigh 1907). But since the envelope of complex high-frequency sounds can create ITDs (Bernstein and Trahiotis 1985; Joris 2003) and low frequencies generate IIDs in the close field, this duplex theory is only valid for pure tones in the anechoic long field (for review: Yin 2002).

The smallest ITDs detectable by mammals are 10-20 microseconds and the smallest IIDs are 1-2 db (for review: Blauert 1997). The resolution of such small IIDs and ITDs implies a very precise and well-timed neuronal network to encode the binaural information.

1.1 The first stages of the binaural auditory pathway in mammals

Auditory signals are processed in the peripheral structures of the ear, the auditory brainstem and several auditory structures in the midbrain and the cortex. The auditory brainstem is the first central relay station of the binaural auditory system. It consists of the cochlear nucleus (CN), the superior olivary complex (SOC) and the lateral lemniscus. The SOC is the first major station of the auditory pathway, where inputs from both ears, the binaural information, are processed (for review: Irvine 1992; Schwartz 1992). The SOC receives inputs from both ventral cochlear nuclei (VCN). The terminals of many auditory nerve fibers projecting to the VCN contain large end-bulb synapses (Rouiller et

al. 1986; Ryugo and Sento 1991). This provides a secure synaptic connection to the bushy cells of the VCN and preserves or even strengthens the precise temporal discharge pattern of auditory nerve fibers (Joris et al. 1994; Smith et al. 1998). The VCN bilaterally excites the medial superior olive (MSO) and monolaterally the ipsilateral lateral superior olive (LSO) (Stotler 1953; Smith et al. 1993; Beckius et al. 1999; for review: Thompson and Schofield 2000). Both nuclei, the MSO and LSO, are additionally inhibited by inputs from the ipsilateral medial nucleus of the trapezoid body (MNTB) (Spangler et al. 1985; Kuwabara and Zook 1992; Sommer et al. 1993), which itself receives strong excitatory inputs from the contralateral VCN (Cant and Casseday 1986; Smith et al. 1991). The synapses of VCN globular bushy neurons onto MNTB neurons (named Calyx of Held) are extremely large and have a special structure to allow precise synaptic transmission (Held 1893; Ramon y Cajal 1907; for review: von Gersdorff and Borst 2002; see inset figure 1.2). In addition to the inhibition from the MNTB, MSO neurons receive inhibitory inputs from neurons of the ipsilateral lateral nucleus of the trapezoid body (LNTB) (Cant and Hyson 1992), which itself gets inputs from the ipsilateral globular bushy cells of the VCN (Cant and Casseday 1986; Smith et al. 1991).

Taken together, the MSO receives bilateral inhibitory and excitatory inputs and the LSO ipsilateral excitatory and contralateral inhibitory inputs.

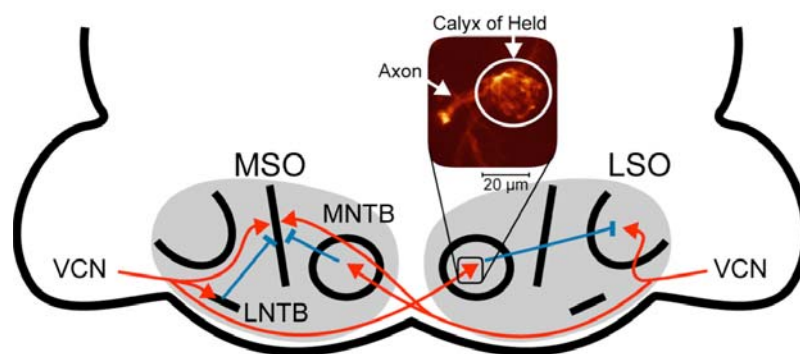


Figure 1.2 Schematic drawing of the neuronal circuitry within the superior olivary complex (SOC, grey area); Ventral cochlear nucleus (VCN), medial nucleus of the trapezoid body (MNTB), lateral nucleus of the trapezoid body (LNTB), medial superior olive (MSO), lateral superior olive (LSO). On the left side the inputs to the MSO are shown, on the right the inputs to the LSO. The inset shows the axon and the colored synapse from the VCN to the MNTB (Calyx of Held) after GFP-Virus injection into the VCN.

1.2 Processing of binaural differences

In mammals, the binaural information is initially processed in the SOC. IIDs are processed by neurons in the LSO via a subtraction mechanism based on excitatory and inhibitory inputs (Boudreau and Tsuchitani 1968; Irvine 2001). Figure 1.3A shows a schematic IID function of a LSO neuron. A positive IID indicates that the sound at the ipsilateral ear is more intense than at the contralateral ear. Since LSO neurons get excitatory inputs from the ipsilateral side and inhibitory inputs from the contralateral side (inset figure 1.3A), these neurons fire maximally at positive IIDs and minimally at negative IIDs.

ITDs are first processed by neurons of the MSO (Moushegian et al. 1964; Masterton and Diamond 1967; Moushegian et al. 1967; Clark and Dunlop 1968; Goldberg and Brown 1968; Watanabe et al. 1968; Guinan et al. 1972; Crow et al. 1978; Caird and Klinke 1983; Langford 1984; Yin and Chan 1990; Spitzer and Semple 1995; Batra et al. 1997a,b; Grothe and Park 1998; Brand et al. 2002), which receive binaural excitatory and inhibitory inputs. A schematic ITD function of an MSO neuron is shown in figure 1.3B. A positive ITD indicates that the sound arrives earlier at the contralateral ear than at the ipsilateral ear. The maximal discharge rate is achieved when the net binaural excitation arrives at the same time (for review: Yin 2002; Grothe 2003).

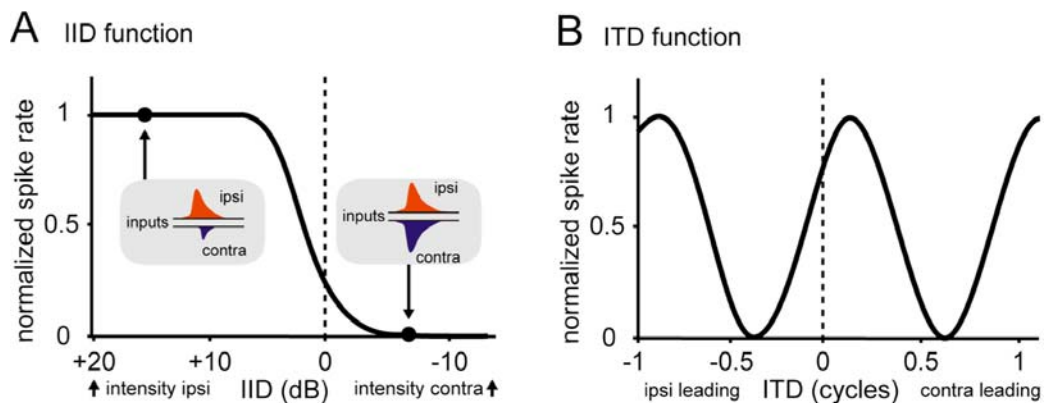


Figure 1.3 Schematic drawing of a normalized IID function (A) and ITD function (B). The neuronal response is plotted against the IID or ITD of the sound. IID sensitivity is processed in the LSO by an ipsilateral excitatory and contralateral inhibitory input (see insets in A).

In general, sounds leading at the contralateral ear generate maximal discharge in the mammalian MSO (Yin and Chan 1990; Spitzer and Semple 1995; Batra et al. 1997a; Brand et al. 2002; see also chapter 1.3).

Furthermore, it has long been suggested that low-frequency LSO neurons are sensitive to ITDs (Caird and Klinke 1983; Joris and Yin 1995; Batra et al. 1997a). This hypothesis has been strengthened by recent findings for a small number of neurons in the low-frequency limb of the cat LSO (Tollin and Yin 2005). In general, ITD sensitivity, which results from MSO-like coincidence mechanisms, is described as peak-type ITD sensitivity. ITD sensitivity, which results from LSO-like coincidence mechanisms, is described as trough-type ITD sensitivity (Yin and Kuwada 1983b; Kuwada et al. 1987; Batra et al. 1997a). Yin and Kuwada established a method to differentiate these two types of ITD-sensitive neurons in peak- and trough-type neurons (Yin and Kuwada 1983b) (figure 1.4). This differentiation is based on the idea that peak-type ITD sensitivity results from binaural coincidence of excitation and trough-type ITD sensitivity from binaural coincidence of excitation and inhibition. Therefore peak-type ITD sensitivity should be generated in the MSO resulting in a maximal discharge rate (peak) to a characteristic ITD regardless of the stimulus frequency (figure 1.4A). In contrast, trough-type ITD sensitivity is described by a characteristic ITD that generates the minimal response (trough) regardless of the stimulus frequency (figure 1.4B). This trough in the ITD function results from a coincidence of excitation from the one ear and inhibition from the other ear. Several studies estimating the ITD sensitivity in the SOC support the existence of peak-type neurons in the MSO and trough-type neurons in the LSO (Spitzer and Semple 1995; Batra et al. 1997a; Tollin and Yin 2005).

For the classical differentiation between these two types of ITD sensitivity, the ITD functions were measured using different stimulus frequencies. The ITDs were normalized to the frequency-dependent duration of cycle (interaural phase differences, IPDs) (Yin and Kuwada 1983b). The stimulus phase changes linearly with frequency. The maximal responses of the IPD functions are plotted versus different stimulus frequencies and the fit-function is extrapolated to zero frequency. The phase at which the graphs intersect with the y-axis (at zero Hz) is called the characteristic phase (CP) of the neuron. A CP around 0 indicates that the maxima of the IPD function occur if the binaural (excitatory) inputs innervate the neuron simultaneously (peak-type neuron, figure 1.4A). A CP of

around ± 0.5 cycles indicates that maximal responses occur when the binaural inputs arrive out of coincidence with an IPD of 0.5 cycles (trough-type neuron, figure 1.4B). This happens when excitation from one side and inhibition from the other side coincide.

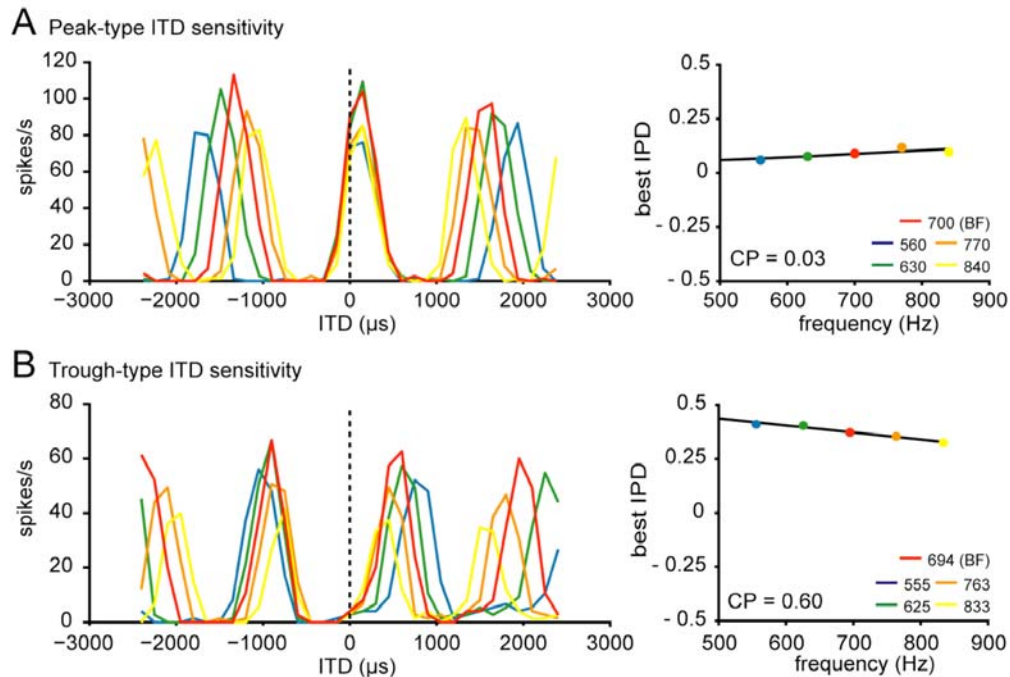


Figure 1.4 Exemplary ITD sensitivity of a peak-type (A) and a trough-type neuron (B). The frequency the neuron is maximally responding to, the best frequency (BF), is plotted in red. On the left side the response to different ITDs measured for different frequencies is shown. For these ITD functions the best interaural phase differences (IPDs) are calculated via vector analysis. The best IPDs are then plotted against the stimulus frequencies to calculate the characteristic phase (CP) as shown on the right side.

It is important to note that the classification of neurons into these two groups is not well defined. Often neurons with a CP between 0 and 0.5 (called intermediate-type neurons) are observed (Fitzpatrick and Kuwada 2001). There is evidence that convergent inputs from brainstem neurons can account for intermediate-type ITD sensitivity at the level of the midbrain (Kuwada and Yin 1983; McAlpine et al. 1998; Cai et al. 1998a; Shackleton et al. 2000; Fitzpatrick and Kuwada 2001; Fitzpatrick et al. 2002). However, several studies found intermediate-type ITD sensitivity already at the level of the SOC (Spitzer and Semple 1995; Batra et al. 1997a).

1.3 Processing of interaural time differences in the MSO

There are two major hypotheses regarding how ITDs are encoded in the MSO. In the first scenario MSO neurons encode ITDs via a coincidence mechanism of two excitatory inputs from the left and the right VCN. The neurons in the MSO are arranged along a delay line from rostral to caudal. This delay line is generated by the different lengths of the incoming axons of the excitatory neurons of the VCN. MSO neurons are excited binaurally and fire when the binaural inputs arrive coincidentally. Depending on the delays of the incoming inputs, every neuron encodes a different ITD by firing maximally at this ITD (Jeffress 1948). In this model all physiological relevant ITDs would be encoded by a maximal discharge rate of a specific neuron depending on its specific place in the delay line. Thus, a “place in space” is translated into a place in the rostral-caudal position of an individual neuron in the MSO. Therefore, this model is called the place-code model. Such a neuronal arrangement could be shown in the nucleus laminaris, the bird’s analogue to the mammalian MSO (Carr and Konishi 1988; Carr and Soares 2002). However, studies in mammals questioned the validity of this model for the ITD processing in mammals (for review: Grothe 2003; McAlpine and Grothe 2003). Anatomical data provide only weak evidence for such a delay line (Smith et al. 1993; Beckius et al. 1999) and physiological data show that especially for small mammals the maximal discharge rates of most of the ITD-sensitive neurons are not within but rather outside the physiologically relevant range of ITDs (Crow et al. 1978; Grothe and Park 1998; McAlpine et al. 2001; Brand et al. 2002; Hancock and Delgutte 2004). Thus, these neurons cannot encode different physiological relevant ITDs at a maximal discharge rate. However, most of the ITD-sensitive neurons change their neuronal response rate over the physiological relevant range of ITDs responding maximally to positive ITDs and minimally to negative ITDs. Based on these findings the second hypothesis, the so-called rate-code model, was formulated. This model suggests that ITDs are encoded by the discharge rate averaged over the population of ITD-sensitive neurons (McAlpine et al. 2001; McAlpine and Grothe 2003). In this rate-code model a small number of ITD-sensitive neurons could encode all the physiological relevant ITDs (Skottun et al. 2001; Shackleton et al. 2003).

Several anatomical (Clark 1969; Perkins 1973; Wenthold et al. 1987; Adams and Mugnaini 1990; Cant and Hyson 1992; Kuwabara and Zook 1992) as well as physiological studies (Grothe and Sanes 1993, 1994; Batra et al. 1997a; Grothe and Park 1998; Magnusson et al. 2005a) supposed that inhibitory inputs contribute to ITD processing in the MSO (see figure 1.2). Further evidence came from *in vivo* recordings in the MSO of gerbils (Brand et al. 2002). After blocking the glycinergic inhibition in the MSO, the maximal discharge rate, which was originally outside the physiological relevant range of ITDs, was shifted to an ITD in the middle of the physiological relevant range (red ITD functions, figure 1.5A). The authors concluded that inhibition shifts the maximal response outside the relevant range of ITDs and the maximal rate change inside the relevant range of ITDs (figure 1.5B). The mechanisms underlying this shift, however, are still a subject of debate. Different models, which incorporate inhibitory inputs to a coincidence detector model, could explain this shift of the ITD function (Brand et al. 2002; Zhou et al. 2005; Leibold and van Hemmen 2005). Taken together, these experiments showed that inhibition changes the ITD coding of the MSO neurons such that they are optimized to encode ITDs via a rate-code.

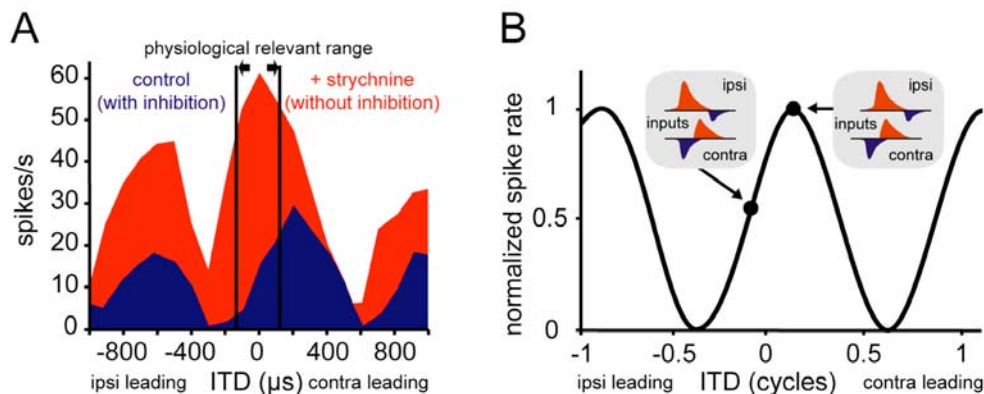


Figure 1.5 A: ITD function of a MSO neuron with (red) and without glycinergic inhibition (blue). Blocking the glycinergic inhibition by applying strychnine increases the discharge rate compared to the control ITD function. The peak of the ITD function is shifted in the physiological relevant range of ITDs (modified from Brand et al. 2002). **B:** Schematic drawing of how preceding contralateral inhibition could suppress the binaural response at zero ITD and thereby generate a maximal response to a positive ITD. The ipsi- and contralateral inputs to the MSO are shown as insets (**B**).

This recent findings, which support a rate-code based coding of ITDs in the MSO, opened controversial discussions about the underlying mechanism for the localization of

low frequency sounds in mammals (Grothe 2003; McAlpine and Grothe 2003; Joris and Yin 2007).

1.4 Issues with the investigation of processing interaural time differences

1.4.1 Processing of interaural time differences in higher stages of the binaural pathway

For several reasons, *in vivo* recordings from low frequency SOC neurons, especially from MSO neurons, are technically demanding. First, the deep location of these neurons in the brainstem makes the experimental access difficult. Second, the compact density of cells within the nuclei and small-sized action potentials of low frequency MSO and LSO neurons, which are due to the high expression of low voltage potassium channels, complicate single cell recordings (Svirskis et al. 2003; Scott et al. 2005). Therefore, data from MSO and LSO neurons are rare and most data about the processing of ITDs derived from recordings in the inferior colliculus (IC) of the auditory midbrain. The abundant convergence of excitatory and inhibitory inputs to the IC complicate the interpretation of data recorded in the IC in terms of general mechanisms of ITD processing (for review: Oliver and Huerta 1992). For example, *in vivo* recordings from the IC (Kuwada and Yin 1983; McAlpine et al. 1998; Fitzpatrick and Kuwada 2001; Fitzpatrick et al. 2002) as well as theoretical considerations (Cai et al. 1998a; Shackleton et al. 2000) indicate that the convergence of only two MSO inputs could create ITD properties that are much more complicated than the ITD sensitivity at the level of the MSO itself.

An alternative approach to investigate the ITD processing may be the recording at another anatomical site such as the dorsal nucleus of the lateral lemniscus (DNLL). The binaural SOC neurons directly innervate neurons of the IC and the DNLL (figure 1.6). MSO neurons send strong collateral projections to the ipsilateral (Shneiderman et al. 1988; for review: Oliver 2000) and, although controversially discussed, to the contralateral DNLL and IC (Glendenning et al. 1981; Willard and Martin 1984; Kudo et al. 1988; Grothe et al. 1994). LSO neurons send inhibitory projections to the ipsilateral IC and DNLL and excitatory projections to the contralateral IC and DNLL (Glendenning et al. 1981; Shneiderman et al. 1988; Shneiderman et al. 1999). Thus, since DNLL neurons

as well as IC neurons receive ITD- and IID-sensitive inputs of MSO and LSO neurons, these neurons are sensitive to both ITDs and IIDs (Brugge et al. 1970; Markowitz and Pollak 1994; Kelly et al. 1998; Fitzpatrick and Kuwada 2001; Kuwada et al. 2006).

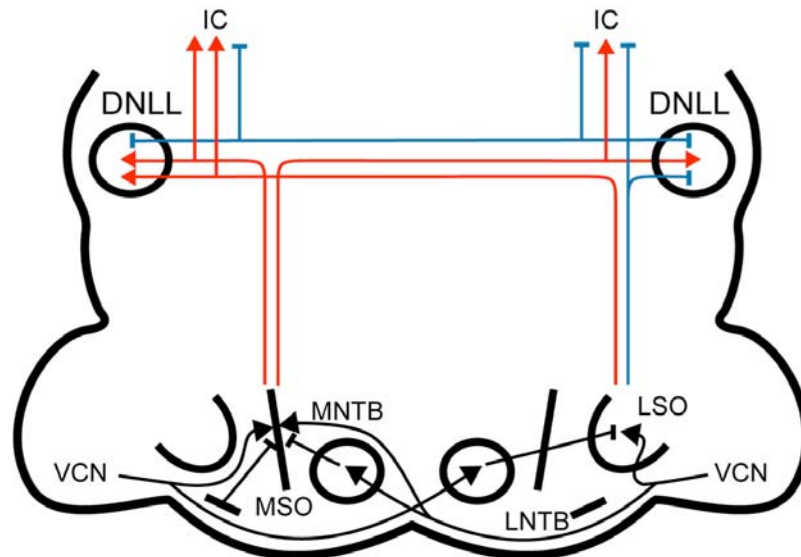


Figure 1.6 Schematic drawing of the binaural inputs to the dorsal nucleus of the lateral lemniscus (DNLL) and the inferior colliculus (IC). On the left side the inputs from the MSO are shown, on the right the inputs from the LSO.

The DNLL is an inhibitory (GABAergic) nucleus and mainly inhibits the contralateral DNLL and both ICs (Adams and Mugnaini 1984; Wu and Kelly 1996; Chen et al. 1999; Shneiderman et al. 1999). However, the convergence of other inputs in the DNLL is less pronounced than in the IC, which makes the DNLL potentially suitable for studying binaural processing.

1.4.2 Localization of multiple sound sources

Until now, most of the neurophysiological studies about localization of low frequency sounds have investigated the processing of one single static sound source, either a pure tone or a noise burst. But this situation does not reflect the natural environment. In nature, sounds are complex mixtures of auditory signals and their reverberations originating from multiple sources (figure 1.7).



Figure 1.7 Schematic drawing of concurrent sounds the gerbil might be exposed in a natural environment.

Obviously, our binaural auditory system is able to extract the relevant cues representing the positions of the sound sources out of this complexity and thus we can localize each of these sources separately. A step towards the understanding of how concurrent sounds are processed would be to investigate the perception of one sound source against a concurrent background noise. Psychophysically, a few studies considered the effect of background noise on sound localization (Cohen and Koehnke 1982; Ito et al. 1982; Stern et al. 1983; Good and Gilkey 1996). A general finding in all these studies is, that the accuracy to localize an auditory signal, measured as just-noticeable differences of ITDs, increases with increasing signal-to-noise ratio. Furthermore, the accuracy decreases if the location of the background noise differed from the location of the signal (Cohen and Koehnke 1982; Ito et al. 1982; Stern et al. 1983). The effects of background noise on the localization of tones were almost absent if the spectral components of the signal and the background noise were highly different (Stern et al. 1983). Hence, the capability to localize sounds against a background noise strongly depends on the level, the location, and the spectral components of the different sources. However, the neuronal mechanisms underlying the localization of multiple sound sources or sounds against background noise are not well understood.

1.4.3 The phenomenon of binaural sluggishness

As described above, the mammalian binaural auditory system relies on a very precise estimation of ITDs in the microsecond range in order to localize low-frequency sounds.

Considering that the duration of an action potential is around 50 times longer than the minimal just noticeable ITDs, this acuity is a biological feat. In contrast to this extraordinary precision, the binaural system has been described as rather slow in following changes in ITDs (for review: Moore 2003). This phenomenon is called binaural sluggishness. Classical experiments by Grantham et al. characterized this phenomenon (Grantham 1982). They estimated the relative resolution of binaural and monaural cues masked by uncorrelated noise and showed that the binaural system is sluggish in contrast to the monaural system. Hence, they postulated that the lower sensitivity or sluggishness of the binaural system might be based on neuronal feedback networks located between a general binaural processor and more centrally located detection mechanisms. Recently Joris et al. searched for a neuronal correlate of binaural sluggishness using the same stimuli as Grantham (Joris et al. 2006). They found neurons at the level of the cat auditory midbrain that follow modulations of interaural correlation which are much faster than estimated from human psychophysical experiments. Therefore, the authors hypothesized that no neuronal substrate exists at the level of the midbrain or at higher brain areas to read out this temporal code, hence the information simply gets lost. The stimulus used in these studies oscillates through stages of a coherent spatial image, a completely diffuse image and a blurred, semi-focused image as produced by interaurally anti-correlated noise. This constellation between a focused and a diffuse image is quite unnatural. Furthermore, neuronal data have been compared with the psychophysical data of Grantham et al. (Joris et al. 2006). This comparison is problematic since the neuronal data express the timing of the neurons to modulations in silence. The psychophysical data, however, express the detection threshold of modulations with increasing masking noise. Electrophysiological experiments that use a naturalistic stimuli and neuronal approach comparable to the psychophysical experiments are still missing.

1.5 The animal model

In order to study sound localization in an animal model, I used the Mongolian gerbil (*Meriones unguiculatus*). Mongolian gerbils (figure 1.8, inset) live in tunnel systems in the Mongolian steppe. High frequency sounds in comparison to lower ones are much

more attenuated particularly in warm and humid air (Huang et al. 2002). It has been hypothesized that gerbils use low frequencies to communicate and detect possible predators in longer distances (Rosowski et al. 1999). Several physiological adaptations such as an unusually tall bulla and a long basilar membrane (Webster and Webster 1975; Webster and Plassmann 1992; Rosowski et al. 1999) are reported to contribute to the low frequency hearing which is unusual for rodents (Ryan 1976; Brown 1987; Heffner and Heffner 1988). Humans and gerbils have the lowest auditory thresholds at 2 to 5 kHz with the whole audiogram of the gerbils being quite similar to that of humans (figure 1.8).

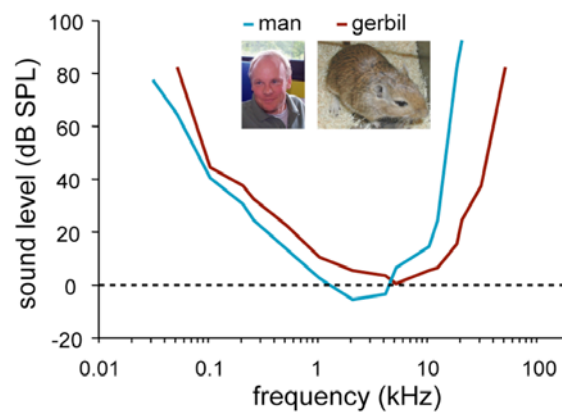


Figure 1.8 Comparison of two auditory threshold curves. The frequency is plotted against the lowest sound level the animal is responding to. The thresholds for a human are shown in blue, and in brown for a Mongolian gerbil (modified from Ryan 1976).

Furthermore, gerbils can resolve ITDs in the microsecond range similar to humans (human: 7-30 μ s, Klumpp and Eady 1956; gerbils 25-36 μ s, Heffner and Heffner 1988; Maier and Klump 2006; for review: Blauert 1997). Therefore, the gerbil is a well-established animal model to study ITD processing of low frequency sounds.

1.6 Aims

The presented work is divided into three parts, in which different novel approaches for the investigation of sound localization are studied:

Part one (chapter 2): My first aim was to carefully analyze DNLL neurons for their suitability as a model to study ITD processing. Using *in vivo* single cell recordings, I investigated general binaural properties and separated the neurons into different groups according to their firing pattern and their sensitivity to ITDs. To understand the origin of the neuronal properties in the DNLL, I investigated the inputs to the DNLL and cross-linked the different properties of the neurons with the inputs of the DNLL. Finally, potential mechanisms underlying the ITD processing were experimentally addressed.

Part two (chapter 3): This study aimed to investigate the ITD sensitivity of DNLL neurons to tones with a concurrent localizable background noise. I focused on the effect of tones on the response to noise as well as on the effect of noise on the response to tones. The following questions were addressed: (i) How do these effects depend on the location of the tone and the noise? (ii) How does the spectral composition of the noise influence the effects? (iii) Which cellular mechanisms mediate the observed effects? The last question was explored in combination with simulation experiments of simple coincidence detector models in cooperation with Christian Leibold.

Part three (chapter 4): My third aim was to investigate the temporal resolution of monaural and binaural processing and to directly link electrophysiological recordings from the gerbil's DNLL to human psychophysical results. Using a newly designed stimulus in combination with already established binaural stimuli, I estimated the speed of the binaural and the monaural neuronal systems. Additionally, I investigated the neuronal responses to the binaural stimuli under increasing masking noise, a setting typically used in psychophysical experiments. This experimental approach allowed the subsequent comparison of the electrophysiological sensitivity of neurons to the psychophysical data obtained in humans using the same stimulus (experiments performed together with Lutz Wiegrebe and Stefan Ewert).

2 Binaural response properties of low-frequency neurons in the gerbil dorsal nucleus of the lateral lemniscus

Siveke I, Pecka M, Seidl AH, Baudoux S, and Grothe B

Published in *Journal of Neurophysiology* 96(3): 1425-40, 2006

2.1 Abstract

Differences in intensity and arrival time of sounds at the two ears, interaural intensity and time differences (IID, ITD), are the chief cues for sound localization. Both cues are initially processed in the superior olivary complex (SOC), which projects to the dorsal nucleus of the lateral lemniscus (DNLL) and the auditory midbrain. Here we present basic response properties of low frequency (<2 kHz) DNLL neurons and their binaural sensitivity to ITDs and IIDs in the anaesthetized gerbil. We found many neurons showing binaural properties similar to those reported for SOC neurons. IID-properties were similar to that of the contralateral lateral superior olive (LSO). A majority of cells had an ITD sensitivity resembling that of either the ipsilateral medial superior olive (MSO) or the contralateral lateral superior olive (LSO). A smaller number of cells displayed intermediate types of ITD sensitivity. In neurons with MSO-like response ITDs that evoked maximal discharges were mostly outside of the range of ITDs the gerbil naturally experiences. The maxima of the first derivative of their ITD functions (steepest slope) however, were well within the physiological range of ITDs. This finding is consistent with the concept of a population rather than a place code for ITDs. Moreover, we describe several other binaural properties as well as physiological and anatomical evidence for a small but significant input from the contralateral MSO. The large number of ITD-sensitive low-frequency neurons implicates a substantial role for the DNLL in ITD processing and promotes this nucleus as a suitable model for further studies on ITD coding.

2.2 Introduction

Interaural disparities in time and intensity are the cues that animals use to localize sounds in the horizontal plane. Interaural intensity disparities (IIDs) are produced by a wavelength-dependent shadowing effect of the head that is more prominent for high- than for low-frequency sounds. In mammals, IIDs are initially processed by neurons in the lateral superior olive (LSO) via a subtraction mechanism based on excitatory inputs from the ipsilateral ear and inhibitory inputs from the contralateral ear (IE; Boudreau and Tsuchitani 1968; Yin 2002). Most LSO cells are tuned to high frequencies. Since low frequencies do not create significant IIDs, interaural time differences (ITDs) are the dominant cue for localizing low frequency sounds (Thompson 1882; Rayleigh 1907). ITDs are first processed in the medial superior olive (MSO), which receives both excitatory and inhibitory binaural inputs. The response of MSO neurons is dominated by a coincidence of the net excitation of the inputs from the two ears (for review: Irvine 1992; Yin 2002). Additionally, it has been speculated that low-frequency LSO neurons might contribute to ITD processing (Joris and Yin 1995). A recent study confirms such an EI-based ITD sensitivity for a small number of neurons in the low-frequency limb of the cat LSO (Tollin and Yin 2005). Unfortunately, data from low-frequency MSO and LSO neurons are sparse because it is notoriously difficult to record from these cells *in vivo*. Accordingly, the few neurophysiologic studies of low frequency MSO and LSO neurons provide small sample sizes compared to studies dealing with other auditory nuclei (Goldberg and Brown 1969; Yin and Chan 1990; Spitzer and Semple 1995; Batra et al. 1997a; Batra et al. 1997b; Brand et al. 2002; Tollin and Yin 2005). Therefore, most data about ITD processing and the neuronal representation of ITDs stems from the auditory midbrain, the inferior colliculus (IC), a direct target of the MSO and LSO projections (Rose et al. 1966; Kuwada and Yin 1983; Yin and Kuwada 1983a; Yin and Kuwada 1983b; Caird and Klinke 1987; Kuwada and Yin 1987; McAlpine et al. 1998, 2001). Unfortunately, a high degree of convergence of both excitatory and inhibitory projections from numerous lower auditory nuclei, from the opposite IC and from intrinsic connections complicates the interpretation of data derived from the IC (for review: Oliver and Huerta 1992). Therefore, large data sets are necessary in order to perform reliable population statistics on IC recordings (Kidd and Kelly 1996; McAlpine et al. 1998;

Fitzpatrick and Kuwada 2001; McAlpine and Palmer 2002; D'Angelo et al. 2005). *In vivo* recordings from IC (e.g. McAlpine et al. 1998) as well as theoretical considerations (e.g. Cai et al. 1998a,b) indicate that the convergence of only two MSO inputs, for instance, could create ITD properties in the IC that are much more complicated than the ITD sensitivity at the level of the MSO itself.

However, the MSO and the LSO also send strong projections to the dorsal nucleus of the lateral lemniscus (DNLL; Glendenning et al. 1981; Shneiderman et al. 1988; Oliver 2000), a hindbrain structure ventral of the IC. This nucleus is easier to record single neuron responses from than MSO and LSO and shows more linear, and hence, predictable response properties than IC neurons, at least for high frequency neurons (Xie et al. 2005). DNLL neurons are known to be sensitive to both IIDs and ITDs (Brugge et al. 1970; Markowitz and Pollak 1994; Kelly et al. 1998; Fitzpatrick and Kuwada 2001; Kuwada et al. 2006). Nevertheless, only a little is known about the role of the DNLL in low frequency sound processing.

Here we show that many low frequency DNLL neurons display response properties strikingly similar to those seen in the superior olivary complex (SOC). However, we also found that a substantial portion of our neurons have response features that are more similar to the properties seen in the IC rather than the SOC.

2.3 Methods

2.3.1 Experimental animals

Auditory responses from single neurons were recorded from 74 Mongolian gerbils (*Meriones unguiculatus*) of both sexes. Mongolian gerbils have a well developed low-frequency hearing and can use ITDs and IIDs for sound localization (Ryan 1976; Heffner and Heffner 1988). Animals used for the experiments were two to three months of age.

All experiments were approved according to the German Tierschutzgesetz (AZ 211-2531-40/01 + AZ 211-2531-68/03).

2.3.2 Surgical procedures

Before surgery, animals were anaesthetized by an initial intraperitoneal injection (0.5 ml/100 g body weight) of a physiological NaCl-solution containing ketamine (20 %) and rompun (2 %). During surgery and recordings, a dose of 0.05 ml of the same mixture was applied subcutaneously every 30 min. Constant body temperature (37-39 °C; Field and Siebold 1999) was maintained using a thermostatically controlled heating blanket.

Skin and tissue covering the upper part of the skull was cut and carefully pushed aside laterally, and a small metal rod was mounted on the frontal part of the skull using UV-sensitive dental-restorative material (Charisma, Heraeus Kulzer, Germany). The rod was used to reproducibly secure the head of the animal in a stereotactic device during recordings. Custom made ear-phone holders were attached to the gerbil head close to the acoustic meatus to form a sealed pressure field sound delivery system allowing the insertion of ear phones and probe-tube microphones. The animal was then transferred to a sound attenuated chamber and mounted in a custom-made stereotactic instrument (Schuller et al. 1986). The animal's position in the recording chamber was standardized by stereotactic landmarks on the surface of the skull (intersections of the bregmoid and lambdoid sutures with the sagittal suture in horizontal alignment) (Loskota et al. 1974). For electrode penetrations to the DNLL, a small hole was cut into the skull extending 1.3-1.6 mm lateral from the midline and 0.5-0.8 mm caudal of the interaural axis. Micromanipulators were used to position the recording electrode according to landmarks on the brain surface and a reference point was used for all penetrations. The dura mater overlying the cortex was removed carefully and during the recording session Ringer solution was applied to the opening to prevent dehydration of the brain. For some recordings the recording electrode was tilted 10° or 5° laterally.

Typical recording periods lasted 10-14 h. After recordings, the animal was sacrificed without awakening by an injection of 0.1ml of T61 (BGA-Reg No T331, Intervet, Germany) and the last electrode position was marked by a current-induced lesion (5 mA for 5 sec after T61 had been applied) using metal electrodes (5 MΩ). Afterwards the head was fixed in 4 % paraformaldehyde for two days. The brain was removed and placed in 30 % sucrose at 4° C for two days. The brains were embedded in tissue-freezing medium (Jung, Leica Instruments GmbH, Germany), frozen solid and mounted in a standard plane

for sections. Transverse sections were cut at 45 μm in a cryostat at $-21\text{ }^{\circ}\text{C}$. Sections were Nissl-stained and the recording sites verified using standard Light Microscopy.

2.3.3 Neuronal recordings

Single-unit responses were recorded extracellularly using tungsten electrodes (1 or 5 $\text{M}\Omega$; World Precision Instruments, Germany) or glass electrodes filled with 1M NaCl ($\sim 10\text{ M}\Omega$). We did not detect any differences between recordings using either type of electrodes in terms of the recording quality (spike to noise ratio, possibility of holding the cells and number of cells recorded per penetration), or neuronal response properties (discharge properties, best frequencies, thresholds, aurality, ITD or IID sensitivity). The recording electrode was advanced under remote control, using a motorized micromanipulator (Digimatic, Mitutoyo, Neuss, Germany) and a piezodriven controller (Inchworm controller 8200, EXFO Burleigh Products Group Inc, USA). Extracellular action potentials were recorded via an electrometer (npi electronics, Germany or Electro 705, World Precision Instruments, Germany), a noise eliminator (Humbug, Quest Scientific, Canada) removing residual line noise picked up by electrode, a band-pass filter (VBF/3, Kemo, Italy) and an additional amplifier (Toellner 7607, Germany) and fed into the computer via an A/D-converter (RP2-1, TDT). Clear isolation of action potentials from a single cell (signal to noise ratio >5) was guaranteed by visual inspection on a spike-triggered oscilloscope (stable shape and amplitude of the action potential) and by offline spike cluster analysis based on stable amplitudes of the positive and negative peaks (Volt) and stable spikes waveform (Brainware, Jan Schnupp, TDT) (see insets figure 2.5 and 2.7).

2.3.4 Stimulus presentation and recording protocols

Stimuli were generated at 50 kHz sampling rate by TDT System II or III (Tucker Davis Technologies, USA). Digitally generated stimuli were converted to analogue signals (DA3-2/ RP2-1, TDT), attenuated (PA5, TDT) and delivered to the ear phones (Sony, Stereo Dynamic Earphones, MDR-EX70LP). The sound field inside the sealed system was controlled using calibrated probe tube microphones (FG 3452, Knowles Electronics,

Inc, USA). The microphone signal was amplified (RP2-1, TDT) and transferred to the computer for offline analysis. The difference of the sound pressure level between the two headphones was less than 5 dB in the range of 100 Hz to 2000 Hz and the phase difference was below 0.01 cycles.

The standard setting was stimulus duration of 200 ms plus squared-cosine rise/fall-times of 5 ms, presented at a repetition rate of 2 Hz. For all recordings, stimulus presentation was randomized. To search for acoustically evoked responses, noise stimuli without interaural time and intensity differences were delivered binaurally. When a neuron was encountered, we first determined its best frequency (BF) and absolute threshold using binaurally identical (IID/ITD = 0) sinus tone stimulation. The frequency that elicited responses at the lowest sound intensity was defined as BF, the lowest sound intensity evoking a noticeable response at BF as threshold. These properties were determined online by audio-visual inspection in all neurons and, in almost all neurons (229/254), confirmed by a careful offline analysis of the frequency versus level response areas. These parameters were used to set stimulus parameters subsequently controlled by the computer. In addition, monaural pure tones and binaural pure tones were presented so that the binaural properties (aurality) could be determined.

Sensitivity to ITDs was primarily assessed by presenting a matrix of pure-tone stimuli with varying ITDs and stimulus frequencies 20 dB above threshold. We presented different ITDs over a range equivalent to at least a cycle of the stimulus frequency (step size 100 or $62500/0.6/BF$ μ s). ITD sensitivity was tested for between three and nine frequencies around BF. ITDs with the contralateral stimulus leading were defined as positive, ITDs with the ipsilateral stimulus leading as negative ITDs. ITD sensitivity was tested setting the IID to 0 dB.

A subpopulation of the binaurally excitable (EE) low-frequency cells was tested with very short downward-frequency-modulated sweeps (“chirps”). To record the waveform of the frequency-modulated-downward sweep stimulus (“chirp”, see figure 2.1) we used a pressure-field $\frac{1}{2}$ ” microphone (Type 4192, Bruel & Kjaer, Denmark) placed about 5 mm in front of the headphone. Headphone and microphone were tightly connected by a plastic tube to mimic the situation at the ear of the animal. The recorded signal was amplified (Calibration amplifier Type 2636, Bruel & Kjaer, Denmark), digitized (RP2.1, TDT) and stored on a PC. The frequency was modulated linearly from 2000 Hz to 100 Hz

in 3 ms, including squared cosine-function rise and fall times of 0.5 ms. The repetition interval was 2.5 Hz. Although these stimuli generate considerable spectral splatter we chose them because, unlike clicks, they did not appear to generate a prolonged ringing response; also, most of the stimulus energy is concentrated in the low frequency band (figure 2.1). The average monaural latencies were assessed for each ear individually by presenting the chirps monaurally. These stimuli evoked either a single discharge or, at most, two discharges with high temporal precision. We could therefore unambiguously determine those discharges that were evoked by the contralateral or the ipsilateral ear, even when the stimuli were presented binaurally, due to the separation by a given ITD. Binaural chirps with varying interaural delays were presented. The stimulation time of the ipsilateral chirp was kept constant and the delay of the contralateral stimulus was varied in steps of 50 μ s, 100 μ s or 200 μ s. Maximal interaural delays were \pm 1 ms or 2 ms. Stimulus amplitudes were adjusted so that cells responded to monaural chirps with one or two action potentials and were then held constant for all further stimulations.

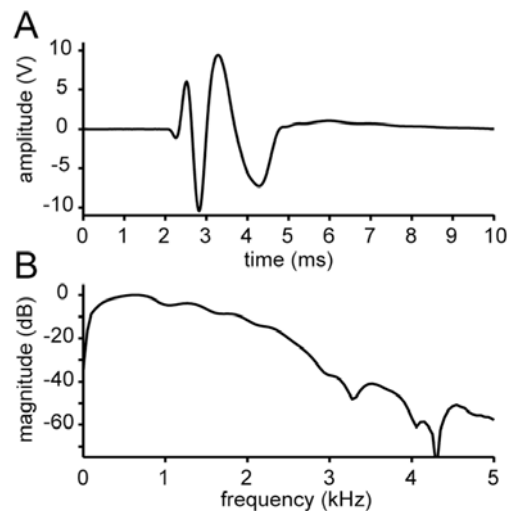


Figure 2.1 Chirp stimulus used to test a subset of neurons. Panel (A) depicts the recorded waveform of the chirp stimulus which was generated by a linear frequency downward modulation from 2 kHz to 0.1 kHz within 3 ms including 0.5 ms rise and fall times. The magnitude spectrum of the waveform in panel (B) illustrates that most of the energy was concentrated in the frequency band below 3 kHz.

In a subpopulation of EI neurons we assessed IID-sensitivity. A combination of different IIDs were presented by holding the intensity on the excitatory ear constant at 20 dB above the binaural (ITD = 0) threshold while varying the intensity on the inhibitory ear in 10 dB steps between 10 dB below and 50 dB above threshold. The resulting IIDs of -30

dB (negative values mark higher intensities on the inhibitory ear) to +30 dB were presented for five different frequencies centered on BF. The repetition rate was 4 Hz.

2.3.5 Data analysis

All quantifications in this study are based on offline analysis. Spontaneous activity was defined as a firing rate higher than 2 Hz. For the analysis of the different response patterns, the mean response to binaural stimuli (IID = 0, ITD = 0) at BF and 20 dB above threshold were used. For analyzing the post-stimulus-time histogram (PSTH), the period histogram, and the inter-spike interval histogram (ISIH) of 184 DNLL neurons we defined different response patterns. The response pattern was defined as onset (response exclusively during the first 50 ms) or sustained (response over the entire duration of the stimulus). Sustained activity was further divided in phase-locked sustained response and non phase-locked sustained response. Neuronal response was classified as phase-locked sustained (s-l) if the vector strength (Goldberg and Brown 1969) was larger than 0.3 and the $P < 0.05$ criterion in the Rayleigh test was fulfilled (Batschelet 1981). Following the description of response pattern of neurons in the cochlear nucleus by Rhode and Greenberg (1992), we divided the non-phase-locked pattern into primary-like (s-p) and tonic sustained (s-t) response patterns. Both patterns did not show regularity in the period histogram or the ISIH. The s-p types were separated from the s-t types by the mean response at the beginning of the response (in the time interval of 12.5- 37.5 ms) and the middle of the response (in the time interval of 87.5 - 112.5 ms). For the s-p types the response at the beginning was approximately three times larger than the response to the middle portion of the stimulus, whereas the response for the s-t types was about the same in both intervals.

ITD sensitivity was carefully analyzed and quantified for cells which showed at least 50 % modulation (reduction of max. spike rate by at least 50 %) in their ITD response rate function when tested at BF. For a detailed analysis of ITD functions we increased our sample size of ITD-sensitive cells by the addition of 105 DNLL cells from earlier, unpublished and published studies (Control group, Seidl and Grothe 2005) using identical equipment and experimental procedures. The quantifications were based on the interaural phase difference (IPD) functions measured with pure tones at different test frequencies

(thereby normalizing the cyclic ITD functions for test frequency). The cells mean interaural phase was calculated for each test frequency via a vector analysis following Yin and Kuwada (1983b). Since stimulus phase changes linearly with frequency, neuronal responses can be plotted as best phase vs. frequency and the functions can be extrapolated to zero frequency. The phase at which the graphs intersect with the y-axis (at zero Hz) is called the characteristic phase (CP), a value between -0.5 and +0.5. Depending on the calculated CP, different groups of ITD-sensitive neurons can be distinguished. “Peak-type” neurons have a CP at or around 0 cycles, reflecting coincidence of binaural excitation, which results in an individual best ITD (eliciting the maximal spike rate) independent of test frequency (Yin and Kuwada 1983b). Similar reasoning is applied to trough-type neurons, although trough-type neurons are characterized by the ITD that generates the minimum responses in the ITD functions. The trough in the ITD function is expected when there is coincidence of excitation from one ear and inhibition from the other. Extrapolations of these phase-frequency plots yield characteristic phases at or around ± 0.5 cycles, reflecting that maximal responses occur when excitatory and inhibitory inputs are out of coincidence.

We defined peak-type neurons by an absolute CP of 0 to 0.125 cycles and trough-type neurons by 0.375 to 0.5 cycles. According to the locations of the peaks and the troughs, we separated these two types into ipsilateral or contralateral peak-type or trough-type neurons, depending on whether the peaks or trough occurred for ipsilaterally or contralaterally leading sounds. Furthermore we defined two intermediate-types: a peak-intermediate-type by a absolute CP within 0.125 to 0.25 cycles and a trough-intermediate-type by a absolute CP within 0.25 to 0.375 cycles. The slope of the linear fit yielded a quantitative measure of the neuron’s characteristic delay (CD) (Rose et al. 1966; Yin and Kuwada 1983a). Phase plots were considered linear if the linear regression component exceeded the 0.005 level of significance using the test of nonlinearity described by Kuwada and colleagues (Kuwada et al. 1987). A subgroup of ITD-sensitive neurons ($n = 81$) was tested for the validity of the assumed linearity of our regression lines of the frequency versus best IPD functions. Of this subpopulation 74 (93 %) neurons showed a significant linearity (following Kuwada et al. 1987). Furthermore we tested if weighting each data point (best IPD at certain frequency) by the vector strength and the mean response in a similar manner to that described by Kuwada et al. (1987) and Spitzer

and Semple (1995) would change the obtained distribution of different types. We could not find any differences. Almost all calculated CPs (71/81, 88 %) were not or at most slightly affected and, hence, their classification of ITD sensitivity was independent of the method used.

To define the point of steepest slope, the ITD function was fitted by a Gaussian (Matlab; The MathWorks, Inc., MA, USA) or sigmoid function (Statistica; StatSoft, Inc., OK, USA) and the inflection point closest to zero ITD was determined. Fitted ITD functions obtaining an R-square below 0.7 were excluded.

Analysis of the responses to binaural chirp stimuli were conducted by defining time slots during which action potentials should occur in response to the ipsilateral or the contralateral stimulus. These time slots (starting point and width) were based on the spike time latencies measured in response to monaural stimulation. The time slots had a width of about 0.25 ms. Response rates in these time windows were assessed. For responses with more than one action potential per stimulation only the first action potential was counted. The average spike time, standard deviation and variance was determined for analysis of the temporal accuracy of a cell's response.

Neurons were defined as IID-sensitive if ipsilateral (inhibitory) stimulation reduced the maximal response elicited by contralateral (excitatory) stimulation by more than 50 %. The IID of maximal inhibition was defined as the smallest IID (lowest intensity at the ipsilateral, inhibitory ear) that caused maximal suppression of the response to the contralateral stimulus. To calculate the maximal inhibition in percent we used the following formula: $(\text{maximal response rate} - \text{minimal response rate}) / (\text{maximal response rate} * 100)$. The IID of 50 % inhibition was graphically extrapolated from the calculated 50 % response rate of the neurons IID-function.

2.3.6 Immunohistochemistry

Three animals were used for anatomical studies in which neuronal tracers were injected into the DNLL after recording. Two different tracer cocktails were used: a mixture of biotin- (10 %; Molecular Probes D-1956, NL) and fluorescein-dextran (10 %, Molecular Probes D-1820, NL), or tetramethylrhodamine-dextran (10 %, Molecular Probes D-1817, NL) dissolved in 0.9 % NaCl. Tracers were injected by iontophoresis (6 μ A for 6 to

10 min). Nine to 10 days after the injection, the animals were deeply anesthetized (Chloralhydrate 50mg/100g) and perfused transcardially with heparinized 0.9 % buffered saline solution for 5 min under deep anesthesia followed by a buffered solution containing 4 % paraformaldehyde and 1% glutaraldehyde for 20 to 30 min. The fixed brain was removed from the skull and placed in 30 % sucrose (until it had sunk) for cryoprotection. Transverse sections of 40 μ m were prepared in a cryostat (Leica Microsystems CM 3050S, Nussloch, Germany).

The histological methods used in this study have been described in detail elsewhere (Malmierca et al. 2002; Oliver et al. 1997). In short, all sections were incubated in 0.05 % TritonX100 for 30 min. For visualization of the biotinylated-dextran amine, the avidin-biotin-diaminobenzidin (DAB) method (ABC Kit, Vector Laboratories, CA, USA) coupled with nickel was used. For permanent staining of the tetramethylrhodamine-dextran, the slices were incubated with anti-tetramethylrhodamine rabbit IgG (Molecular Probes, NL) over night followed by 30 min incubation with biotinylated anti rabbit (Jackson, PA, USA), and avidin-biotin-DAB. Every third section was counter-stained (Nissl) to allow a clear allocation of the labeled cells. Camera lucida drawings were made with the aid of a drawing tube attached to a Leitz microscope (Dialux 20, Leitz, Wetzlar, Germany). Photomicrographs were made with a digital camera (Polaroid, USA). The retrogradely labeled and DAB-stained neurons in the SOC of three animals were counted under the light microscope and pooled for each nucleus (as defined via the Nissl staining).

2.4 Results

2.4.1 General response features of DNLL cells

BFs ranged from 70 Hz to 5.6 kHz, but more than 2/3 of the neurons (185/254) had BFs below 2000 Hz, which we refer to as low-frequency neurons. Twenty percent of the low frequency DNLL neurons we tested were spontaneously active (38/185; 20.5 %) (rate about 2 Hz).

Low frequency DNLL neurons ($BF < 2$ kHz) exhibited five different discharge patterns when tested at $ITD=0$.

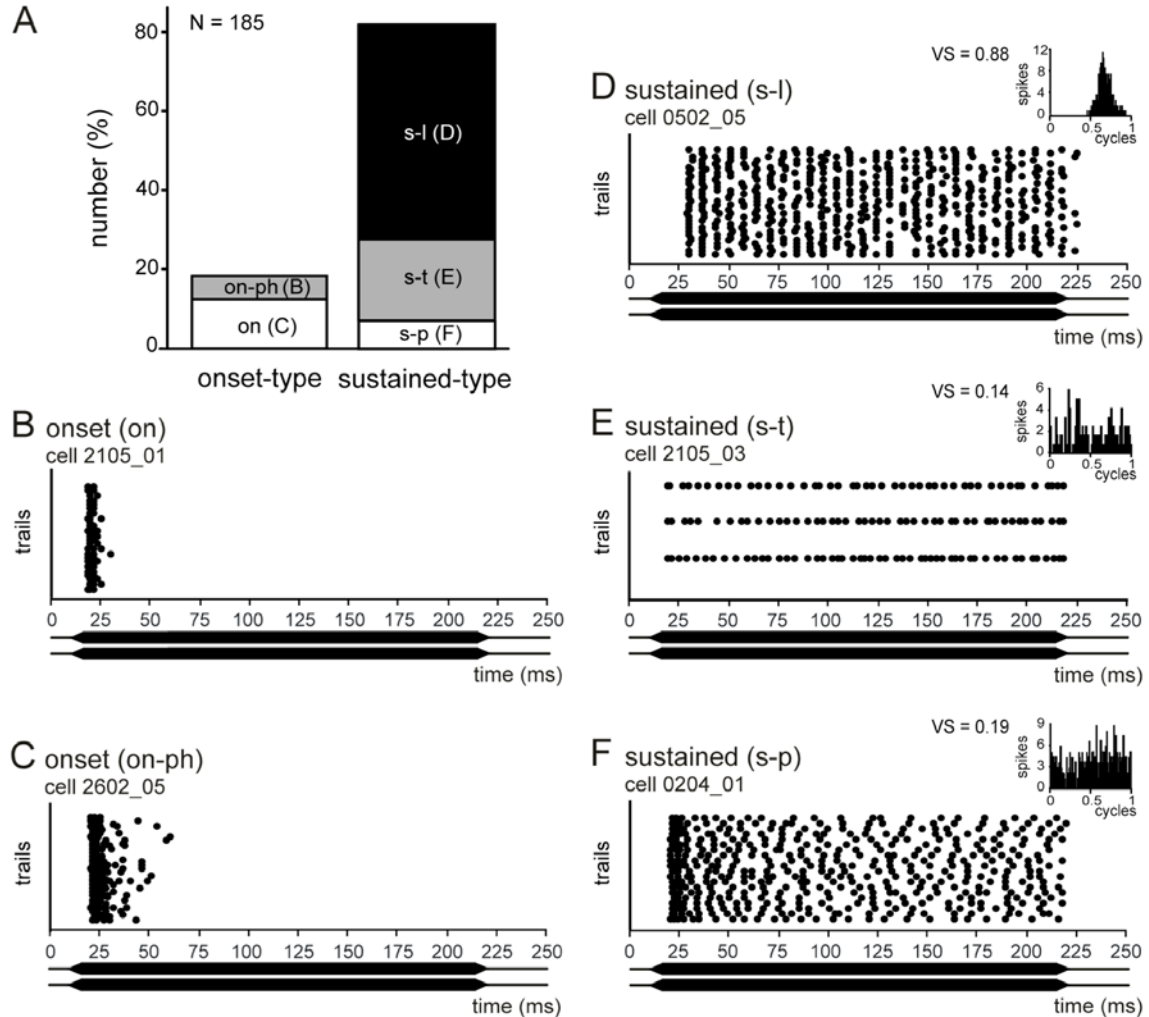


Figure 2.2 Response types of binaural DNLL neurons in response to binaural 200 ms pure tones at BF, 20 dB above threshold. **A**: Distribution of response types. **B-F**: Examples of different response types showing discharges as raster plots and phase-histograms (insets) average the responses on a cycle-by-cycle basis. Stimuli are indicated below the dot raster as black bars. **B**: Example of an on-type response with one or two action potentials per stimulus presentation (on). $BF = 1300$ Hz. **C**: On-type neuron with multiple spikes at the beginning of the stimulus (on-ph). $BF = 800$ Hz. **D**: Response of a neuron with a sustained response showing nearly perfect phase-locking as apparent from the phase histogram (inset) and the high vector strength (VS) derived from it (s-l). $BF = 200$ Hz. **E**: Neuron with a sustained response, which was not phase-locked to the stimulus (s-t). $BF=1300$ Hz. **F**: Typical primary-like discharge pattern with a prominent on-component and a weaker ongoing component (s-p). In this case the ongoing component was weakly phase-locked. $BF = 1000$ Hz.

A small group of neurons (34/185, 18 %) showed onset responses (figure 2.2A). Of these, two thirds (23/34; 68 %) fired one to three spikes per stimulus with an extremely short

onset (on; figure 2.2B), whereas 32 % (11/34) showed a phasic-on type response (on-ph; figure 2.2C). Most neurons (151/185; 82 %) had sustained discharge patterns. About two thirds of the sustained neurons (101/151; 67 %) showed a significant phase-locked response (s-l) to the low frequency pure tones (figure 2.2D). Non-phase locked but sustained neurons exhibited either primary-like (s-p) (14/151; 9 %) or tonic (s-t) discharge patterns (36/151; 24 %). S-t neurons exhibited a nearly constant discharge rate throughout the entire stimulus duration (figure 2.2E), whereas s-p neurons had a stronger response at the beginning of the response period (figure 2.2F).

We tested the distribution of binaural properties using 127 low frequency DNLL neurons (figure 2.3). Except for a small number of monaural neurons (16/127; 13 %), which were excited by the contralateral ear and unaffected by ipsilateral stimulation (E0), most low frequency DNLL neurons (111/127; 87 %) were binaurally sensitive. Most of these binaural sensitive neurons (73/111; 65 %) showed evidence for binaural excitation either by responding to monaural stimulation of either ear alone or by exhibiting binaural facilitation. These neurons were classified as excitatory-excitatory (EE). A substantial number of neurons (33/111; 30 %) were excited by the contralateral and inhibited by stimulation of the ipsilateral ear (EI) and a smaller number of the neurons (4/111; 5 %) were excited by ipsilateral and inhibited by binaural stimulation (IE).

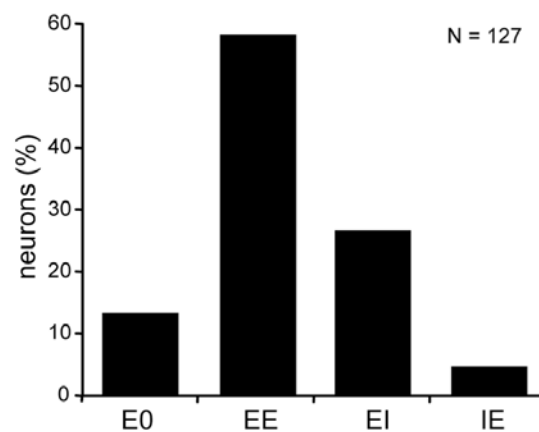


Figure 2.3 Distribution of aural types of low frequency DNLL neurons. The first letter indicates the overall effect of the contralateral, the second letter of the ipsilateral ear. E = excitatory, I = inhibitory, 0 = no effect. Note that this notation does not distinguish between excitation and facilitation.

We looked for correlations between temporal response patterns with the binaural response type (table 2.1).

Table 2.1 Correlation between the binaural types and the response pattern of the low-frequency neurons. Total number of types is 82. n = 8, 57, 5, and 12 for OE, EE, IE, and EI, respectively. Parentheses enclose percentages.

Response pattern	Binaural Types			
	OE	EE	IE	EI
Onset	1 (13)	12 (21)	0 (0)	0 (0)
Sustained (phase-locked)	5(63)	33(57)	3 (60)	5 (42)
Sustained (tonic/primary-like)	2 (25)	12 (21)	2 (40)	7 (58)

Interestingly we found that all onset neurons were EE or OE whereas sustained responding neurons showed all binaural response types. All monaurally inhibited neurons (EI and IE) showed sustained response patterns. EI and IE type neurons showed s-l and s-p response types to an equal extent, while the EE and EO types showed more s-l type than s-p type responses. 50% of the binaural neurons exhibited s-p type activity.

2.4.2 Features of ITD-sensitive neurons

We evaluated responses to a wide range of ITDs in 189 binaural low-frequency DNLL neurons. ITD-sensitive neurons were divided into two main groups: peak-type neurons and trough-type neurons (as defined in Methods). Representative ITD functions of these two types of ITD-sensitive neurons are shown in figures 2.4 and 2.5. Both example neurons exhibited a sustained phase-locked discharge pattern (insets figure 2.4) at favorable ITDs (maxima or “peak” of the functions), and a decreased response rate with only an on-discharge remaining at unfavorable ITDs (minima or “trough” of the function). Where the peak-type neuron had a peak response at a common best ITD independent of the test frequency (figure 2.5A), the trough-type neuron showed a trough at a common ITD independent of the test frequency (figure 2.5B). The characteristic phase (CP, see methods) of the peak-type neuron was around 0 cycles (figure 2.5A; CP =

-0.068 cycles), the CP of the trough-type neuron around ± 0.5 cycles (figure 2.5B; CP = -0.514 cycles).

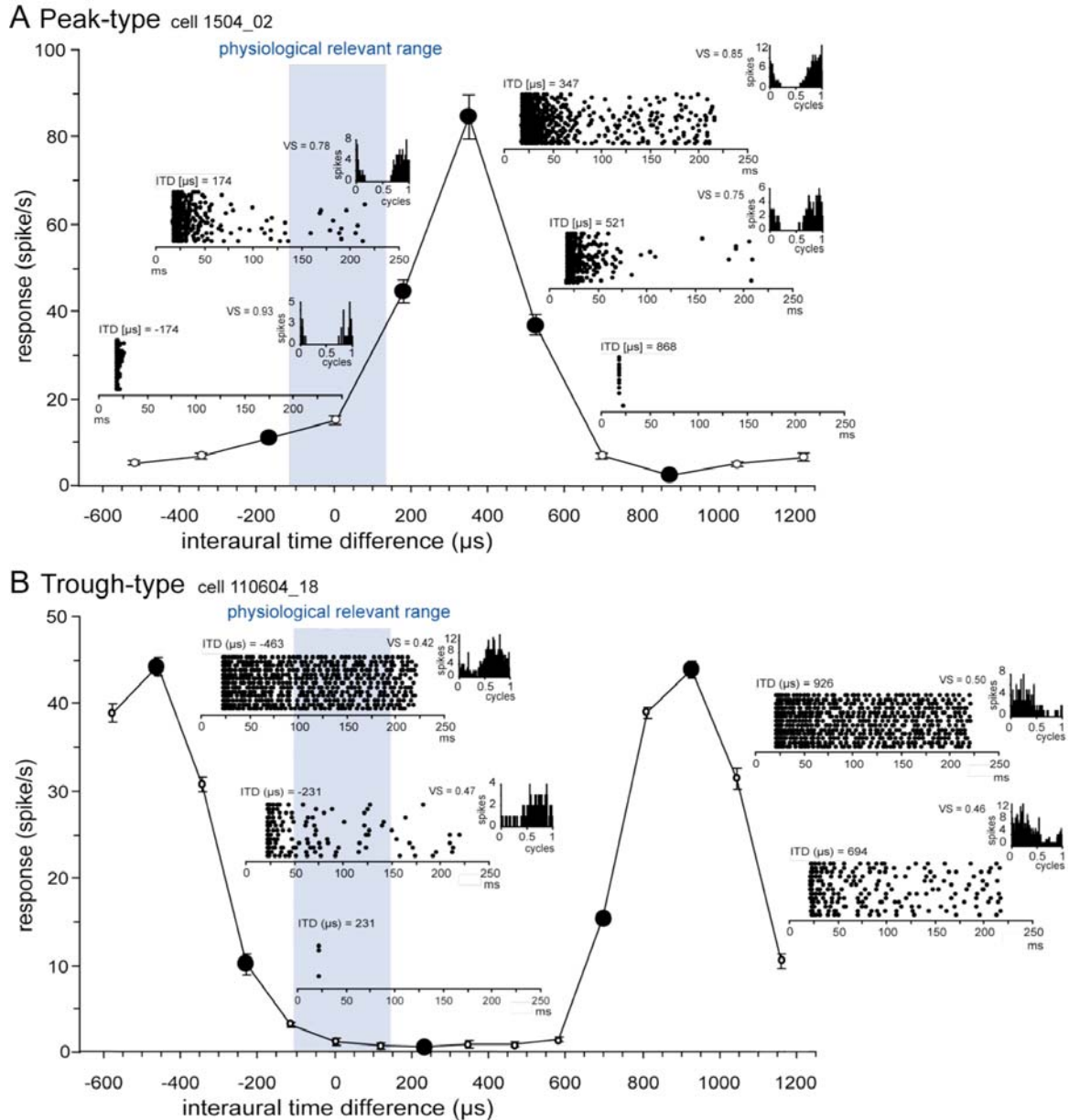


Figure 2.4 ITD-sensitive responses of a typical EE (A) and EI neuron (B). The dot raster plots (corresponding to the ITDs marked as black dots) reveal the neuron’s sustained response to favorable ITDs and its onset-response to unfavorable ITDs. *Inset*: period histograms show that the sustained response as well as the onset response are phase-locked to the same phase angle. **A**: neuron’s ITD sensitivity was tested at BF (600 Hz) 20 dB above threshold and the ITD sensitivity classified as peak-type response (see response of the same neuron to different frequencies figure 2.5A). **B**: The neuron was tested at BF (700 Hz) 20 dB above threshold and the ITD sensitivity classified as trough-type response (see response of the same neuron to different frequencies figure 2.5B). The shaded areas indicate the physiologically relevant range of ITDs for the gerbil. Error bars = SE.

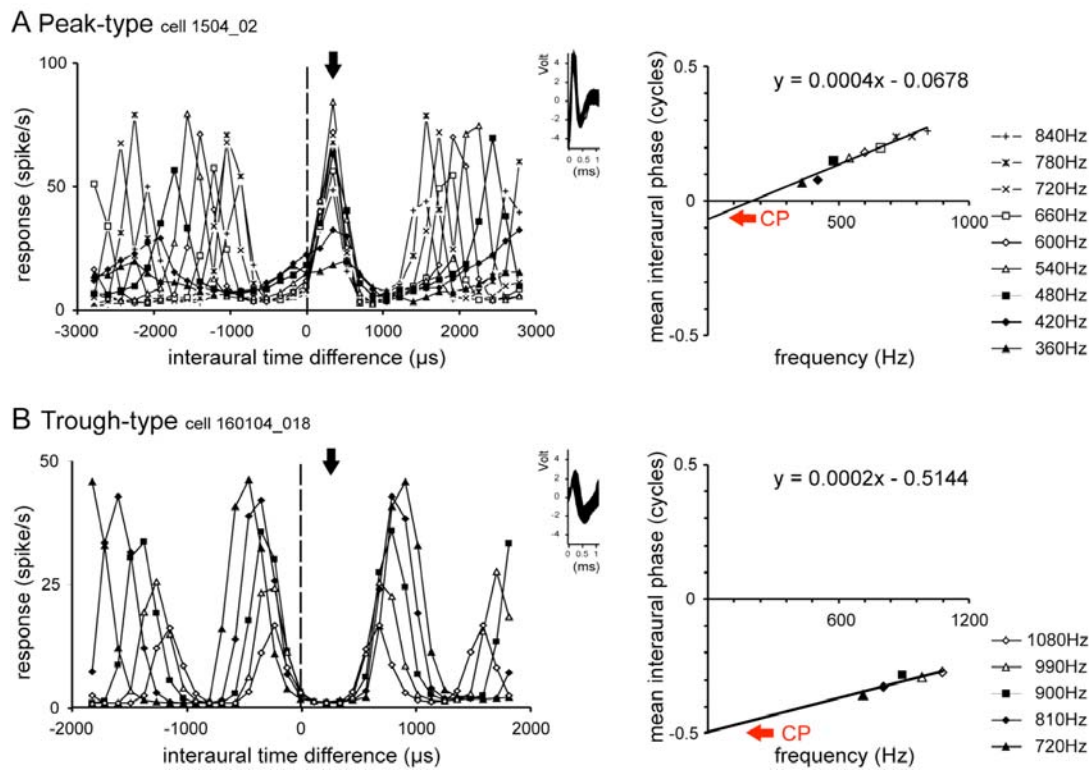


Figure 2.5 A: Typical peak-type ITD sensitivity in response to different test frequencies (same neuron as in figure 3A). As shown in the left figure, the neuron exhibited a maximum discharge at an ITD of 350 μs (contralateral stimulus leading, indicated by the black arrow) independent of test frequency. All other peaks and troughs of the cyclic ITD functions change systematically (according to the length of the cycle) with test frequency. **B:** The trough-type response (same neuron as in figure 2.3B) exhibited a minimal discharge at about 200 μs (contralateral stimulus leading, indicated by the black arrow), independent of test frequency. The shapes of the action potentials of all spikes recorded for this stimulation are shown as insets. On the right side the frequency phase-plot is shown. For each test frequency the best interaural phase difference (IPD) was calculated via a vector analysis of the IPD function. The intercept with the y-axis gives the characteristic phase (CP). For the neuron shown in **A**, the CP is close to 0, indicating the peak-type characteristic of the neuron's ITD sensitivity. In **B**, the CP around ± 0.5 indicates a trough type characteristic (**B**, right panel). The slope of the regression line gives the characteristic delay (400 μs for the peak-type neuron and 200 μs for the trough-type neuron in **B**).

We found that the large majority of the peak-type neurons were contralateral (70 %; 56/80) and that a smaller group was ipsilateral peak-type neurons (30 %; 24/80). The trough-type neurons were roughly equally distributed between ipsilateral (44%; 14/32) or contralateral trough-type neurons (56 %; 18/32).

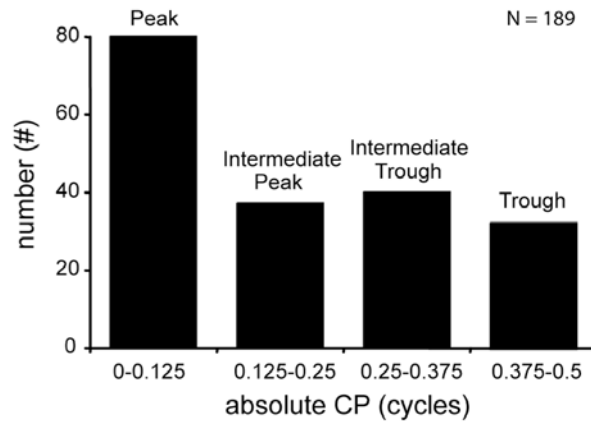


Figure 2.6 Distribution of different types of ITD sensitivity found in the population of DNLL cells tested. See text for details.

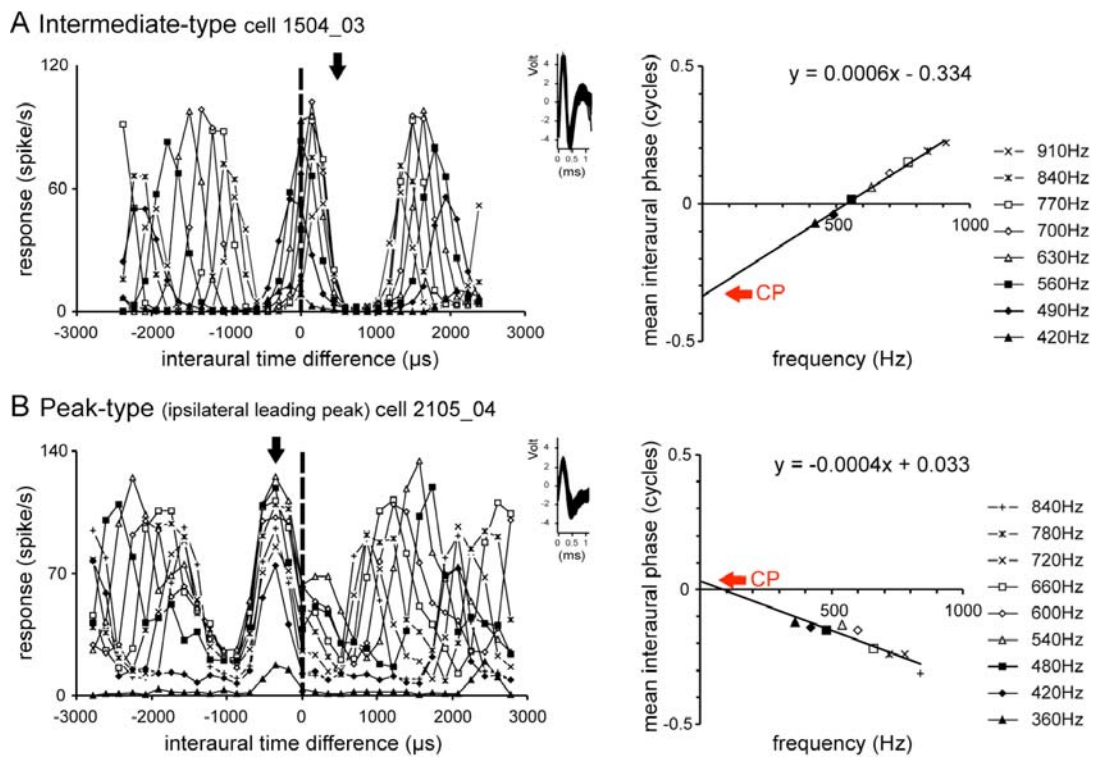


Figure 2.7 A, ITD sensitivity of a neuron that showed neither a stable peak nor a stable trough across different test frequencies. The frequency phase-plot shows a CP far from 0.5 and 0, confirming the intermediate type of the ITD sensitivity. The neurons BF was 700 Hz. **B**, ITD sensitivity of a neuron representative of a small population of cells that had stable peaks at negative ITDs (ipsilateral stimulus leading) with a small second-peak at positive ITDs, particularly when tested with frequencies close to BF (540 Hz). Format as in figure 2.5.

The peak-type neurons and trough-type neurons are the most distinct examples of ITD tuning. Peak-type neurons were the most common type of ITD function and comprised

42 % of the sample (80/189). Trough-type neurons were the least common and comprised 17 % (32/189) of our sample (figure 2.6). A large group of neurons, however, showed an ITD sensitivity between these two extremes; 41 % (77/189) of the neurons showed an intermediate type ITD sensitivity ($0.125 < CP < 0.375$ cycles; figure 2.7A). According to our definition (see methods) we found 20% intermediate peak-type neurons (37/189; $0.125 < CP < 0.25$) and 21 % intermediate trough-type neurons (40/189) ($0.25 < CP < 0.375$ cycles; figure 2.7A).

Based on qualitative visual inspections, we observed secondary peaks in the ITD functions in 23 % (44/189) of our sample. An example neuron is illustrated in figure 2.7B. In some cases the secondary peak was evoked by one frequency but in other neurons it was evoked by all of the tested frequencies. Secondary peaks were not evenly distributed among the groups of ITD-sensitive types. 11% of the contralateral peak-type neurons (6/56) had secondary peaks and were the least likely type to have secondary peaks. Significantly more (Chi^2 ; $p < 0.001$) secondary peaks were found in ipsilateral peak-type neurons (50 %; 12/24).

For a small number of peak-type neurons we compared the ITD sensitivity of the first spike to the ITD sensitivity of the ongoing component of the response. A typical example is shown in figure 2.8. Comparing the tone-delay-functions at BF the ITD sensitivity of the first spike showed the same feature as the ITD sensitivity of the whole response. In 12 of the 16 neurons (75 %) we found the first spike to have a similar sensitivity to ITDs as the ongoing component of the response.

We tested for correlations between types of ITD sensitivity three features: the frequency tuning of the neurons (data not shown), the temporal response pattern (upper part table 2.2), and the binaural response type (lower part table 2.2). Note that this subgroup is representative as it has the same distribution of different ITD-sensitive types as the entire sample. We could not find differences in the frequency tuning of the neurons dependent on the type of ITD sensitivity. Also, the temporal response patterns were not specific for any of the groups. Interestingly, the response pattern could change for different ITDs (figure 2.4). The neurons tended to respond to unfavorable ITDs with onset response pattern and to favorable ITDs with sustained response pattern. The response patterns were tested with pure tones at zero ITD, a common standard procedure, which obviously leads to a somewhat arbitrary classification for binaural neurons. Around 80% of the peak and

intermediate-peak type neurons showed clear signs of binaural excitation. Some intermediate-trough and trough-type neurons were binaurally excited, but the combined number of EI and IE neurons was much higher in these groups.

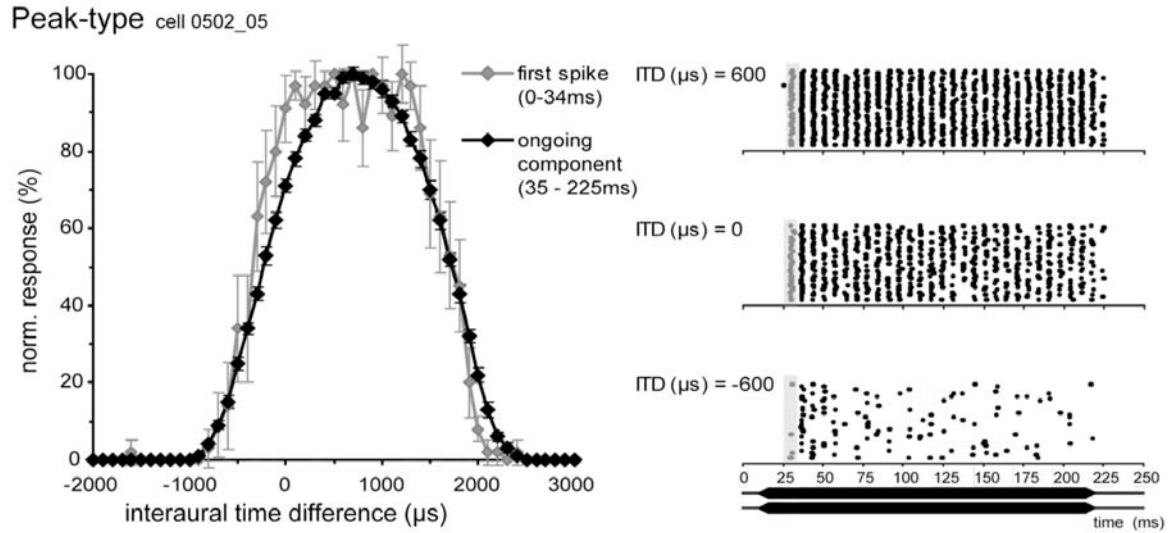


Figure 2.8 ITD sensitivity of the first spike of the response of a peak-type neuron in comparison with the ITD sensitivity of the ongoing response. The figure shows the neuronal response to a tone-delay-stimulation at BF (BF = 200 Hz). *Right*: PSTHs of the response to three different ITDs. The shaded area indicates the area of the 1st spike. Error bars = SE.

Table 2.2 Correlation between type of ITD sensitivity, response pattern, and aurality. n = 35, 15, 20, and 12 for peak type, intermediate peak type, intermediate trough type, and trough type, respectively. Percentage in parentheses.

Response pattern/ Aurality	Type of ITD sensitivity			
	Peak-type	Intermediate peak-type	Intermediate trough-type	Trough-type
Onset	7 (20)	5 (33)	1 (5)	1 (8)
Sustained (phase-locked)	18 (51)	6 (40)	13 (65)	9 (75)
Sustained (tonic/primary-like)	10 (29)	4 (27)	6 (30)	2 (17)
OE	2 (6)	3 (20)	2 (10)	1 (8)
EE	31 (89)	11 (73)	10 (50)	6 (50)
IE	1 (3)	0 (0)	2 (10)	1 (8)
EI	1 (3)	1 (7)	6 (30)	4 (33)

2.4.3 Distribution of ITDs across frequency

The head width of adult gerbils creates ITDs ranging from 0 μs for sounds emanating straight ahead, to about 120 μs for sounds located 90 degrees laterally (Maki and Furukawa 2005). Hence, the maximal ITDs gerbils can experience range from -120 μs to +120 μs (= “physiological range”). However, the best ITDs of the peak-type neurons when tested at BF were distributed between +527 and -470 μs as shown in figure 2.9. The average mean interaural phase of the peak-type neurons was 0.13 cycles (+/-0.1 cycles). The majority of peak-type neurons had best ITDs well outside the physiological range of ITDs (figure 2.9A). In contrast to the peaks, the points of steepest slopes of the functions were distributed around 0 ITD and almost all within the physiological relevant range (figure 2.9B). This holds not only for contralateral but also for ipsilateral peak-type neurons, although the latter had a larger variance in their distribution.

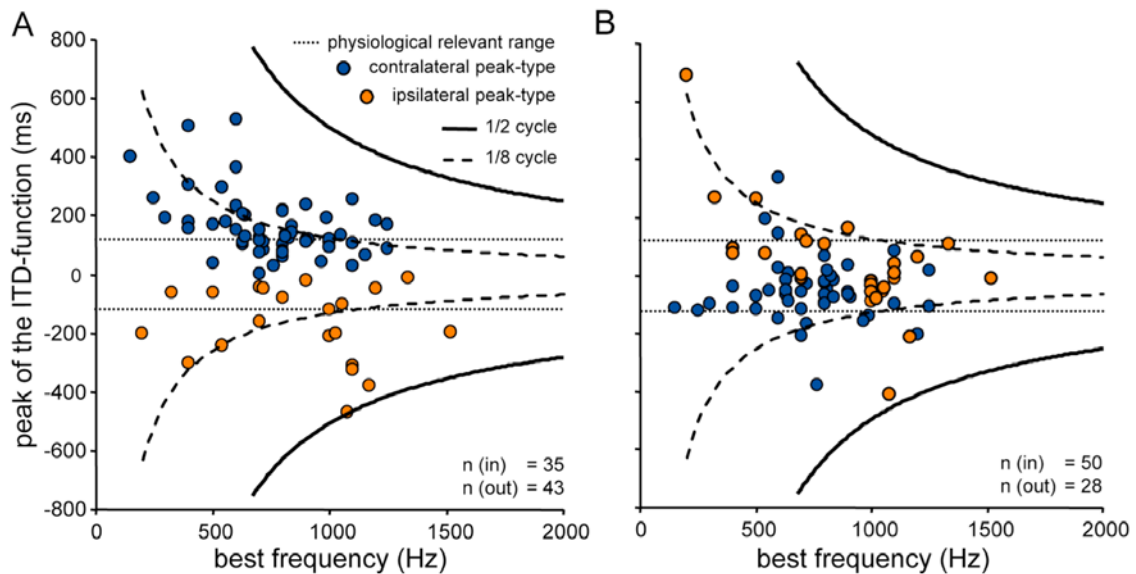


Figure 2.9 Peaks and slopes of the ITD functions of peak-type neurons as a function of BF. Values derived from the ITD functions measured at BF. Horizontal dotted lines indicate the range of ITDs gerbils can experience naturally (about $\pm 120 \mu\text{s}$). **A:** Best ITDs as a function of the neurons’ BFs. Note that best ITDs are not independent of BF and that most best ITDs are outside the physiological range of ITDs. **B:** Points of steepest slopes of ITD functions as a function of the neurons’ BFs. Points of steepest slopes are independent of BF (in contrast to the best ITDs). The majority of points of steepest slopes are close to 0 ITD and well within the physiological range of ITDs. n(out) = number of point outside the physiological relevant range, n(in) = number of point inside the range.

2.4.4 DNLL neurons are sensitive to ITDs evoked with brief chirps

A model based on the circuitry of the MSO suggested that contralateral preceding inhibition from the medial nucleus of the trapezoid body (MNTB) might shape the ITD functions (Brand et al. 2002). Here we utilized chirp stimuli that could provide some evidence for the existence of a leading contralateral inhibition. The first panel in figure 2.10 shows separate responses evoked by stimulation of each ear at an ITD of $-900 \mu\text{s}$ (contralateral signal lagging). The shaded areas depict the expected time of response derived from monaural stimulation of the ipsilateral (left shaded area) and contralateral (right shaded areas) ear respectively. The response to contralateral stimulation was influenced by the leading ipsilateral stimulus, as it was slightly delayed compared with the monaural response whereas the response to the leading ipsilateral stimulus occurs within the expected time frame. When the contralateral signal was lagging by $600 \mu\text{s}$ the contralateral response was almost absent. Note that shortening the lag of the contralateral stimulus led to a remarkable decline in the accuracy of the ipsilaterally evoked response although the response to the leading (ipsi) stimulus still occurred several hundred microseconds before the expected response to the lagging (contra) stimulus. The standard deviation of the latency at $900 \mu\text{s}$ ITD was $58.7 \mu\text{s}$ and increased to $313.0 \mu\text{s}$ at the ITD of $600 \mu\text{s}$ for this example neuron. The most significant feature occurred when the contralateral stimulus lagged the ipsilateral signal by $300 \mu\text{s}$ (third panel). Now the leading inhibition evoked by the contralateral ear suppressed almost all discharges evoked by the ipsilateral signal. When both stimuli were presented simultaneously (fourth panel), the cell responded with a single spike, and with re-established excellent temporal accuracy (STD of latency $69.2 \mu\text{s}$, variance $4.8 \mu\text{s}$).

We tested 24 EE cells for contralateral inhibition preceding excitation with these chirp stimuli. In 14 of those neurons (58 %), presentation of a contralateral chirp shortly after an ipsilateral chirp changed the response to the ipsilateral stimulation even though the contralateral net excitation always occurred clearly after the ipsilateral one. In 12 of the 14 cells the influence was seen as a substantial decrease of the spike rate to the ipsilateral chirp ($>50\%$ to maximum spike rate; average decrease of 12 cells was 88.5 %) as depicted in figure 2.10. In two cells, no decrease in the response was detected, but a strong increase in the jitter of the timing of the response was observed (increase of the standard deviation of the average response latency by more than 60 %, the average

increase in jitter was 66.0 %). This effect was furthermore accompanied in these two neurons by a sudden but consistent increase of the average latency. Three cells showed both an increase in latency simultaneously with a decrease in spike rate and one neuron showed an increase in jitter and a decrease in spike rate.

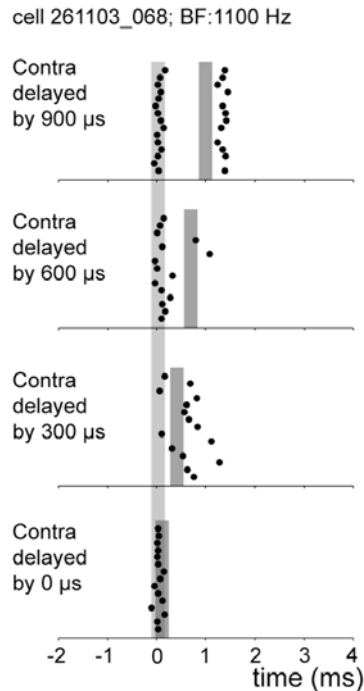


Figure 2.10 Example neuron (EE) with apparent inhibition from the contralateral side preceding contralaterally driven excitation. Raster plots show the occurrence of single action potentials in response to “chirps”. The stimulus amplitude was set to a level that elicited one spike per stimulus when presented monaurally at either ear. The shaded area gives the expected response based on monaural stimulation to the ipsilateral (left shaded area) or contralateral ear (right shaded area). When the contralateral stimulus was delayed by 900 μ s, both stimuli elicited spikes. Note that the response to the lagging, contralateral stimulus was already influenced by the leading stimulus in that it was slightly delayed. A decrease of the interaural delay to 600 μ s caused the lagging response to the contralateral stimulus to vanish. Also, the response to the ipsilateral stimulus became less accurate (higher jitter), although the response to the contralateral stimulus is expected to occur long after the response to the ipsilaterally evoked response. At an interaural delay of 300 μ s, the ipsilaterally evoked response was strongly suppressed. Coincidence of the two excitatory inputs seems to occur at 0 ITD, resulting in one spike per stimulus, but with higher accuracy (lower jitter) compared to the monaural responses.

2.4.5 IID-sensitive neurons in the DNLL

Although we were mainly concerned with ITD processing in this study, we also tested 106 cells for sensitivity to IIDs by holding the intensity at the contralateral ear constant

and varying the intensity at the ipsilateral ear. Of the 106 cells, 46 (43 %) were sensitive to IIDs, which were all of EI aural type. IID-sensitive EI cells had BFs that ranged from 200 Hz to 5400 Hz (average 2011.5 + 1167 Hz). Sixty one percent (28/46) of the cells had BFs below 2000 Hz and were therefore in the low frequency range.

We measured three features of IID-functions for 45 EI cells. We determined the maximal inhibition as a percent of the peak response to binaural stimulation, the point of 50 % inhibition of the IID-function, and the point of maximal inhibition (figure 2.11A). No significant differences could be found in the IID-characteristics of low and high frequency neurons. Note that our “high frequency” cells had BFs still in the range of frequencies that, under natural conditions in the free field, would only create significant IIDs in the near field (Maki and Furukawa 2005).

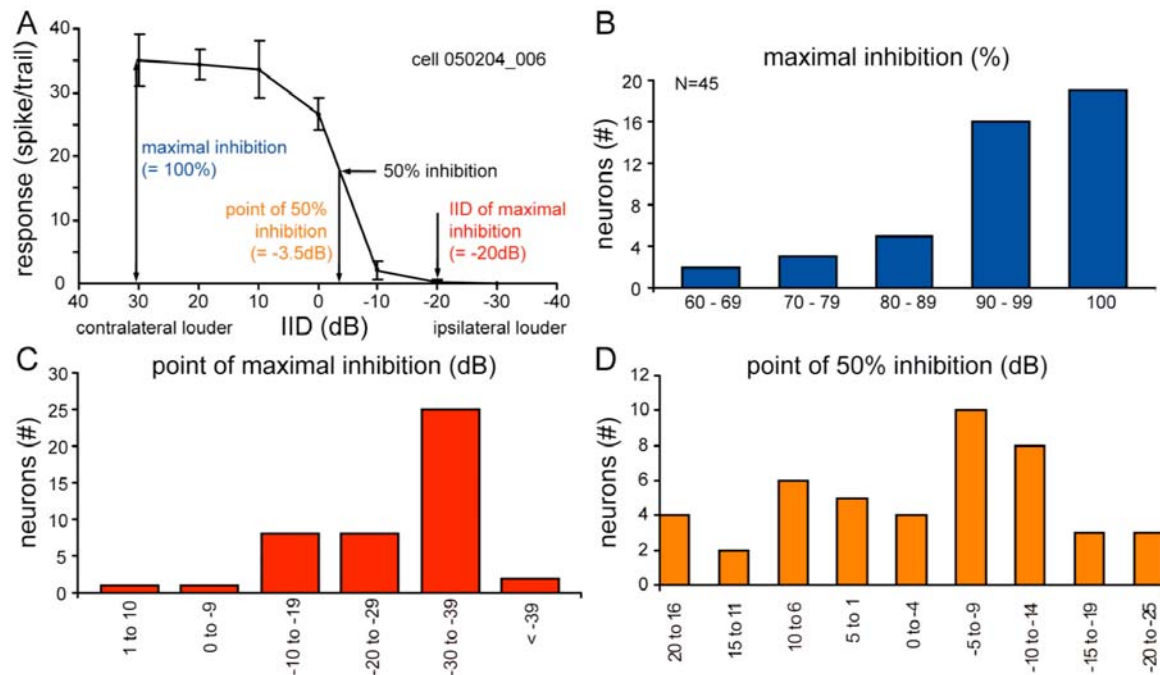


Figure 2.11 A: IID-function of a typical EI neuron. Maximal inhibition occurred when the ipsilateral (inhibitory) stimulus was at least 20 dB more intense than the contralateral (excitatory) stimulus. The response was inhibited by about 50% when the stimulus level at the inhibitory ear was about 3.5 dB more intense, (-3.5dB IID, extrapolated from the IID-function). The contralateral stimulus intensity was kept constant (30 dB above threshold) for all values. BF: 2.400Hz. **B-C:** Quantification of the IID-functions measured. **B:** Degree of maximal suppression (in %). **C:** IID of maximal suppression. In the majority of cells the response could be reduced by at most 100%, preferable at negative IIDs (ipsilateral stimulus more intense). **D:** IIDs of 50% inhibition (IID in dB) showing a rather broad distribution.

More than three-quarter of the neurons (35/45) showed a reduction in the response rate of 90 % or more and 19 of these units (42 %) exhibited a total inhibition of spikes (figure 2.11B). The response of 5 neurons could not be inhibited by more than 80 % by ipsilateral stimulation. Almost three-quarters of the cells (33/45; 73%) showed 50 % points between IIDs of +10 and -14 dB. The peak of the distribution was at slightly negative values as 18 units had 50% points between -5 and -14 dB (figure 2.11C). The average point of 50 % inhibition was at -3 dB (+-10.8 dB). The point of maximal inhibition for the majority of the neurons (25/45; 55.6%) ranged between -30 and -39 dB (figure 2.11D). Two cells were already inhibited maximally for IIDs > -10 dB.

2.4.6 Anatomy

We injected retrograde tracers bilaterally in the DNLL of three animals to evaluate the projections of the SOC to the DNLL. After recording from the DNLL, we injected a mixture of biotin and fluorescein-dextran in the left DNLL and tetramethylrhodamine-dextran in the right DNLL (figure 2.13B). The injections on both sides were made in locations that evoked strong activity to low frequencies. Nevertheless, as almost the whole nucleus was transfected by the injections, we are not able to comment on any frequency dependence in the staining.

We counted the labeled neurons in the SOC of all three animals under the microscope. In all three cases, we found labeled cells in the contralateral DNLL and in various nuclei of the superior olivary complex (SOC) on both sides (figure 2.13A,B; table 2.3). In agreement with previous studies, strong labeling was found in the ipsilateral MSO (174 of 195 labeled MSO neurons). However, we also found a much smaller number of labeled cells in the contralateral MSO (11%, 21/195). Interestingly, there were also a few double-labeled MSO cells (7%, 14/195), suggesting that some MSO cells project bilaterally to the DNLL (figure 2.13C). Large numbers of labeled cells were found in both the contra- and ipsilateral LSOs, with about equal numbers of labeled cells in each LSO (contralateral 44%, 248/641; ipsilateral 56%, 357/641). Note that we focused on the MSO projections, those sections are shown in figure 2.13 that support the notion that MSO projects bilaterally to the DNLL. Since LSO and MSO only partially overlap in the sections, only a small portion of the LSO is shown (under representing the labeling of

LSO cells). As with the MSO (figure 2.13C), some LSO cells were also double labeled (5%, 37/696).

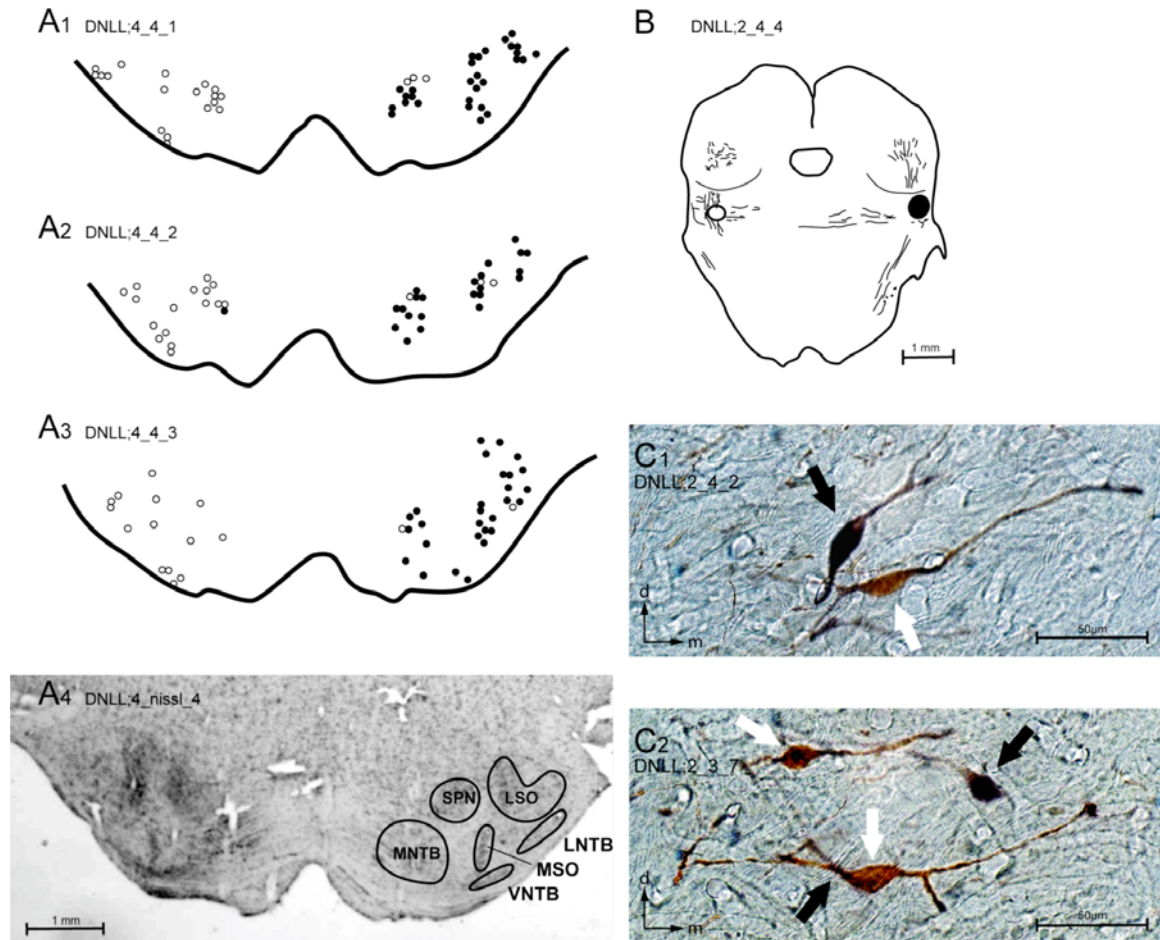


Figure 2.12 Retrograde labeling in the superior olivary complex (SOC) after bilateral tracer injections into the DNLL on both sides. Biotin/flourescein-dextran was injected into the left DNLL, tetramethylrodamine-dextran into the right DNLL. Injection sites are given in **B**. **A1-3**, Biotin (○) and rodamin (●) labeled somata of neurons in the SOC in three consecutive sections (from rostral to caudal). **A4**, Nissl-counterstained section of the SOC. The principal nuclei are outlined. **C1-2**, Retrogradely labeled MSO neurons showing the typical bipolar outline with the dendrites oriented orthogonally to the dorso-ventral axis of the nucleus. In some cases, biotin- (↔) and rodamin-labeled cells (↔) could be found in juxtaposed positions in one MSO. **C2** depicts a double labeled cell (white and black arrow). Quantifications are given in table 3. d = dorsal; m = medial.

Many labeled cells were also located in the nuclei of the trapezoid body with the strongest labeling in the ipsilateral MNTB (95%, 380/401), while 5% of the labeled cells were found in the contralateral MNTB (21/401). All labeled MNTB neurons were principle neurons. Much weaker labeling was seen in the other nuclei of the trapezoid body. 24 labeled cells were found in the lateral nuclei of the trapezoid body (LNTB) at

both sides, 15 cells in the ipsilateral ventral nucleus of the trapezoid body (VNTB) and 41 cells in the ipsilateral superior paraolivary nucleus (SPN).

Table 2.3. Retrograde labeling of SOC neurons. Pooled number of labeled cells in the superior olivary complex after injecting biotin/fluorescein-dextran into the left and tetramethylrhodamine-dextran into the right DNLL of three Mongolian gerbils. LNTB: lateral nucleus of the trapezoid body; LSO: lateral superior olive; MNTB: medial nucleus of the trapezoid body; MSO: medial superior olive; SPN: superior paraolivary nucleus; VNTB: ventral nucleus of the trapezoid body; +++ = heavy labeling (>200 cells); ++ = moderate labeling (>100 cells), + = weak labeling (>10 cells), (+) = few cells labeled (< 10 cells), - = no labeling.

Number of labeled cells			
Nucleus	Ipsilateral	Contralateral	Double
LSO	+++ (357)	+++ (284)	+ (37)
MSO	++ (160)	+ (21)	+ (14)
MNTB	+++ (380)	+ (21)	- (0)
VNTB	+ (15)	- (0)	- (0)
LNTB	+ (13)	+ (11)	- (0)
SPN	+ (41)	(+) (2)	- (0)

2.5 Discussion

We found the majority of low-frequency ITD-sensitive cells to show either peak-type or trough-type characteristics. Peak-type responses were more prevalent than other response types indicating a dominance of pure MSO input characteristics. Some cells' responses, however, seemed to reflect pure LSO inputs and a substantial number of ITD-sensitive cells were neither pure peak-type nor pure trough-type neurons, but rather met criteria for intermediate types. Some neurons, mostly trough- and intermediate-type, showed

secondary peaks in their ITD functions, a feature not reported for cells in the SOC. In two-thirds of the peak-type neurons maximal responses occurred at ITDs that correspond to sound sources in the contralateral sound field. However, a subpopulation of DNLL neurons preferred ipsilateral sounds, a finding that may correspond to the weaker but nevertheless substantial contralateral MSO input found in the tracer experiments. Best ITDs of most peak-type neurons were evoked at ITDs that gerbils would never experience, at least not as direct irradiation. However, the slopes of their ITD functions were steepest in the physiological range of ITDs.

The abundance of low frequency cells we found in the DNLL is consistent with the well developed low frequency hearing capabilities in the Mongolian gerbil (Ryan 1976). It is, however, important to stress that we actively focused on low frequency neurons. Normally, the distribution of BFs in the DNLL reflects the entire audiogram of an animal (mustache bat: Markowitz and Pollak 1993; big brown bat: Covey 1993; free-tailed bat: Burger and Pollak 2001; rat: Bajo et al. 1998; cat: Aitkin et al. 1970) and our unpublished results confirm the existence of a large number of high-frequency neurons in the gerbils DNLL (M Pecka, B Saunier-Rebori, unpublished observation).

Most of the binaural neurons we found were binaurally excited. This is consistent with findings in the DNLL of cats and rabbits which, like gerbils, are well adapted to hear low frequencies (Brugge et al. 1970; Kuwada et al. 2006). In contrast, EI type neurons have been found to dominate in animals that do not hear low frequencies like rats (Bajo et al. 1998; Kelly et al. 1998) and bats (Covey 1993; Markowitz and Pollak 1994).

We found phase-locked sustained discharge patterns to clearly dominate in the gerbil DNLL. These discharge patterns, however, may change depending on the binaural context. Changes of discharge patterns have been suggested to contribute in sound localization (Middlebrooks et al. 1994; Koch and Grothe 2000) but were not systematically investigated in the present study.

2.5.1 Peak- and trough-type DNLL neurons inherit their ITD features from the SOC

The ITD functions of the peak and trough-type neurons we found in DNLL are similar to the ITD functions reported in previous studies for MSO and LSO neurons. As for MSO cells, the maximal responses (i.e. peaks) in peak-type neurons were evoked at the same

ITD across frequency, and thus their phase-frequency plots were linear with a characteristic phase at or around 0.0 cycles (Yin and Chan 1990; Spitzer and Semple 1995; Batra et al. 1997a; Batra et al. 1997b; Brand et al. 2002), indicative of binaural excitation (EE). Similarly, the minimal responses (i.e. troughs) of trough-type neurons were evoked at a common ITD across frequency as has been reported for low frequency LSO cells and as indicative of an interaction of excitation and inhibition (Batra et al. 1997a; Batra et al. 1997b; Joris and Yin 1998; Brand et al. 2002; Tollin and Yin 2005). The peak responses of DNLL trough-type neurons also had linear phase-frequency plots with a characteristic phase at or around 0.5 cycles. In addition to these features, we observed that in most peak-type neurons the maximal responses were evoked by ITDs generated in the contralateral sound field, which is consistent with the strong projections to the DNLL deriving from the ipsilateral SOC (Glendenning et al. 1981; Shneiderman et al. 1988; Oliver 2000). In a small number of peak-type neurons the maximal responses were, however, evoked by sounds that would emanate from the ipsilateral side. This finding can be explained by the contralateral projection we found by tracer injections or by the fact that at least a small number of MSO cells has been found to prefer ipsilaterally leading sounds (Yin and Chan 1990; Batra et al. 1997a). Contralateral projections from the MSO, particularly to the IC, are not uncommon but there is a remarkable species-specific difference concerning their prevalence (for review: Grothe 2000). We also found a substantial number of ipsilateral trough-type neurons, responding minimally to a sound in the ipsilateral sound field, consistent with studies of the SOC of rabbits (Batra et al. 1997a,b). This may reflect differences in the latencies of the excitatory and inhibitory inputs to LSO neurons (Park et al. 1996; Irvine et al. 2001). Such latency differences would not only lead to different positions of troughs, but also to a widespread distribution of the ITDs of maximal inhibition as found for EI DNLL cells in this study and previously shown for LSO neurons (Markowitz and Pollak 1994; Park 1998) All of these features are consistent with the hypothesis that peak and trough-type neurons in the DNLL inherit their basic ITD properties from the MSO and LSO respectively. Kuwada et al. (2006) found a similar distribution of ITD properties in the rabbit DNLL with a large number of neurons showing peak-type sensitivity with maximal responses mostly for stimuli generated in the contralateral sound field. They also found a small number of peak-type neurons that would prefer sounds in the ipsilateral sound field. As in our experiments, the

peak-type and trough-type sensitivity in the rabbit DNLL could not be exclusively explained by the binaural properties of the neurons. Nevertheless, both studies show that most EE neurons show peak-type and most EI neurons trough-type characteristics.

Although many DNLL neurons seem to simply reflect their SOC input it is important to note that DNLL cells receive not only excitatory inputs from LSO and MSO but also glycinergic inputs from the LSO and GABAergic innervation from the opposite DNLL via the commissure of Probst (for review: Schwartz 1992). In addition, our data confirm the strong glycinergic input from the ipsilateral MNTB earlier shown for cats and rats (Glendenning et al. 1981; Spangler et al. 1985; Sommer et al. 1993). It appears likely that projections from the opposite DNLL or from sources other than the MSO and LSO may affect processing in DNLL, although the nature of this influence requires further study. To date two interpretations are available. The first by Kuwada and colleagues (Fitzpatrick and Kuwada 2001; Kuwada et al. 2006) suggest that ITD functions are sharpened along the ascending auditory pathway and that first signs of this sharpening are visible in the DNLL. However, their analysis comes from a dataset that does not account for the best frequency of neurons. As long as ITD functions are simply created by pure EI and EE interactions and as long as these binaural inputs are perfectly matched in terms of their frequency tuning, one could see such a sharpening in the population statistic irrespective of BF. There is, however, abundant evidence for inhibitory input to all MSO neurons (for review: Grothe 2003), and even the simple EI model for LSO function has become questionable (Kil et al. 1995; Magnusson et al. 2005b). Therefore, a quantitative analysis of the ITD width has to account for BF and can not be performed far from BF where small differences in the frequency tuning of the multiple inputs may account for significant changes in the ITD functions due to different cochlear delays (compare: Shamma et al. 1989). Rather, our data suggest that the straightforward processing of ITDs during static tone bursts, in anesthetized animals, is a simple reflection of the processing in the MSO for peak-type neurons and in the LSO for trough-type neurons. Furthermore, our data may suggest a second possible explanation. High frequency DNLL neurons have been shown to inherit their IID-sensitivity from the LSO. What distinguish them from LSO neurons may not be the response to static stimuli but the response in a more complex temporal spatial context. Pollak and colleagues (for review: Pollak et al. 2003) concluded that DNLL neurons may be involved in echo suppression. Alternatively, they

may be involved in processing other dynamic changes in the spatial-temporal domain. Further studies are necessary to elucidate these processes.

2.5.2 ITD tuning of peak-type neurons in the DNLL

The maxima of the ITD functions are clearly outside of the physiologically relevant range for direct sound irradiation for the majority of cells tested. It should be noted, however, that become more complex when reverberations are present. They, via de-correlation, may create larger ITDs. This could be one possible explanation for finding large best ITDs. However, if maximal ITDs matter as such, one would expect the highest density at ITDs that correspondent to the highest behavioral resolution, namely around 0 ITD (Hafter et al. 1975; Makous and Middlebrooks 1990). The fact that only few maxima are found around 0 ITD stipulates a different interpretation. The key issue seems to be that, in contrast to the maxima, the slopes of almost all ITD functions cross the midline (ITD = 0). This finding is consistent with studies in the kangaroo rat and gerbil MSO, the IC in guinea-pigs and cats (Crow et al. 1978; McAlpine et al. 2001; Brand et al. 2002; Hancock and Delgutte 2004) but appears to be in contrast to the recently published study on the rabbit DNLL that describes most peaks to be within the physiological range (Kuwada et al. 2006). However, Kuwada et al. do not distinguish between best ITDs recorded at BF and those recorded at other stimulus frequencies and they do not provide any data concerning the slopes of ITD functions for the stimuli that drive a neuron best (BF). Recording in the low-frequency tail of high frequency neurons (as discussed by Kuwada et al. 2005) might lead to a very different distribution of best ITDs than recording from neurons with low BFs, in particular if BFs and best ITDs are correlated in order to adjust the slopes of ITD functions to the physiologically relevant range. If the response peaks underlies ITD coding rather than slopes it would be difficult to interpret the contribution of low-frequency trough-type neurons (also described for the rabbit DNLL) for which best ITDs change as a function of test frequency. Theoretical considerations suggest that a coding strategy with the maximal slopes close to ITD = 0 would be of considerable advantage at least for low frequencies and, in particular, for small animals because it optimizes the change in firing rate in face of small changes in ITD (Skottun et al. 2001; Harper and McAlpine 2004; Leibold and van Hemmen 2005). Common standards for

dealing with ITD data will be needed to determine if the differences observed in studies of ITD coding are species specific. The existence of different coding strategies would imply that different principles of neuronal representations of ITDs are used by different groups of animals, while similar observations would suggest that all mammals use a common strategy.

This incompleteness of our current knowledge also concerns the role of the inhibitory MSO inputs in ITD processing. There is increasing evidence that the MSO output does not reflect a perfect cross-correlation based on binaural excitation (Batra and Yin 2004). Several anatomical (Clark 1969; Perkins 1973; Cant and Hyson 1992; Kuwabara and Zook 1992) as well as *in vivo* studies proposed an involvement of inhibitory inputs in ITD coding (Moushegian et al. 1964; Goldberg and Brown 1969; Carney and Yin 1989; Spitzer and Semple 1995; Grothe and Park 1998; Brand et al. 2002). Specific roles of synaptic inhibition have been suggested based on *in vitro* recordings (Grothe and Sanes 1993; Grothe and Sanes 1994; Magnusson et al. 2005a) and modeling (Han and Colburn 1993; Batra et al. 1997a; Brand et al. 2002; Zhou et al. 2005). The model by Brand et al (2002) suggests fast contralateral inhibition preceding excitation driven by the same ear that delays the effective contralateral EPSPs, to be an important element in the ITD encoding neuronal circuit in the MSO (Brand et al. 2002; Grothe 2003). However, an alternative model by Zhou and colleagues (Zhou et al. 2005) assumes a comparatively slow inhibition but still reliably simulates the effects observed during blockade of inhibition in the MSO (Brand et al. 2002). The fact that we found the first spike of the response to be as sensitive to ITDs as the ongoing component speaks for an immediate and fast effect of the inhibition, but direct evidence of a fast preceding inhibition at the MSO is lacking.

Carney and Yin (1989) showed a suppressive effect they called “early inhibition” which preceded contralateral excitation in ITD-sensitive cells in the IC in response to clicks. The time courses of suppression they found were similar to the effects we obtained in the DNLL by using chirp stimuli. While Carney and Yin hypothesized that preceding inhibition could be generated in the IC, our results show that this inhibition is already present below the midbrain. The fact that both the IC and the DNLL receive prominent inputs from the MSO supports the idea that preceding inhibition is already created at the MSO, the initial site of ITD processing.

One problem in interpreting the time course of the apparent inhibition elicited by broadband stimuli like clicks or chirps is the possible involvement of cochlear delays. Because of the time course of the traveling wave in the cochlea, high frequencies elicit earlier responses than low frequencies (Ruggero et al. 1992). Therefore, a mismatch in the frequency tuning of MSO inputs could cause a precedence of one of the inputs due to shorter cochlear delays (compare: (Shamma et al. 1989). The use of downward frequency modulated chirps in the present study might even enhance such effects. However, a comparison of ITD functions measured with pure tones and noise in the MSO itself revealed similar ITD tuning for both stimuli (Yin and Chan 1990), a finding that can hardly be explained by cochlear delays.

2.5.3 Intermediate-type ITD sensitivity

It is unclear to what extent intermediate type ITD sensitivity in DNLL is a result of interactions of multiple inputs and to what extent it is imposed by SOC inputs. Spitzer and Semple (1995) as well as Batra and colleagues (Batra et al. 1997a, b) found intermediate type neurons in the SOC of gerbils and rabbits, respectively. They might be a result of convergence of at least three inputs (Batra et al. 1997b). Similarly, intermediate-type neurons have been found at higher stations like the IC (Yin and Kuwada 1983b; McAlpine et al. 1998; Fitzpatrick and Kuwada 2001) but there is evidence that convergence at the level of the IC itself can account for intermediate type ITD sensitivity at least in some neurons (McAlpine et al. 1998). Our present study was not designed to, and therefore cannot distinguish between the two possible alternatives.

The feature that is likely to be constructed in the DNLL, and not inherited, is the occurrence of secondary peaks that we observed in many ipsilateral peak-type and intermediate peak and trough-type neurons. A simple explanation for this would be that these cells received inputs from several cells that had the same best frequency, but the CD of at least one of the inputs was slightly different from the CD of the other inputs or even at the opposite side (via contralateral MSO inputs) and, therefore, caused a second peak in the ITD function. Such second peaks have not been seen in the ITD functions of SOC neurons and thus are almost surely a property created in the DNLL.

In summary, it appears that pure peak and trough-type neurons express ITD sensitivity and other properties that are nearly identical to those seen in the MSO and LSO. This suggests that peak and trough-type neurons in the DNLL may be appropriate substitutes for the SOC, although the connections from other sources suggest the processing may be different in these neurons with stimuli more complex than tones, like multiple or dynamic stimuli.

3 Spectral composition of concurrent noise affects neuronal sensitivity to interaural time differences of tones in the dorsal nucleus of the lateral lemniscus

Siveke I, Leibold C, and Grothe B

Published in *Journal of Neurophysiology* doi: 10.1152/jn.00275.2007, 2007

3.1 Abstract

We are regularly exposed to several concurrent sounds, producing a mixture of binaural cues. The neuronal mechanisms underlying the localization of concurrent sounds are not well understood. The major binaural cues for localizing low-frequency sounds in the horizontal plane are interaural time differences (ITDs). Auditory brainstem neurons encode ITDs by firing maximally in response to “favorable” ITDs and weakly or not at all in response to “unfavorable” ITDs. We recorded from ITD-sensitive neurons in the dorsal nucleus of the lateral lemniscus (DNLL) while presenting pure tones at different ITDs embedded in noise. We found that increasing levels of concurrent white noise suppressed the maximal response rate to tones with favorable ITDs and slightly enhanced the response rate to tones with unfavorable ITDs. Nevertheless, most of the neurons maintained ITD sensitivity to tones even for noise intensities equal to that of the tone. Using concurrent noise with a spectral composition in which the neuron’s excitatory frequencies are omitted reduced the maximal response similar as obtained with concurrent white noise. This finding indicates that the decrease of the maximal rate is mediated by suppressive cross-frequency interactions, which we also observed during monaural stimulation with additional white noise. In contrast, the enhancement of the firing rate to tones at unfavorable ITD might be due to early binaural interactions (e.g. at the level of the superior olive). A simple simulation corroborates this interpretation.

Taken together, these findings suggest that the spectral composition of a concurrent sound strongly influences the spatial processing of ITD-sensitive DNLL neurons.

3.2 Introduction

In natural environments, sound stimuli are often complex and originate from a number of different sources. Obviously, our binaural auditory system is able to extract the relevant cues representing the positions of the sound sources amidst this complexity. Thus we can localize each of these sources and detect or segregate them based, among other cues, on spatial information (Culling and Summerfield 1995; Darwin and Hukin 1997; Drennan et al. 2003). A step towards the understanding of how concurrent sounds are processed is to investigate the perception of tones in the presence of a noise source. The detection and segregation of tones from background noise has been studied psychophysically (Blauert 1997) and, furthermore, could be correlated to electrophysiological results (Langford 1984; Caird et al. 1991; McAlpine et al. 1996; Jiang et al. 1997a,b; Palmer et al. 1999; Lane and Delgutte 2005). But most of the work on sound localization has been performed for single sources and the localization of tones in background noise has not been thoroughly investigated. The small number of psychophysical studies showed that the capability to localize sounds in noise strongly depends on the location, the level, and the spectral components of the noise source (Cohen and Koehnke 1982; Stern et al. 1983; Good and Gilkey 1996). However, the neuronal mechanisms underlying the localization of tones in background noise are not well understood.

In this study, we focused on the neuronal mechanisms underlying the localization of low-frequency tones (< 2000 Hz) in the presence of localizable noise. The most important spatial cue for low-frequency sounds in the horizontal plane is the difference in the arrival time of sound at the two ears, the interaural time difference (ITD) (Rayleigh 1907). ITDs are processed by coincidence-detector neurons in the medial (MSO) and lateral superior olive (LSO) (Goldberg and Brown 1969; Yin and Chan 1990; Tollin and Yin 2005). These neurons receive precisely timed monaural inputs from both ears. Both the strength as well as the exact timing of the monaural inputs determines the response rates of these coincidence-detector neurons. MSO and LSO neurons project to the dorsal

nucleus of the lateral lemniscus (DNLL) (for review: Oliver and Huerta 1992). Many DNLL neurons faithfully reflect the ITD sensitivity of their MSO and LSO inputs (Seidl and Grothe 2005; Siveke et al. 2006; Kuwada et al. 2006). Therefore we used the population of ITD-sensitive DNLL neurons as an approach to studying binaural processing at the level of the coincidence-detectors.

We recorded from ITD-sensitive neurons in the DNLL of the anesthetized gerbil and found complex interaction between pure tones and noise. Furthermore the findings suggest that the spectral composition of a concurrent sound influences the processing of ITD-sensitive neurons.

3.3 Methods

Single neurons (N = 111) in the DNLL were recorded from Mongolian gerbils (*Meriones unguiculatus*) of both sexes two to three months of age. All experiments were approved according to the German Tierschutzgesetz (AZ 55.2-1-54-2531-57-05).

The detailed methods in terms of surgical preparation, acoustic stimulus delivery, stimulus calibration, and recording techniques have been described previously (Siveke et al. 2006) and will only be described briefly here.

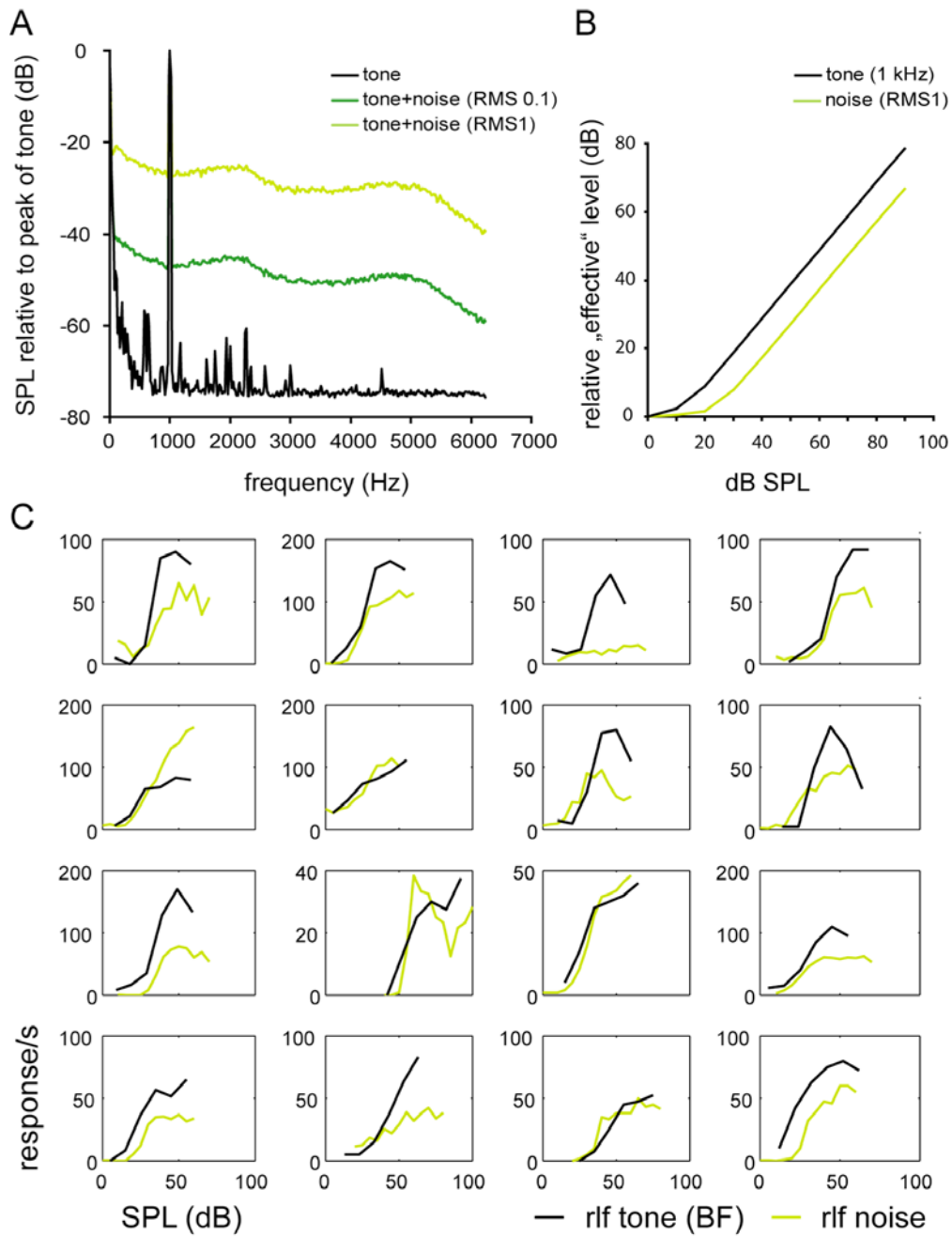
3.3.1 Animal preparation, recording procedures

The animals were anaesthetized by a physiological NaCl-solution containing ketamine (20 %) and xylazine (2 %). During recordings, the animal was placed in a sound-attenuated chamber and mounted in a custom-made stereotaxic instrument allowing reproducible positioning of the skull (Schuller et al. 1986). Ear-molds were attached to the head allowing the insertion and fixation of earphones and probe tube microphones. For electrode penetrations, a small hole was cut into the skull and the dura mater was removed extending 1.3 - 2.6 mm lateral to the midline and 0.5 - 0.8 mm caudal of the interaural axis. Micromanipulators were used to position the recording electrode. For some recordings the recording electrode was tilted 10° or 5° laterally.

Single-cell responses were recorded extracellularly using glass electrodes filled with 1M NaCl (~10 M Ω). The recording electrode was advanced under remote control, using a motorized micromanipulator (Digimatic, Mitutoyo, Neuss, Germany) and a piezodriven (Inchworm controller 8200, EXFO Burleigh Products Group Inc, USA). The amplified and filtered action potentials were fed into the computer via an A/D-converter (RP2-1, TDT-Tucker Davis Technologies, USA). Clear isolation of action potentials from a single neuron (signal to noise ratio > 5; see waveform of the recorded spikes in figure 3.3, 3.4, and 3.5) was guaranteed by visual inspection (stable size and shape) on a spike-triggered oscilloscope and by offline spike cluster analysis (Brainware, Jan Schnupp, TDT). Stimuli were generated at 50 kHz sampling rate by TDT System III. Digitally generated stimuli were converted to analog signals (RP2, TDT), attenuated (PA5, TDT) and delivered to the ear phones (Sony, Stereo Dynamic Earphones, MDR-EX70LP).

3.3.2 Stimuli

Stimuli were presented randomized with a repetition rate of 2 Hz. All binaural stimuli were applied with an interaural intensity difference of 0 dB. Unless indicated otherwise, stimulus duration was 200 ms plus 5 ms rise and fall times of a squared cosine. As search stimulus we used uncorrelated binaural noise bursts. Using pure tones we first determined the neuron's characteristic frequency (CF) and absolute threshold audio-visually to set the stimulus parameters subsequently controlled by the computer. The frequency that elicited responses at the lowest sound intensity was defined as CF, the lowest sound intensity evoking a noticeable response at CF as threshold. For all neurons both CF and threshold were later confirmed by a careful offline analysis of the frequency versus level response areas (9 frequencies, step size CF/5, 10 dB steps). For a subpopulation of neurons, we additionally measured the response threshold for noise stimulation by rate-level-functions (supplementary figure). In some of these neurons the response to noise showed an increase already at the threshold level for tones at BF with the same RMS.



Supplementary figure A: Power spectrum of stimuli used: tone alone, tone with noise (RMS 20dB below RMS of tone) and tone with noise (same RMS as tone). **B:** The “effective” level of the tone and noise stimuli with the same RMS in the most relevant frequency band (500-1500 Hz). A and B are measured using a FFT Network analyzer (Stanford Research System, USA). **C:** Rate-level functions of a randomly chosen subpopulation of neurons tested with either tone alone or noise alone.

Sensitivity to ITDs was assessed by measuring noise delay functions (NDFs) and tone delay functions (TDFs) 20 dB above threshold to pure tones at CF (for details concerning the relationship of levels for tone and noise stimulation see supplementary figure). The

frequency, which evoked the maximal response at a given neuron's best ITD, we refer to as "best frequency" (BF). For NDFs and TDFs we presented different ITDs over a range equivalent to ≥ 2 cycles of BF (step size BF/10). ITDs with the contralateral stimulus leading were defined as positive, ITDs with the ipsilateral stimulus leading as negative. TDFs were tested for five stimulus frequencies around BF. Each stimulus was repeated at least three times. NDFs were determined from 16 iterations. To obtain best ITDs the position of the peaks of the NDF or TDF at BF were estimated and used to compute the signals for further experiments.

For the first set of tone-in-noise experiments (used for figures 3.1 to 3.4) we presented a 100 ms tone at BF while varying the ITD. This stimulus was presented alone or embedded in a 250 ms Gaussian noise starting 10 ms before the tone. Assuming a neuronal delay of less than 20 ms to the DNLL, we defined and analyzed the neuronal response to the tone in the time window from 20 ms to 120 ms after onset of the tone. The binaurally correlated noise was varied in amplitude (noise level 20 dB below tone level and noise level equal to tone level) and ITD. The noise stimuli were applied with two different ITDs, 0 ms and the best ITD. In most of the neurons ($n = 61$) best ITDs were derived from the NDF. For 19 neurons the best ITDs were derived from the TDF. For a subgroup of neurons we additionally tested the monaural responses to the same tone-in-noise stimuli presented either ipsilaterally or contralaterally.

For the second set of tone-in-noise experiments (used for figure 3.5) we constructed neuron-specific spectrally adjusted "tuned" and "notched" noise stimuli. These were created online using the computer program *Matlab* (The MathWorks Inc., Natick, MA, USA). Tuned noise contained the frequency domain of the excitatory tuning curve, whereas notched noise was constructed as the difference between white noise and tuned noise, hence, reflecting the spectral areas outside the excitatory tuning curve of a given neuron. More specifically, we again determined response areas of neurons with eight repetitions of frequency versus level stimulations using pure tones at the best ITD at BF. From these frequency-versus-level response areas we determined the thresholds for all stimulated frequencies. The thresholds were defined as the intensity, which evoked 20 % of the maximal firing rate plus spontaneous activity following Sutter et al. (1999). For frequencies other than the stimulated ones, thresholds were obtained by linear interpolations (figure 3.5B). The resulting threshold curve was used as a weighting

function for the spectral content of notched and tuned noise. For notched noise spectral power was depressed proportional to this weighting function, whereas for tuned noise spectral power was depressed proportional to the maximal level minus the threshold curve. Therefore the weighting function, i.e. the threshold curve, was constructed such that the neurons still weakly responded to the notched noise. The overall sound intensities (*root-mean-square value, RMS*) of the three noise stimuli were chosen equal to the intensity (RMS) of the pure tone stimulus (20 dB above threshold). In contrast to the first set of tone-in-noise experiments, in the second set of experiments (used for figure 3.5) noise and tone were played in an overlapping sequence. The three noise stimuli were presented for 200 ms at the best ITD of the NDF. After 100 ms a 200 ms BF tone was added with varying ITD. The resulting stimulus sequence is: noise alone for 100 ms, tone and noise for 100 ms, and tone alone for 100 ms. To avoid overlapping of the responses, again assuming a neuronal delay of 20 ms, the time windows for the different sets of data were set as follows: the response to noise alone was derived for the interval from 20 to 100 ms, the response to tone and noise from 120 to 200 ms, and the response to the tone alone from 220 to 300 ms after stimulus onset. All tone and noise stimulus combinations were presented 10 to 20 times.

3.3.3 Data analysis

In the whole study all averaged quantities are denoted as mean \pm standard error of the mean (SEM). Unless mentioned otherwise, significance was always determined by the Student's two-tailed paired *t*-test with a level of significance $P < 0.05$.

Monaural tone and noise were defined as “excitatory” if the firing rate was significantly increased and as “inhibitory” if the firing rate was significantly decreased when compared to the spontaneous rate. The vector strengths of the monaural and binaural responses were calculated as described by Goldberg and Brown (1969).

Neurons were classified as ITD-sensitive if the Rayleigh test (Batschelet 1981) showed a significant ($P < 0.001$) deviation from a uniform distribution of response rates. The neuron's mean interaural phase, eliciting the maximal spike rate, was calculated for each test frequency via a vector analysis following Yin and Kuwada (1983b). We calculated the characteristic phase (CP) of the neurons using mean interaural phase versus frequency

plots weighting each data point by the vector strength and the mean response (Kuwada et al. 1987; Spitzer and Semple 1995). Peak-type neurons, described for the MSO, fire maximally at a characteristic ITD for which coincidence occurs. Trough-type neurons, described for the LSO, encode ITDs by being maximally suppressed at the ITD at which coincidence accrues. We defined peak-type neurons by an absolute CP of 0 to 0.25 cycles, trough-type neurons by an absolute CP of 0.25 to 0.5 cycles.

ITD sensitivity of a single neuron is defined as the ability to respond with a different firing rate to different ITDs. Therefore we additionally measured the ITD sensitivity of the neurons to tones in the presence of noise via the standard separation (D) of the response to the peak (R_p) and the trough (R_T) of the TDF (Sakitt 1973). We used a modified version of the standard separation, described by Jiang et al. (1997a). This index gives a simple interpretation of discrimination that is independent of any assumptions about the underlying distributions. The calculation of D is described in the following equation:

$$D = \frac{R_p - R_t}{\sqrt{SD(R_p) \times SD(R_T)}} .$$

$SD(R_p)$ and $SD(R_T)$ denote the SDs of the respective response distributions. Random rating would produce $D = 0$ and perfect discrimination would produce an infinite D. We defined neurons as sensitive to ITDs, if D had a value above 2 (which is a quite conservative estimation).

Neuronal responses to combined tone-in-noise stimuli were classified as proposed by Jiang et al. (1997b) (see figure 3.7, schematic drawings). They presented correlated noise (ITD = 0, constant level) and measured the response rates to additional pure tones (signal) with increasing level. The signals were either presented with an ITD of zero (S_o) or phase inverted at one ear (S_π). If at some signal level the discharge rate to a combined tone-in-noise stimulus became one standard separation (D) larger than the discharge rate to noise alone, the neuron was classified as P-type (positive D-value). Conversely, a neuron was classified as N-type (negative D-value) if there a signal level existed at which the discharge rate to the tone-in-noise stimulus became lower than that to the noise alone. Since there are two stimulus conditions (S_o , S_π), each neuron was characterized by two letters (PP, PN, NP, NN). The first letter denoted the change in response for the signal S_o , the second one referred to S_π . In contrast to Jiang et al. (1997b) in the present study we

used stimuli with varying noise levels and a constant tone level. Thus we could not calculate standard separation as a function of the level of the pure tone. Instead we classified the neuron as P(N)-type, with respect to a significant increase or decrease in firing rate for the two tested noise levels independently (noise RMS equal to tone RMS and 20 dB below; ITD = 0). For all tested neurons, changes in firing rate were significant ($P < 0.05$).

3.3.4 Binaural correlation and model

The acoustic signals arriving at the ipsi- and contralateral ear were presented to the auditory nerve (AN) model by Tan and Carney (2003), which requires the characteristic frequency of the nerve fiber as a single parameter. In all simulations shown in this paper this characteristic frequency was chosen to be 1 kHz. The output of this model provides a firing probability per unit time. The resulting model outputs of the ipsi- and contralateral fibers are denoted by $a_{\text{ipsi}}(t)$ and $a_{\text{contra}}(t)$, respectively. These quantities were interpreted as proportional to the presynaptic input rates to a coincidence-detector neuron in the superior olivary complex.

To quantify the amount of binaural correlations that are present in these input rates for different ITDs, we calculated their coefficient r of correlation as:

$$r = \frac{\langle (a_{\text{ipsi}} - \langle a_{\text{ipsi}} \rangle)(a_{\text{contra}} - \langle a_{\text{contra}} \rangle) \rangle}{\sqrt{\text{var}(a_{\text{ipsi}}) \cdot \text{var}(a_{\text{contra}})}},$$

in which

$$\langle a \rangle = \frac{1}{T} \int_0^T dt a(t)$$

denotes averaging over the duration T of the stimulus (here $T = 100$ ms) and var is the variance over time. As a next step, to understand the subthreshold temporal summation of binaural synaptic inputs, we also assessed the temporal average $\langle (a_{\text{ipsi}} + a_{\text{contra}})^2 \rangle$ of the squared binaural synaptic input rates (cf. Batra et al. 1997a), figure 12 A).

To also study subthreshold neuronal discharge rate we simulated two neuron models. Both were based on a simple integrate-and-fire mechanism (Gerstner and van Hemmen

1994) at which the ipsi- and contralateral input rates a_{ipsi} and a_{contra} are convolved with an epsp kernel:

$$\kappa(t) = \left(e^{-t/\tau_1} - e^{-t/\tau_2} \right) \quad \text{for } t \geq 0, \tau_1 > \tau_2$$

and $\kappa(t) = 0$ for $t < 0$ to yield a mean membrane potential:

$$v(t) = \int_{t_0}^t dx \kappa(t-x) \left(a_{\text{ipsi}}(x) + a_{\text{contra}}(x-\Delta) \right).$$

Since synaptic inputs are of stochastic nature, we derived a noisy voltage trace by adding a Gaussian random variable η to the mean input rates $a_{\text{ipsi/contra}}$. The variance of η (in a small time interval of length dt) was set to a value of $a(t)dt/N$ as it would be expected from N independent AN fibers per ear firing with Poisson statistics. Here, we assumed $N = 200$. Each time the noisy membrane potential hit a threshold (θ), the neuron generates an action potential and the voltage is reset to its resting potential $v = 0$. To limit the instantaneous firing rate to 200 Hz, we additionally introduced a refractory time of 5 ms. The shape κ of the excitatory postsynaptic potential was modeled using an exponential decay time τ_1 of 200 μs and an exponential rise time τ_2 of 100 μs (compare: Scott et al. 2005). The contralateral input was delayed by $\Delta = 150 \mu\text{s}$. This model we refer to as Jeffress-type model, since it incorporated a combination of coincidence detection and temporal delay (Jeffress 1948). The firing threshold (θ) of this neuron was adjusted to obtain a mean maximal firing rate of about 60 Hz for pure tone stimulation. In the second neuron model, we did not use a contralateral temporal delay, i.e., $\Delta = 0$. Instead, we added phase-locked contralaterally driven inhibition which is able to delay the effective contralateral excitation, if it arrives shortly before this excitation (Brand et al. 2002). The inhibitory kinetics was modeled with the same kernel κ as the excitation except that it was multiplied with a constant factor $g = 2/3$. To obtain the same best ITD as for the Jeffress-type model, the contralateral inhibition was modeled to arrive $\Lambda = 150 \mu\text{s}$ before excitation (Leibold and van Hemmen 2005). The noise in the inhibitory inputs was determined by assuming $N = 100$. The resulting subthreshold dynamics of the membrane potential v is thus expressed by the convolution integral:

$$v(t) = \int_{t_0}^t dx \kappa(t-x) \left(a_{\text{ipsi}}(x) + a_{\text{contra}}(x) - g a_{\text{contra}}(x+\Lambda) \right).$$

The firing threshold θ was adjusted to obtain similar firing rates as for the previous model. All TDFs of the spiking neuron models shown in figure 3.6 were derived from 100 repetitions of the auditory stimulus.

3.4 Results

Data presented here were derived from single cell recordings from 111 ITD-sensitive DNLL neurons. We first studied the effect of different levels and ITDs of white noise on the response to tones presented at different ITDs ($N = 80$). To differentiate between effects arising from monaural processes and those caused by binaural interactions at the coincidence-detectors in MSO and LSO, we also investigated the monaural responses to tones in noise ($N = 32$) as well as the binaural responses to tones with spectrally adjusted noise ($N = 31$). Since these recordings suggested that lateral frequency integration decreases the response to tones, we compared our experimental data for narrow band noise stimuli with numerical simulations of a model of a coincidence-detector neuron.

3.4.1 Effects of binaural noise on tone delay functions

ITD-sensitive neurons show a distinctive maximum and minimum in their response to a favorable and an unfavorable ITD, respectively. To study the effects of noise on the ITD processing of pure tones, we focused on these two prominent response features evoked by the favorable and the unfavorable ITD. We used white noise at two different levels: one with the same level (RMS) as the tone and the other one 20 dB lower, corresponding to the threshold level for tones at BF.

Adding this noise to tones at favorable and unfavorable ITDs affected the maximal and minimal responses in opposite directions (figure 3.1). Noise suppressed the response to the favorable ITD (figure 3.1A) but slightly increased the response to the unfavorable ITD of the pure tone (figure 3.1B). Both effects became stronger with an increasing level of noise. All of these effects were statistically significant ($P < 0.001$) for the higher level of noise. For the lower level of noise the decrease of the response to the favorable ITD of the pure tone with noise at best ITD (figure 3.1A2) was significant ($P < 0.001$). The

change of the TDFs was measured for two different ITDs of the noise stimulus. If the ITD of the noise (noise level = tone level) was set to 0 μs , which evoked an intermediate firing rate for most of the neurons, the peak response was decreased to $46 \pm 5.9\%$ ($P < 0.001$) of the peak response to pure tone stimulations (117 ± 7.4 spikes/s) (figure 3.1A2, left). The trough response was significantly increased from $2.7 \pm 0.5\%$ to $4.7 \pm 0.8\%$ of the peak response to pure tone stimulation ($P = 0.044$) (figure 3.1B2, left). If the ITD of the noise (noise level = tone level) was set to the best ITD, the average peak responses were reduced to about $62 \pm 6.6\%$ ($P < 0.001$) (figure 3.1A2, right) and the trough response statistically significantly increased from $2 \pm 0.5\%$ to $6.1 \pm 1\%$ of the peak response to the pure tone stimulation ($P < 0.001$) (figure 3.1B2, right).

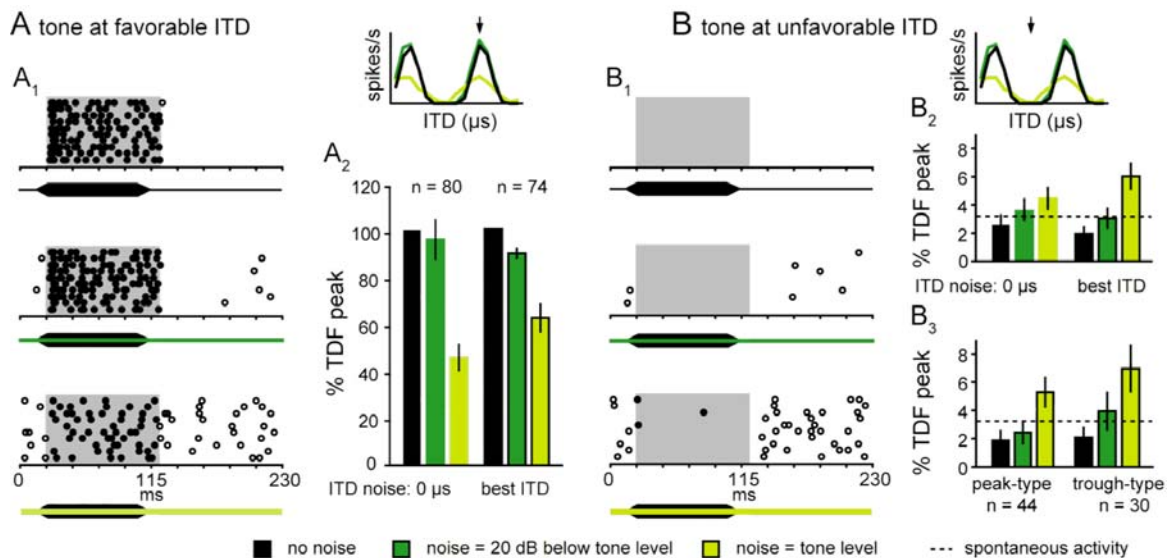


Figure 3.1 Effects of increasing the level of white noise at 0 or best ITD on the response to tones at favorable (A) and unfavorable (B) ITD. **A1, B1:** Raster plots of a single-unit response to tones at favorable (+420 μs) and unfavorable ITD (-280 μs) with increasing noise at best ITD (neuron: 050106_07; BF = 750 Hz). Analysis windows with a standard delay of 10 ms after stimulus onset are displayed by the light gray area underlying the raster plots. The presentation of the tone is indicated by the black bar, the noise level by the color-coded line below the plots. **A2, B2-3:** Summarize population statistics. The maximal and minimal firing rates of the TDFs with noise are normalized to neuron's maximal response of the TDF and then averaged over the population. **B3:** minimal average firing rate to tones in noise at best ITD are shown separately for the peak and trough types. All of these effects were statistically significant ($P < 0.001$) for the higher level of noise. For the lower level of noise the decrease of the response to the favorable ITD of the pure tone with noise at best ITD (figure 3.1A2) was significant ($P < 0.001$). Error bars = standard error of the mean (SEM).

The effects of the noise on the firing rate to tones at favorable and unfavorable ITDs did not differ between peak- and trough-type ITD-sensitive neurons. The average responses to unfavorable ITDs for both types are shown in figure 3.1B3.

To investigate how the noise-induced changes of peak and trough firing rates influence ITD sensitivity of the neurons, we calculated the standard separation (D) of the responses to the tone at favorable and unfavorable ITD (figure 3.2, see methods). Even for large D -values, a considerable fraction of the neurons remains ITD-sensitive under all noise conditions tested (figure 3.2A). The percentage of ITD-sensitive neurons was a decreasing function of noise level, but was rather independent of the ITD of the noise (figure 3.2A). If we applied a conservative separation threshold of $D > 2$ we found that 96 % (77/80) of the neurons remained ITD-sensitive to tones when the noise was presented at ITD = 0 and 97 % (72/74) of the neurons remained sensitive for noise presented at best ITD. These fractions were obtained presenting additional noise with intensities 20 dB below the tone level. If the noise was presented at the same level as the tones the fractions were reduced to 71 % (57/80) for noise with ITD = 0 and 74 % (55/74) for noise presented at best ITD (figure 3.2). Hence, the ITD sensitivity of DNLL neurons to tones showed a high robustness against additional noise.

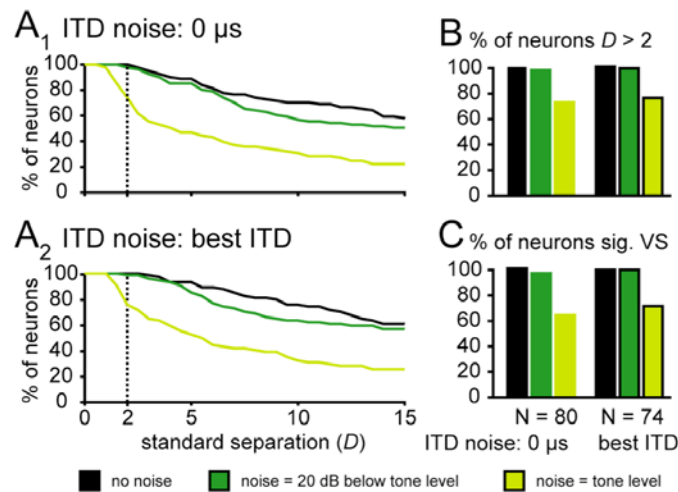


Figure 3.2 Effect of increasing white noise on the ITD sensitivity of the neurons. ITD sensitivity is measured by the standard separation D of the response to tones at favorable and unfavorable ITD (A, B). **A**: The percentage of neurons defined as ITD sensitive versus D -value. The effects of increasing noise were similar for noise at 0 μ s ITD (A1) or at best ITD (A2). **B**: Percentage of neurons classified as ITD-sensitive with $D > 1.5$. **C**: Percentage of neurons with significant vector strength (VS).

From a different point of view, the pure tone reduces or enhances the response to white noise. Therefore in addition to the question of how noise effects the localization of pure tones, we also addressed how the location of pure tones affected the response to noise. This was quantified through the differences between the average response rate to the noise alone and the response rate with additional tones at favorable or unfavorable ITDs. We refer to these differences as tone-induced reduction and tone-induced enhancement of the response to noise (figure 3.3A). On average with increasing noise level the response to noise increased ($P < 0.001$) (figure 3.3B) but the tone-induced enhancement significantly decreased ($P < 0.001$). Furthermore, with increasing noise levels, the increase of the response to noise alone was much stronger (figure 3.3B) than the increase of the response to the combination of noise and tones at unfavorable ITD (figure 3.1B).

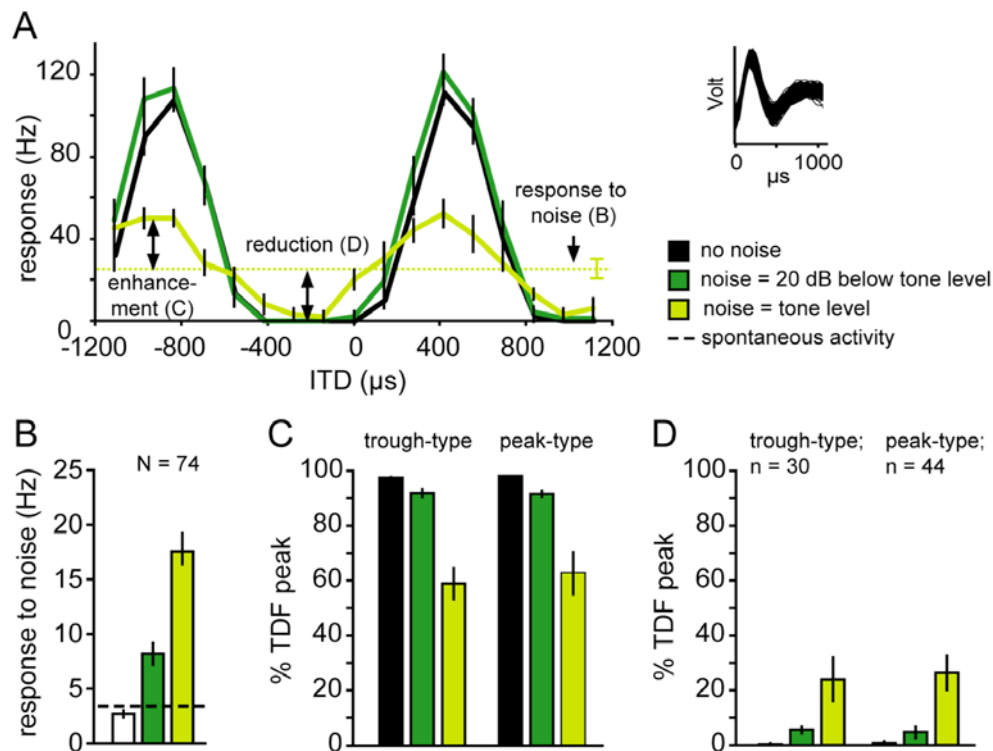


Figure 3.3 Effects of tones on the response to white noise with increasing level. **A**: Exemplary firing rates of a single-unit and calculation of the three measures from TDFs with increasing noise level (neuron: 151205_05; BF = 700 Hz; the shapes of the recorded action potentials on the right demonstrate a single cell recording). **B-D**: Summarized population statistics. **B**: The response to noise at best ITD increased with increasing level. **C**: The enhancement of the response to noise induced by tones at favorable ITD decreased. **D**: The reduction of the response to noise induced by tones at unfavorable ITD increased with increasing noise level. All described changes were significant for both levels of noise. Error bars = standard error of the mean (SEM).

Therefore in contrast to the tone-induced enhancement the tone-induced reduction got stronger with increasing noise level ($P < 0.001$) (figure 3.3C). The effects of tones on the responses to noise were independent of whether the neuron was a peak- or a trough-type neuron (compare figure 3.3C and 3.3D left and right). All described changes shown in figure 3.3 were significant for both levels of noise.

To conclude, white noise presented at levels up to equal that of the tone decreased the maximal response to tones at favorable ITDs, but the minimal response at the unfavorable ITD slightly increased. The strong tone-induced reduction of the response to noise accounted for the robustness of the ITD sensitivity against additional noise.

3.4.2 Monaural contributions to the noise-induced effects on tone delay functions

To distinguish which of the noise-induced effects on TDFs are due to binaural interactions at the level of the coincidence-detectors in the superior olivary complex and which can be explained independently of binaural interactions we also recorded responses of DNLL neurons to monaural tones in monaural noise. The neuronal discharge rate (see raster plots figure 3.4A left panel) evoked by monaural excitation was generally lower than that to binaural stimulation at the best ITD of the neurons. Nevertheless a considerable number of the ITD-sensitive DNLL neurons were significantly excited by contra- (27/32; 84 %) or ipsilaterally (19/32; 59 %) applied pure tones (example shown in figure 3.4A, average response in figure 3.4B, black bars). Adding monaural noise to the monaurally presented tones on average decreased the responses for both, ipsi- ($P < 0.001$) and for contralateral stimulations ($P = 0.055$) (figure 3.4B). The temporal structure of the firing pattern was quantified by the vector strength of phase locking to the pure tone stimulus. The vector strength was slightly lower for monaural as for binaural stimulations (see phase plots figure 3.4A, right panel). Moreover, phase locking slightly decreased by adding noise, both in monaural and binaural stimulations (figure 3.4C). The relative decrease of monaural response rates was similar to the noise-induced decrease of the responses at favorable ITDs obtained with binaural stimuli. Therefore, we hypothesize that the noise-induced reduction of the binaural response to tones at favorable ITDs has the same origin as the decrease of the monaurally evoked firing rates. On the other hand, the small but significant increase of the binaural response to tones with unfavorable ITD

with increasing noise level could not be attributed to any of the monaural effects. Thus the tone-induced reduction of noise responses was likely to originate from binaural interaction at the coincidence-detectors at the level of the superior olivary complex.

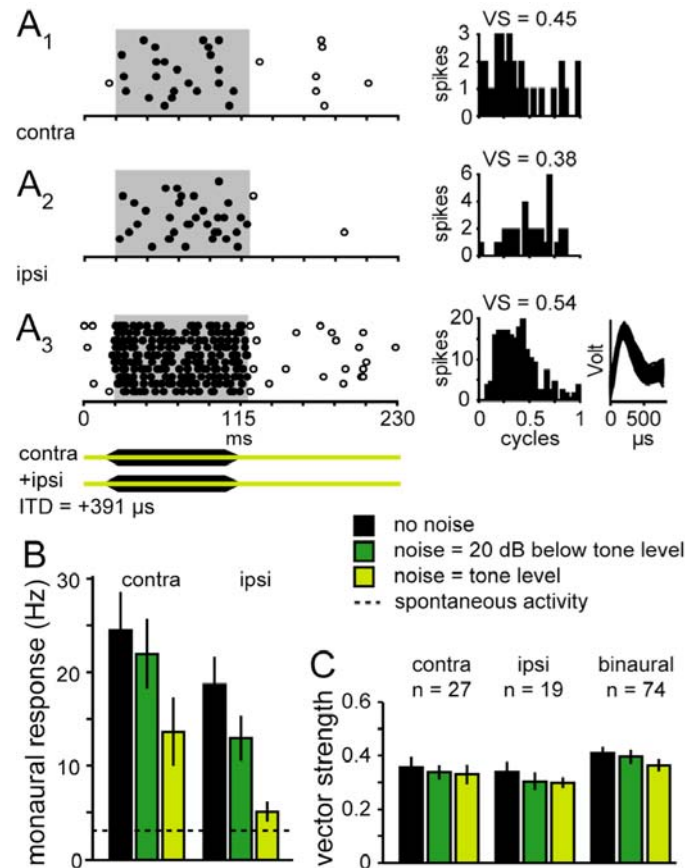


Figure 3.4 Monaural and binaural responses to tone in white noise. **A:** Raster plots and period histograms of single-unit responses to contralateral (**A1**), ipsilateral (**A2**), and binaural (**A3**) stimulations with tone and noise presented at the same time. The shapes of the recorded action potentials on the right demonstrate a single cell recording (neuron: 151205_02; BF = 800 Hz). The noise level was 20 dB below the tone level. **B-C:** Summarized population statistics. **B:** Average contralateral and ipsilateral responses to tone and noise stimulation decreases with increasing noise level. **C:** The average vector strength (VS) of the monaural and binaural responses is slightly decreased by additional noise. Error bars = standard error of the mean (SEM).

3.4.3 Effects of notched noise and tuned noise on TDFs

The response rate of ITD-sensitive coincidence-detector neurons can be influenced by the frequency composition of the stimulus as well as the binaural correlations of their inputs. To distinguish the observed effects of noise on the TDFs in terms of these two

mechanisms, we used three different noise stimuli: white noise, notched noise, and tuned noise. Notched noise should mainly stimulate the frequency components a neuron is not excited by. Tuned noise was intended to cover the excitatory spectral components. All three noise-stimuli were presented at best ITD and at the same level (RMS) as the pure tones.

As shown in the example in figure 3.5, notched noise consists of frequencies the neuron was only weakly responding to (see methods and figure 3.5A and 3.5B). Therefore the response to notched noise was smaller than the response to white noise (figure 3.5C). Consistent with this example the average responses to notched noise (23.8 ± 3.5 spikes/s) were significantly smaller ($P < 0.001$) than these to white noise (31.8 ± 3.6 spikes/s) (figure 3.5D). The effects of notched noise on the response to tones at favorable as well as at unfavorable ITDs were very similar to the effects of white noise (single response in figure 3.5C; average response in figure 3.5E); The responses to favorable ITDs were decreased, whereas the responses to unfavorable ITDs of the tones were slightly increased by adding both white noise or notched noise. Since the response to white noise was stronger than that to notched noise, the tone-induced enhancement at favorable ITDs was smaller and the tone-induced reduction at unfavorable ITDs was stronger in the white noise condition (figure 3.5F and 3.5G). Taken together, although the tone-induced effects were slightly different, notched noise and white noise had similar impact on TDFs.

Tuned noise was constructed from frequencies strongly exciting the neuron (see methods and figure 3.5A and 3.5B). Therefore the responses to the tuned noise (average response: 99.0 ± 6.9 spikes/sec) were stronger than the average response to white noise ($P < 0.001$) (figure 3.5C, figure 3.5D). Adding tuned noise to a tone with favorable ITD on average slightly but not significantly ($P = 0.21$) enhanced the response rate by 5 % (figure 3.5E, left), in contrast to white or notched noise, which decreased the response rate. Furthermore tuned noise also elevated the firing rate for tones at unfavorable ITDs (figure 3.5E, right). Despite a small increase of the response to the favorable ITD with increasing the level of tuned noise (figure 3.5E), the tone-induced enhancement was decreased and the tone-induced reduction of the noise was increased (figure 3.5F); the latter effects were a direct consequence of the strongly increased response to tuned noise alone (dark blue dashed line in figure 3.5C). Although the responses to the different spectral noise composites showed clear differences, the proportion of neurons which were sensitive to

ITDs was almost unchanged when the noise level for each condition was equal to the tone level. For tuned noise, all neurons remained ITD-sensitive, whereas 77 % (24/31) of the neurons (figure 3.5G) remained ITD-sensitive for both notched and white noise. Importantly, while the response rate to tones strongly depended on the spectral components of the added noise, the ITD sensitivity to the tone was preserved with all different types of added noise.

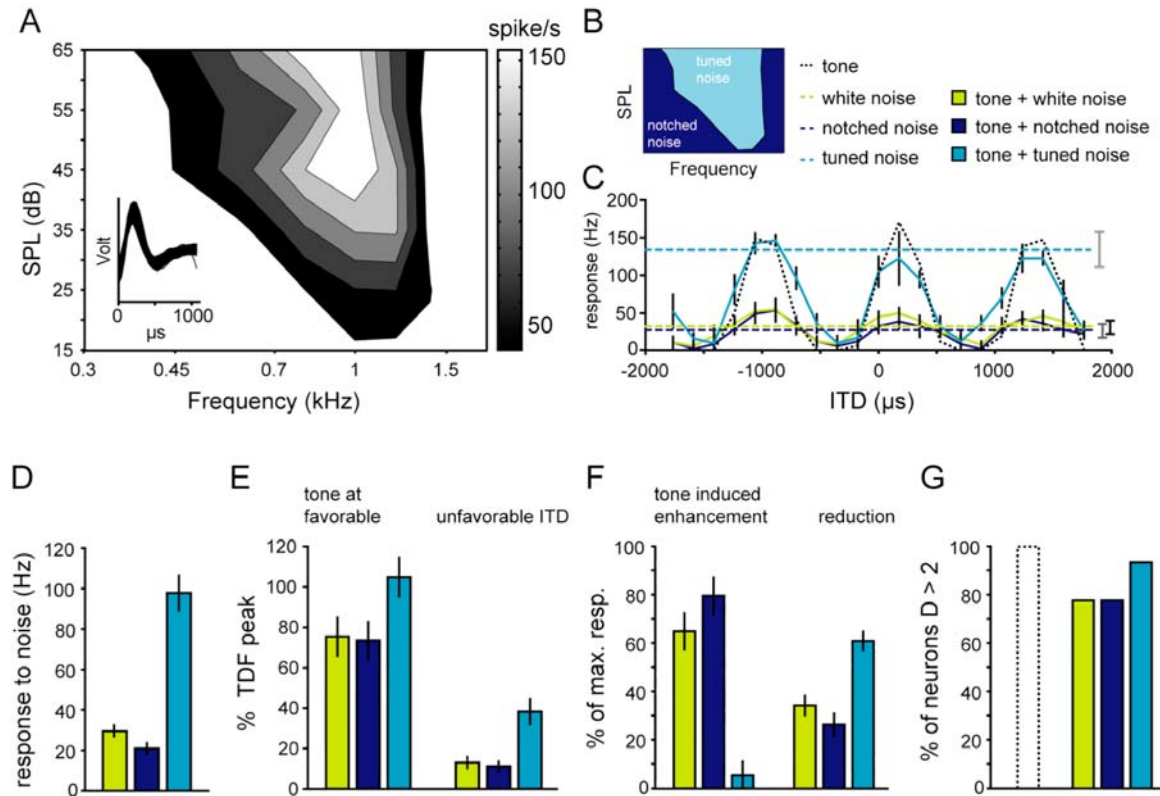


Figure 3.5 Effects of white, notched, and tuned noise on TDFs. From the frequency-versus-level response areas (A; neuron: 181006_04, BF = 1000 Hz) we calculated the neuron's notched and tuned noise (B). C: Single-unit response to the three different types of noise at best ITD are shown in dashed lines. The error bar on the right side shows the standard error of the response to the noise. The TDFs with concurrent presented noise are shown with lines, the TDF without noise in a dotted line. (neuron: 061006_04, BF = 800 Hz). D-G: Summarized population statistics. D: The response to noise E: The maximal and minimal response to tones in noise F: The enhancement and reduction of the response to noise by tones. G: Although there are differences in the response rate the ITD sensitivity to tones remained in more than 75 % of the neurons independent of the spectral component of the added noise. Error bars = standard error of the mean (SEM).

We note that all three types of noise stimuli were presented at best ITD and with the same RMS as the RMS of the pure tones. The effective levels of these different types of noise

for a particular neuron may thus be very different. In particular the effective level of the spectrally shaped noises, which are composed of fewer spectral components as the white noise, will presumably be higher. The conclusions of our paper, however, refer to *changes* of firing rates in dependence of noise intensity for each different type of noise separately. Therefore, though we might underestimate the effective level of the notched or tuned noise, the general trends are supposed to be the same.

3.4.4 Simulated effect of the noise level on binaural correlations

Tuned noise had been constructed in order to reduce cross-frequency interactions or effects caused by lateral suppression. We thus assumed the NDFs derived from tuned noise stimulation to be largely inherited from the coincidence-detector neurons in the superior olivary complex within the same frequency channel. To understand the neuronal responses to tuned noise, we investigated how binaural correlations are temporally processed and translated to firing rates in a neuronal model receiving input from a single frequency channel. We therefore derived binaural input rates of the coincidence-detector neurons from feeding the acoustic stimuli into the AN model of Tan and Carney (2003) for a characteristic frequency of 1 kHz. However, before studying a cellular model we first calculated the coefficient of correlation between the binaural input rates as a function of pure tone ITD (figure 3.6A1). As expected, with increasing noise level, the coefficient of correlation becomes less dependent on the pure tone ITD and saturates at a constant value of 1. The coefficient of correlation thus is not a good model for the discharge rate of the coincidence neuron since it cannot explain the noise-induced increase in the peak rate, though it might qualitatively explain the increase of the trough-firing rate (figure 3.6A2).

As a next step to also include subthreshold integration of the binaural signal we calculated the temporal average of the squared input rates and interpret this as a firing rate (figure 3.6B). Energy models like such are long and widely used in visual (e.g., Adelson and Bergen 1985) and auditory systems neuroscience (Batra et al. 1997a; Gollisch 2006) and incorporate the probably simplest non-linearity. The outcomes of this model show that an increase of the noise level yields an increase in both the response to the favorable as well as the unfavorable ITD and hence at least qualitatively can account

for the observed *in-vivo* responses. The sound intensity (20 dB above neuronal threshold) of the tuned noise used in the experiment roughly corresponded to a noise level of 30 dB SPL (above standard threshold of audibility) in the model. Consistent with our empirical DNLL data for tuned noise stimulation, the peak response at 30 dB SPL (in the model) was slightly enhanced as compared to the peak response obtained from pure tone stimulation. However, the increase of the trough response was considerably larger than that observed in the data. The latter discrepancy could be resolved by applying the input rates to simple integrate-and-fire-type spiking neuron models (figure 3.6C, 3.6D). As a result of the threshold non-linearity, the trough-firing rate at 30 dB SPL was only slightly enhanced as compared to the trough of the TDF.

The best ITD of the model neurons was shifted to 0.15 ms to match the averaged best ITDs of recorded DNLL units. In the first model (figure 3.6C) this shift was achieved by an additional temporal delay of contralateral excitatory inputs that might arise from longer axonal conduction. This way of shifting the best ITD dates back to the model of neuronal ITD representation by Jeffress (1948). Recently, another computational model of how to neurally encode ITDs has been proposed by Brand et al. (2002), who showed that phase-locked inhibition evoked by inputs to the contralateral ear can also induce a shift of the best ITD if this inhibition arrives slightly earlier. We also implemented a model using contralateral phase-locked inhibition (figure 3.6D) to test whether the mechanism that accounts for the peak shift is crucial to explain the effects of tuning noise upon the TDFs of a coincidence-detector neuron. However, the phase-locked inhibition model exhibits both peak and trough firing rates with a virtually identical dependence on noise intensity as the Jeffress-type model (compare figure 3.6C and 3.6D). Hence our modeling cannot make a prediction on the mechanism of the peak shift.

To conclude, our models show that additional binaurally correlated noise does not reduce the peak-firing rate of the TDF as noise intensity increases. The model thus corroborates the interpretation that the suppressive across-frequency interactions resulting in a reduction of the peak firing rate under notched and white noise stimulations are due to either inhibitory or binaurally uncorrelated contributions from lateral frequency bands. A second conclusion from our models is that the increase of the firing rate at the trough of the TDF with increasing noise level can be explained by a simple binaural coincidence-detector acting on binaural AN inputs. For the AN model by Tan and Carney (2003), the

threshold noise intensity of about 30 dB SPL, at which the trough firing rate starts to linearly increase, is in good quantitative agreement with our DNLL data.

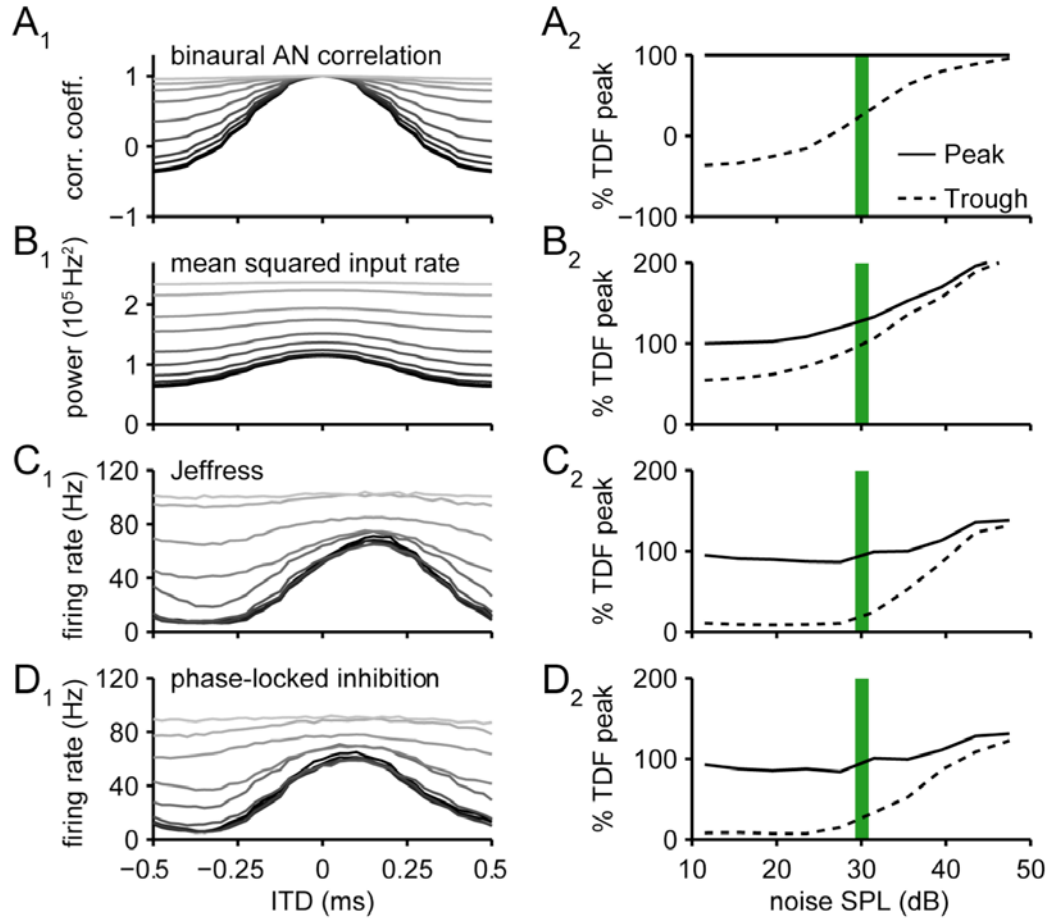


Figure 3.6 TDFs (left column) derived from models. Concurrent noise was applied with different levels and at best ITD. Gray levels encode the noise intensity from 10 (dark) to 50 dB SPL (light). Peak and trough firing rates as a function of noise level are depicted in the right column. The green areas indicate the noise level used in the experiment. **A**: Coefficient of correlation between ipsi- and contralateral AN model responses. **B**: Mean squared binaural sum of AN rates (see Methods). **C**, **D**: Firing rates derived from simple neuronal threshold models of either Jeffress- (**C**) or phase-locked inhibition-type (**D**).

3.5 Discussion

The present study investigated the effect of a concurrent noise source on the sensitivity of DNLL neurons to ITDs of pure tones and vice versa. Although the neurons were responsive to binaural white noise, we found that, for the combination of white noise and

pure tone, the neuronal response to the tones at best ITD decreased with additional noise. The response to unfavorable ITD slightly increased with additional noise. However, for all tested noise levels (up to RMS-identical tone and noise levels) it remained below the firing rate evoked by the noise stimulus alone. From a different point of view, a pure tone at unfavorable ITD could thus be considered to reduce the response to white noise.

The decrease of the response to a tone at favorable ITDs and the increase of the response to tones at unfavorable ITDs can be explained by two different mechanisms: monaural across-frequency interactions and temporal summation at the level of the coincidence-detector.

The influence of noise on TDFs was strongly dependent on the spectral composition of the noise. Notched noise, which was constructed to specifically stimulate suppressive side bands, had similar effects on TDFs as white noise. In contrast, tuned noise, which consists primarily of excitatory spectral components, did not suppress the neuronal discharge rate evoked by a pure tone at favorable ITD. Therefore these results support the hypothesis that the suppression of the response to favorable ITDs results from a spectral integration with a dominating role of suppressive side bands. The fact that noise presented at levels below excitatory thresholds for pure tones stimulation affected response rates to TDFs indicates sub-threshold across-frequency interactions. The lateral suppression, however, could already occur prior to the binaural processing stage, e.g. in the cochlear nucleus or in the cochlea. Our monaural data also showed a decrease in the response to tones with increasing level of additional noise. This strengthens the idea that lateral suppression decreases the response to tones at favorable ITDs with increasing noise level.

Lateral suppression, however, cannot explain the observed small increase of the response to the unfavorable ITDs. Hence, the increase of the response to unfavorable ITDs by adding noise is likely to result from binaural interactions at the level of the coincidence-detector in the superior olivary complex. Simulations of simple coincidence-detector models receiving input from a single frequency channel corroborate this interpretation. In these models, adding binaural noise results in an increase of both the trough and the peak-firing rate.

3.5.1 Comparison with previous monaural studies

Neuronal responses to stimulations with tones in combination with noise have been electrophysiologically studied in monaural structures i.e. the auditory nerve (Rhode et al. 1978; Young and Barta 1986) and the cochlear nucleus (Greenwood and Maruyama 1965; Goldberg and Greenwood 1966; Gai and Carney 2006). There, neurons generally respond stronger to tonal stimuli than to noise stimuli and the response to a combination of tone and noise is weaker than the response to tones alone. Furthermore, Kiang and Moxon (1974) also showed substantial across-frequency interactions at the level of the auditory nerve. These findings are consistent with the results from monaural and binaural notched noise stimulations presented in this study (figure 3.4). Therefore part of the suppressive effects caused by spectral integration we observed in the DNLL with spectrally adjusted noise stimuli could be explained by mechanisms, which might take place already at the level of the cochlea.

3.5.2 Comparison with binaural studies on the detection of tones in noise

Previous psychophysical studies showed that noise substantially affects the ability to detect pure tones and, moreover, that this ability is strongly influenced by the ITD of the tone (for review: Blauert 1997): the detection threshold for tones with 0 ITD (S_0) in noise with 0 ITD (N_0) improves dramatically when the phase of the tone at one ear (S_π) is inverted. These results correlate with change of the firing rate of single neurons in the inferior colliculus (IC) (Caird et al. 1991; McAlpine et al. 1996; Jiang et al. 1997a,b; for review: Palmer and Shackleton 2002). Furthermore, in these studies the neurons are classified according to their changes of the firing rate to noise and tones (N_0S_0 or N_0S_π) with increasing tone intensity. Since the main focus of our study was not detectability but rather localization of pure tones we varied the ITD of the tones and used two different noise levels. We therefore cannot make statements on whether the IC neuron's detection capability is present at the level of the DNLL. However, for N_0S_0 versus N_0S_π stimulation we did the same classification for our set of 80 neurons as in the IC literature (figure 3.7; Jiang et al. 1997b). While there were small differences between the results for the two noise levels, most of the neurons (66/80 for noise level at 20 dB below tone level, and 65/80 for noise level at tone level) showed an increase in the response to noise with

additional tones with zero ITD (S_0) (Type-PP or Type-PN). As in the IC a few neurons showed a decrease in the response with additional tones at zero ITD (Type-NP or Type-NN). Altogether the fractions are similar to those reported from the population of IC neurons measured by Jiang and colleagues (Jiang et al. 1997b). We thus conclude that the ITD-dependent detectability of tones in noise shown in the IC reflects the one we observed on the level of the DNLL. Since the DNLL is a mainly inhibitory nucleus and therefore almost certainly not solely responsible for the features of IC neurons, the similarity indicates that the superior olivary complex is the potential site providing the relevant computational mechanisms.

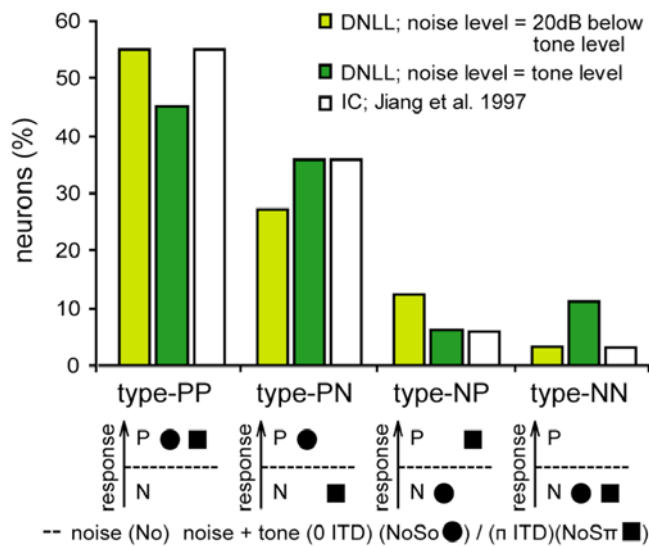


Figure 3.7 Different types of binaural masking. Comparison of our DNLL data with the population of IC neurons measured by Jiang et al. (1997b). The schematic drawings describe the responses underlying the division into the different types.

3.5.3 Comparison with binaural studies on the localization of tones in noise

The psychophysical studies investigating the localization of tones in background noise showed that accuracy and discrimination ability declines with increasing level of background noise (Stern et al. 1983; Good and Gilkey 1996). This finding is consistent with the single neuron responses we report in this study, since background noise reduces the discriminability of peak and trough firing rates and, hence, the fraction of ITD-sensitive neurons (figure 3.2).

Furthermore, psychophysical studies have shown that, in contrast to the detection of pure tones, the ITD discrimination of a signal (pure tone or narrow band noise) is improved, if the ITD of the background noise has the same ITD as the signal (Cohen 1981; Ito et al. 1982). In the present study, however, we only see a small reduction of ITD-sensitive neurons if we change the noise ITD from best ITD to 0 ITD (figure 3.2). Our results therefore cannot provide a link between single cell recordings in the DNLL and psychophysics.

3.5.4 Functional relevance

Our data reveal a complex interaction between the concurrent sound sources, in our example of tones and noise. The overall firing rates of the ITD-sensitive DNLL neurons to tones are strongly modulated by noise and vice versa the firing rate to noise is strongly modulated by tones. Furthermore, we observed a complex interaction between the spatial and the spectral cues. Different values of the neuronal firing rate seem to encode different spectral properties of the acoustic stimulus composition. Therefore we hypothesize that in contrast to these spectral cues, the spatial cues are encoded independently of the actual firing rate via activity patterns in a population of neurons (Jeffress 1948; Fitzpatrick et al. 1997; Hancock and Delgutte 2004; Harper and McAlpine 2004; Stecker et al. 2005).

4 Perceptual and physiological characteristics of binaural sluggishness

Ida Siveke, Stephan D. Ewert, Benedikt Grothe, and Lutz Wiegand

Prepared for submission to the *Journal of Neuroscience*

4.1 Abstract

The mammalian auditory system is the temporally most precise sensory modality: To localize low-frequency sounds in space, our binaural system resolves differences in the interaural arrival times of sound waves with microsecond precision. In contrast, the binaural system has been described to be very sluggish in updating dynamically changing interaural time differences as they arise from a low-frequency sound source moving along the horizontal plane. For a combined psychophysical and electrophysiological approach, we created a new stimulus type that allows transmitting very rapid and plausible auditory motion. With this stimulus, the binaural psychophysical performance in humans is significantly better than reported previously with different stimuli and is comparable to the monaural performance for detecting amplitude modulations. Neuronal performance estimated from the electrophysiological recordings of binaural brainstem neurons in the gerbil predicts the improvement of the psychophysical performance quantitatively. The results indicate that the binaural system can be as fast as the peripheral monaural system. Thus, the current data provide both psychophysical and physiological evidence against a general, hard-wired binaural sluggishness.

4.2 Introduction

The mammalian auditory system relies on exquisitely precise estimation of the differences in interaural arrival time (ITDs) to localize low-frequency sounds in space. For low-frequency pure tones and noise, e.g., human psychophysical experiments showed that ITD differences as low as 10 to 20 μs can be resolved. In contrast to this extraordinary neuronal precision, the binaural system has been described as rather slow in following the changes in ITDs, elicited by a low-frequency sound source moving in space. Previous experiments recruited the binaural system's capability to unmask spatially divergent signals from maskers to characterize binaural sluggishness (Grantham and Wightman 1979; Kollmeier and Gilkey 1990). Grantham (Grantham and Wightman 1978; Grantham 1982) used a low-pass noise with time-varying ITD or time-varying interaural correlation to estimate the temporal precision of the binaural system by means of a binaural time constant of about 50 – 200 ms. The speed of monaural temporal processing, using amplitude-modulated stimuli, was quantified with time constants between 1.1 and 2.5 ms (Viemeister 1979; Dau et al. 1999; Ewert and Dau 2000). Together these studies provided evidence that the binaural system is sluggish compared to the monaural system.

A recent study by Joris et al. (2006) searched for a neuronal correlate of binaural sluggishness in the cat using stimuli with oscillating interaural correlation as used in Grantham (1982). At the level of the cat auditory midbrain, neurons were well capable to lock to modulations of interaural correlation that are an order of magnitude faster than was estimated from human psychophysical experiments (Grantham 1982). The authors argued that the fast binaural modulations presumably created in the superior olivary complex and recorded in the inferior colliculus might not be adequately processed by subsequent auditory stages, creating the apparent binaural sluggishness in detection tasks. However, the oscillating-correlation (Oscor) stimulus used in these studies does not generate changes in ITD over time like a natural sound source rotating around the listener. Instead, the Oscor stimulus oscillates through stages of a perceived coherent spatial image, produced by interaural correlated noise, and through stages of a completely diffuse spatial image, produced by uncorrelated noise. Between these two extremes a blurred, semi-focused image produced by interaurally anti-correlated noise is perceived.

Thus, the Oscor never resembles a “meaningful” binaural input that shares similarities to any naturally occurring binaural stimulus.

To compare the speed of monaural and binaural processing directly, a stimulus, which creates strong and unambiguous auditory motion, the ‘Phasewarp’, was created. A combination of human psychophysical experiments and electrophysiological recordings in the auditory brainstem of a well-established animal model of human sound localization, the Mongolian gerbil, is presented in the current study. The psychophysical data show that with the Phasewarp, the auditory system can detect binaural modulations much faster than estimated previously. This psychophysical improvement is reflected in the responses of binaural cells in the dorsal nucleus of the lateral lemniscus (DNLL).

Parts of this work have been presented at the 14th International Symposium on Hearing, 2006.

4.3 Methods

4.3.1 Stimuli

To create a monaural modulation, dichotic Gaussian noise was multiplied with a sinusoidal modulator varying in amplitude between zero and two. The phase was randomized over trials, but it was identical for the two ears. The Oscor was generated according to Grantham (1982) starting with two independent noise samples. One was fed directly into the left ear. A copy of this noise sample was multiplied with a sine modulator. The other sample was multiplied with a cosine modulator. The two modulated waveforms were added and fed to the right ear. The generation of the Oscor is illustrated in figure 4.1A. The Oscor01 was generated also with two independent noise samples where one was fed directly to the left ear. A copy was multiplied with the square root of a raised-sine modulator, varying in amplitude between zero and one. The other sample was multiplied with the square root of the 180-degree phase shifted raised-sine modulator and the resulting waveforms were added and fed into the right ear. The generation of the Oscor01 is illustrated in figure 4.1B. Phasewarp stimuli were generated in the frequency domain using a frequency independent magnitude and a random phase for the

components of the spectrum of the stimulus for the left ear. For the spectrum of the right ear's stimulus, the phase components of the left ear were shifted along the frequency axis by an amount equal to the modulation frequency (MF). The generation of the Phasewarp stimulus is illustrated in figure 4.1C.

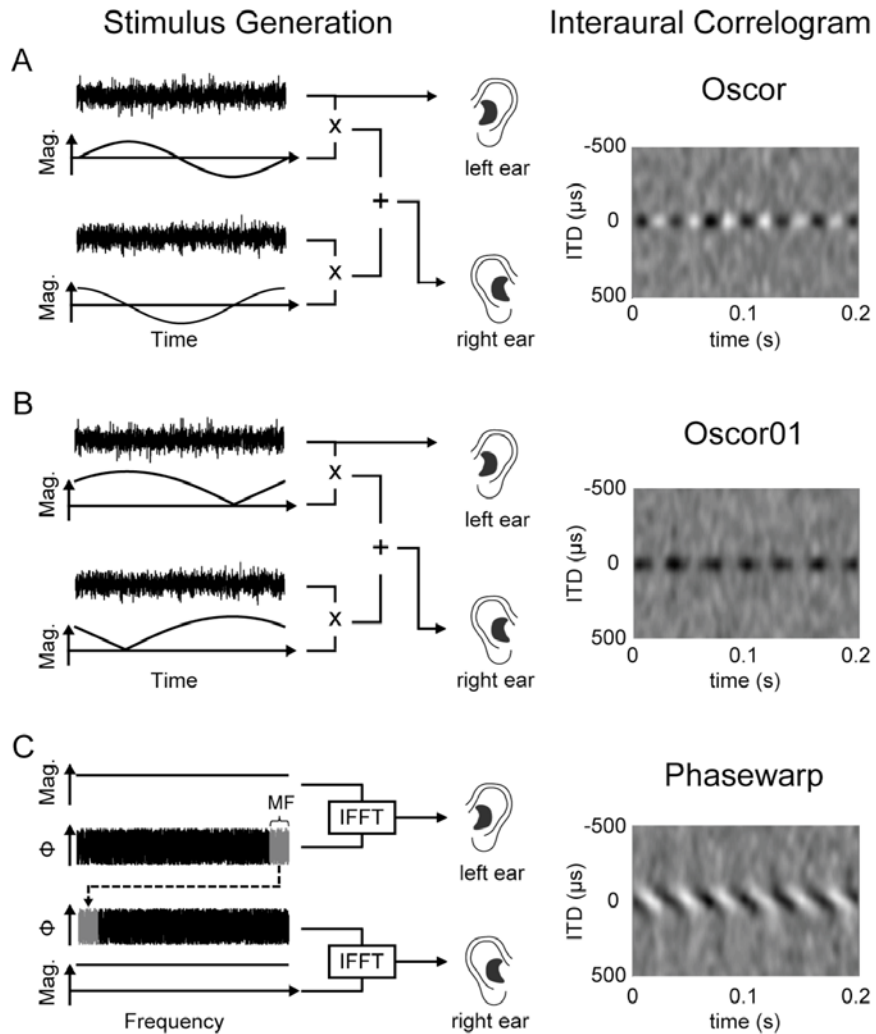


Figure 4.1 Illustration of the generation of binaurally modulated stimuli: Oscor (A), Oscor01 (B), and Phasewarp (C). See text for a detailed description of the stimulus generation (left-side panels). The right-side panels show interaural cross-correlograms as an illustration of a binaural display of these stimuli: The degree of interaural correlation is color coded as a function of time and interaural time difference with black representing the highest correlation. Note that while the Oscor and Oscor01 produce modulation only along the time axis, the Phasewarp produces binaural modulation both along the time- and ITD axis.

All stimuli were generated with MFs ranging from 2 to 512 Hz or from 8 to 1024 Hz in doublings. The right column of figure 4.1 shows the interaural correlation as a function of

ITD and time for the three types of binaural modulations low-pass filtered at 5 kHz. While the three types of binaural modulations share the same MF of 8 Hz, the Phasewarp stimulus shows a pattern of correlation, which is modulated both along the ITD and the time axis, while the Oscore and Oscore01 stimulus is only modulated along the time axis. None of the binaural stimuli illustrated in figure 4.1 produced any monaural amplitude modulation.

The standard (unmodulated) stimuli for the psychophysical experiments were samples of dichotic noise. In case of the Oscore01 measurements, a noise was used as standard where the interaural correlation roved around the average long-term interaural correlation of the Oscore01, 0.5. The magnitude of the rove was ± 0.25 . This was done to prevent listeners from attending to the width of the binaural image instead of the modulation. In case of the Oscore the average interaural correlation is 0 as for the dichotic noise standard.

In addition to the Phasewarp measurements with dichotic noise standard, a second standard was used in a control experiment: The interaural envelope correlation of the Phasewarp stimulus in different auditory bands increases monotonically with the fraction characteristic-frequency (CF)/MF of the band. For high-frequency channels, where phase-locking is only observed to the envelope, the Phasewarp results in an increased interaural correlation of the internal signals relative to the dichotic-noise standard. This is particularly prominent for low MFs. Subjects are able to perceive correlation increase as a narrowing of the spatial image in the high-frequency channels. To estimate this effect for human psychophysics, the interaural envelope correlation for different ratios CF/MF was analyzed in a 2000 Hz 4th -order gammatone filter (Patterson 1994). Since the effect depends on the CF/MF ratio and the gammatone filter-shape scales with CF, only a single exemplary filter needed to be analyzed. The new standard, the Phasewarp-equivalent correlation (PWEC) noise, was generated by mixing a diotic and an interaurally independent dichotic noise with a frequency dependent mixing ratio. This mixing ratio followed an empirically adjusted function that led to the same interaural envelope correlation as the Phasewarp stimulus at the output of the 2000 Hz gammatone filter. The correlation was analyzed for ratios of MF and the equivalent rectangular bandwidth (ERB) of the filter of MF/ERB = [0.01 0.02 0.04 0.08 0.16 0.32 0.64 0.96 1.28 1.96 2.56 3.84 5.12 10.24]. The root-mean-square (RMS) difference of the envelope correlation of the Phasewarp and the PWEC noise could be minimized to 1.6%. The PWEC noise was

generated in the frequency domain and the mixing ratio, mix , of the frequency component, $freq$, was

$mix = \exp(-1.1 * fm. / (ERBbandwidths))$, with $ERBbandwidths = 24.7 + freq/9.265$.

As a result, the PWEC noise has the same envelope correlation in all filters of a gammatone filterbank as the Phasewarp but it lacks the binaural modulation along the time and ITD axis of the Phasewarp.

4.3.2 Psychophysics

In an adaptive three-alternative, forced-choice procedure, four listeners (21 to 24 of age) were asked to detect the interaurally or monaurally modulated stimuli following a two-down, one-up rule. This procedure estimates the 70.7 % correct point on the psychometric function. The dependent variable was the relative level of uncorrelated noise added to the monaural or binaural modulations. The experiment was carried out with broadband versions of the modulated stimuli and with high- and low-pass filtered versions of the Oscor and the Phasewarp. The cut-off frequencies for the low-pass filtered stimuli was 1500 Hz, the cut-off for the high-pass stimuli was 5000 Hz. Filters were implemented as ‘brick-wall’ filters which, due to an Fourier-transform based algorithm, produce filter slopes in excess of 100 dB per octave. The remaining frequencies were filled with uncorrelated noise of the same spectrum level to preclude the use of off-frequency cues (see below).

Stimulus duration was one second including 20 ms raised-cosine ramps. Listeners were seated in a sound-attenuated room. The Stimuli were presented from an RME Audio Digi 96/8 soundcard (Haimhausen, Germany) through Sennheiser HD580 headphones (Wedemark, Germany) at a sound pressure level of 60 dB SPL. The headphones were digitally compensated to produce a frequency-independent response on a Bruel&Kjaer 4153 artificial ear (Naerum, Denmark).

For each listener and stimulus condition, at least three adaptive runs were acquired. Individual data were only used for further analysis if a threshold could be determined in all three runs. Data averaged across listeners are shown only if an average threshold could be determined for each tested listener.

4.3.3 Neurophysiology

Auditory responses from 87 single neurons were recorded from 26 adult Mongolian gerbils, *Meriones unguiculatus*. The detailed methods in terms of surgery, acoustic close-field stimulation, stimulus calibration, and recording techniques have been described previously (Siveke et al. 2006). All experiments were approved according to the German Tierschutzgesetz (AZ 55.2-1-54-2531-57-05).

The anaesthetized animals (20% ketamine and 2% xylacine) were placed in a sound-attenuated chamber and mounted in a custom-made stereotaxic instrument. Using motorized Micromanipulators (Digimatic, Mitutoyo, Neuss, Germany) and a piezodriven (Inchworm controller 8200, EXFO Burleigh Products Group Inc, Quebec, Canada) the electrode (tilted 10° or 5° laterally) were penetrated 1.3-2.6 mm lateral to the midline and 0.5-0.8 mm caudal of the interaural axis. Single-unit responses were recorded extracellularly using glass electrodes filled with 1M NaCl (~10 MΩ). The amplified and filtered action potentials were fed into the computer via an A/D-converter (RP2.1, TDT-Tucker Davis Technologies, Alachua, USA). Clear isolation of action potentials from a single neuron (signal to noise ratio > 5; see waveform of the recorded spikes in figure 4.4, 4.6) was guaranteed by visual inspection (stable size and shape) on a spike-triggered oscilloscope and by offline spike cluster analysis (Brainware, Jan Schnupp, TDT).

Stimuli were generated at 50 kHz sampling rate by TDT System III. Digitally generated stimuli were converted to analog signals (RP2.1, TDT), attenuated (PA5, TDT) and delivered to the ear phones (Sony, Stereo Dynamic Earphones, MDR-EX70LP, Tokyo, Japan).

Randomized broadband and narrow-band ($\pm 10\%$ around BF) noise stimuli (duration: 200 ms, repetition rate: 2 Hz, raise-fall time: 1ms) were presented to determine the level (20 dB above threshold; rate-level functions, 5 dB steps) and the maximal ITD (noise-delay functions, 0.15 cycles steps). For broadband and narrow-band noise, the specific level and maximal ITD was determined separately. We considered a unit ITD-sensitive if the noise-delay function was modulated by $\geq 50\%$ (i.e., if the minimum discharge rate was less than half of the maximum rate). Response were defined as sustained if the neurons responded over the entire duration of the stimulus and not exclusively during the first 50 ms. For the first part, neuronal responses of 68 neurons to 10 repetitions of the monaural and binaural modulation stimuli with 1-s duration and a repetition period of

1.5 s and a cosine-squared gating raise-fall time of 20 ms were obtained. For the second part, neuronal responses of 19 neurons to 10 repetitions of the Oscor and Phasewarp stimuli with 500-ms duration and a repetition period of 750 ms and a cosine-squared gating raise-fall time of 20 ms were obtained. As in the psychophysical study, additional binaurally uncorrelated noise was applied at a signal-to-masker ratio (SMR) of -19, -16, -13, -10, -7, -3, 2, 10 and ∞ dB.

The vector strength (VS) for each MF was calculated according to Goldberg and Brown (1968) and determined as significant if the $P < 0.001$ criterion in the Rayleigh test was fulfilled (Batschelet 1981). For the second set of data, receiver operation characteristics (ROC) analysis (Green and Swets 1966; Britten et al. 1992) was used to generate a neurometric function. As standard condition, the -19 dB SMR was used. The analysis was either based on the rate or timing of the response. For the timing analysis at the infinite SMR standard, normalized period histograms (P) with x bins were calculated for each MF. For the ROC analyses, the differences between the standard period histogram (P) and the normalized period histograms for all different SMRs (Q) were calculated by the Kullback-Leibler-divergence (KL):

$$KL(P, Q) = \sum_x p(x) * \log \frac{p(x)}{q(x)}.$$

4.4 Results

4.4.1 Psychophysics

The human sensitivity to a monaural modulation and three types of binaural modulation are shown in Fig. 2a. Modulation detection was quantified in terms of the signal-to-masker ratio (SMR) at threshold with a dichotic-noise masker. The data show that a monaural modulation is detectable at a SMR of about -14 dB (figure 4.2A, green line). In line with previous findings (Viemeister 1979), the threshold SMR increased for MFs above 64 Hz. The three other plots depict human sensitivity to different types of binaural modulations (figure 4.2A, orange, red, and black line). Overall binaural sensitivity was worse than monaural sensitivity by about 10 dB SMR. Moreover, with the Oscor

stimulus, sensitivity decreased relatively quickly with increasing MF larger than 8-16 Hz. For MFs higher than 128 Hz, not all four listeners could detect the modulation in the Oscor stimulus (black line). This faster decrease in sensitivity compared to monaural sensitivity could be attributed to an additional binaural sluggishness with a time constant ≥ 10 ms. Thresholds for binaural modulation detection with the Phasewarp stimulus are shown in red. For low MFs, thresholds were very similar to those with the Oscor but for higher MFs, thresholds with the Phasewarp decreased only slowly and the modulations were detectable by all four listeners up to the highest MF of 1024 Hz.

The low-pass characteristic of binaural modulations elicited by the Phasewarp is considerably shallower than the six dB-per-octave slope of a first-order low-pass filter, which can be quantified with a time constant. Thus, no explicit time constant was derived from the empirical data. However, the overall slope of decrease in sensitivity with increasing MF is similar to that of the monaural modulation. This shows that using the Phasewarp stimulus, there was no indication of additional binaural sluggishness.

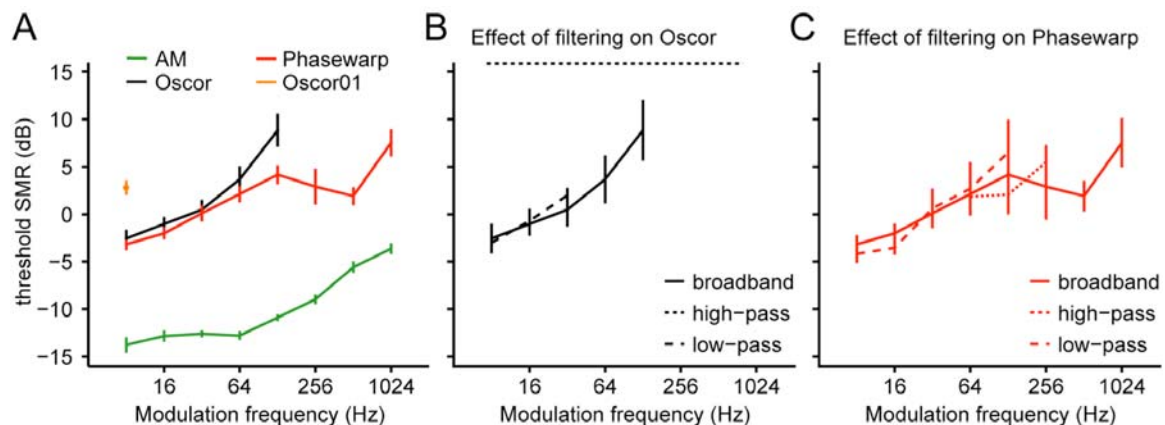


Figure 4.2 Psychophysical sensitivity to monaural modulations and three types of binaural modulations. Result with broad-band stimulation are shown in **A**. Sensitivity, expressed in terms of the SMR at modulation-detection threshold is highest for the monaural modulations and worst for the Oscor01. The decrease of the sensitivity with increasing MF is very similar for the monaural modulations and the binaural modulations elicited by the Phasewarp. In contrast, with binaural modulations elicited by the Oscor, sensitivity decreases fast with increasing MF. With the Oscor01, binaural modulations could only be detected at the lowest tested MF of 8 Hz. The effect of filtering on binaural modulation sensitivity is illustrated in **B** and **C** for the Oscor and Phasewarp, respectively. See text for details.

The fourth stimulus (orange) was a modified version of the Oscor stimulus denoted ‘Oscor01’ (see methods). The Oscor01 differed from the Oscor in that the modulation of

interaural correlation only varies between one and zero and not between one and minus one. With the Oscor01, sensitivity to binaural modulation decreased dramatically. The binaural modulation was only detectable for the lowest presented MF of 8 Hz. A time constant or cut-off frequency cannot be estimated from this single data point. However, the data could be interpreted as indicating a considerably higher binaural sluggishness for the Oscor01 than found for the Oscor and Phasewarp.

The psychophysical experiments were carried out with broadband stimuli and thus, it cannot be determined which frequency range was used by the listeners to detect the binaural modulation. The experiments were consequently repeated with filtered versions of the Oscor and the Phasewarp. To avoid edge effects at the filter slopes and off-frequency listening, the filtered stimuli were added to inversely filtered uncorrelated noise (see methods). Results with the filtered stimuli are shown in figure 4.2B for the Oscor and in C for the Phasewarp stimulus. In the low-pass condition (1.5 kHz, dashed lines in figure 4.2B and C), listeners' sensitivity to low MFs was unchanged compared to the broadband condition. However, with increasing MF, sensitivity in the low-pass condition deteriorated more rapidly. This indicates that faster modulations were better preserved in higher frequency channels.

All listeners could still discriminate the high-pass Phasewarp from the uncorrelated-noise standard for at least some MFs (figure 4.2C). Some listeners could even detect the high-pass filtered Phasewarp at all MFs and some listeners could detect the high-pass filtered Oscor at some MFs (not shown). Since the human auditory system is no longer capable of encoding carrier information at frequencies of 5 kHz and above (Moore 2003), subjects must have been able to use a detection cue other than the interaural modulation. As described in the stimulus section (see methods), the Phasewarp stimulus leads to an increasing interaural envelope correlation inversely related to the ratio MF/CF. The decrease of the envelope correlation is perceivable by the auditory system also at frequencies of 5 kHz and higher. This decrease could provide a static detection cue, a narrowing of the spatial image width, in comparison the standard stimuli consisting of binaurally uncorrelated noise.

Results of a control experiment, which precludes the (static) envelope correlation cue, are shown in figure 4.3. In this control experiment, the standard stimuli were PWEC noise, which was designed to elicit the same increase of interaural correlation with increasing

frequency as it is expected from the Phasewarp (see methods). The data in the left panel show the performance with the standard stimulus used before (figure 4.2) and the data in the right panel show the performance with the PWEC noise as standard stimuli. The data with the PWEC noise show that in the broadband condition, the high sensitivity to the binaural modulation elicited by the Phasewarp was preserved. In the high-pass condition with the PWEC-noise standard, however, none of the listeners could detect the binaural modulation anymore. This control experiment demonstrates that while listeners could use the spatial image-width cue in the high-pass condition, the results of the main broadband experiment are not influenced by a potential usage of this cue.

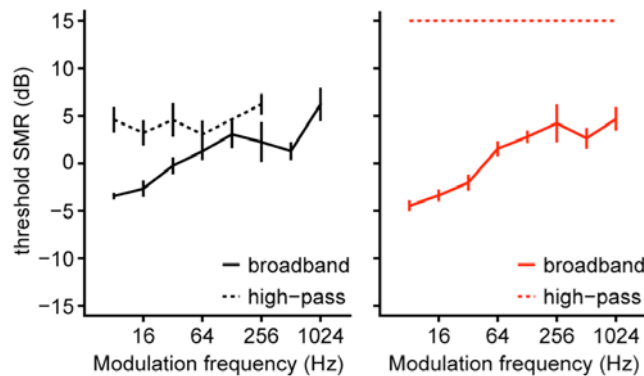


Figure 4.3 Control experiment concerning the contribution of perceptual binaural image width to binaural modulation detection. Results for the detection of the binaural modulation elicited by the Phasewarp in the broadband and high-pass conditions are shown in **A**. A repetition of these experimental conditions with the PWEC as standard stimuli is shown in **B**. While the listeners' performance in the broad-band condition is unaffected by the different standard, none of the listeners could detect the Phasewarp in the high-pass condition. These data show that while perceptual image width can mediate the Phasewarp detection in high-frequency channels, this perceptual cue does not underlie the good sensitivity for the binaural modulation of the Phasewarp.

In summary, the psychophysical data show that perceptual sensitivity to binaural modulation is much better with the Phasewarp than with the classic Ocor and well comparable with the low-pass characteristics of monaural temporal processing.

4.4.2 Electrophysiology

Responses to monaural modulation and the three types of binaural modulation were obtained from a total of 87 single neurons in the gerbil dorsal nucleus of the lateral lemniscus (DNLL). All neurons exhibited sustained response, a best frequency below

2 kHz and ITD sensitivity to noise stimulation. The modulated stimuli were adjusted to each neuron's best ITD as determined by the noise-delay function. For low MFs, most neurons could synchronize their spike timing to the modulation period of either the monaural or the binaural modulation. Responses of a DNLL neuron with a best frequency of 1000 Hz is shown in figure 4.4. The 8 Hz modulation of the stimuli is reflected both in the raster plots (figure 4.4A) and in the period histograms (figure 4.4B) of the neuronal responses. As a measure of how precise the neuronal response reflects the modulation of the stimulus, the vector strength (VS) was calculated from the period histograms. The VS as a function of MF is plotted in figure 4.4C. For the three binaural modulations, the VS was unchanged up to a MF of about 64 Hz and decreased with further increasing MF. In contrast, for the monaural modulations, VS increased with increasing MF up to 64 Hz and decreased with further increasing MF.

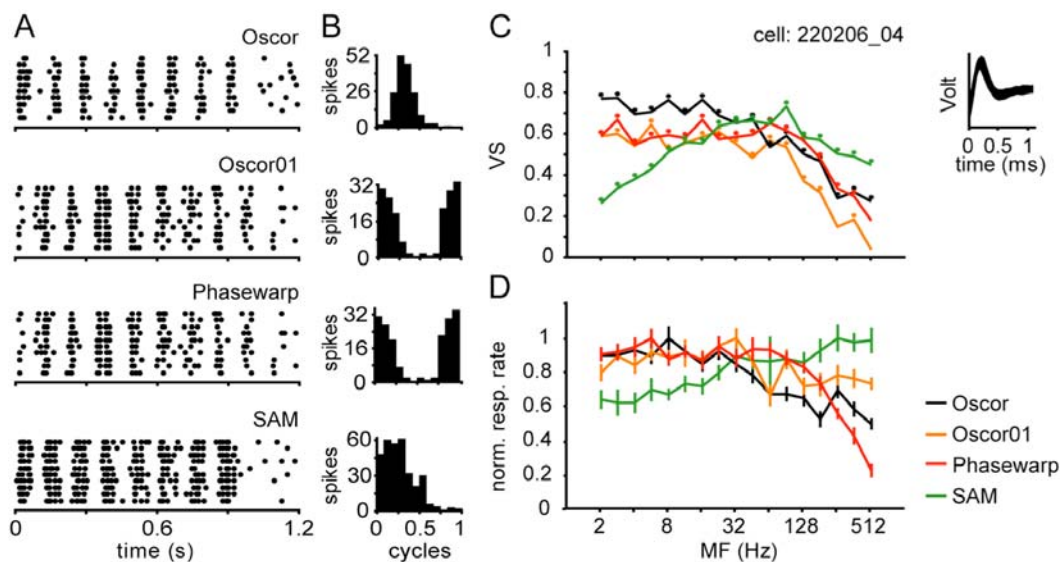


Figure 4.4 Single-cell responses of a gerbil DNLL cell to the three types of binaural modulations and the monaural modulation elicited by SAM noise. Raster plots and period histograms in response to stimuli with a MF of 8 Hz are shown in **A** and **B**, respectively. Temporal response characteristics, expressed as vector strength, and the response rates of this cell are shown as a function of MF in **C**. The vector-strength analysis shows a low-pass characteristic with very similar sensitivity for the three types of binaural modulation and a band-pass characteristic for the monaural modulation. The response rate also shows a low-pass characteristic for the three types of binaural modulations but a slight high-pass characteristic for the SAM (**D**). Error bars represent standard errors of the mean across stimulus repetitions. The inset in **C** shows the spike waveform which was very stable throughout the recording.

Changes in the response rate as a function of MF are shown in figure 4.4D. While for the three binaural modulations, the response rate decreased slightly with increasing MF, the rate increased with increasing MF in response to monaural modulations.

Both the temporal and rate-response characteristics described for a single neuron are reflected in the population data shown in figure 4.5. As in the single-neuron data, population VS as a function of MF showed a low-pass characteristic with a cut-off frequency of 32 to 64 Hz in response to binaural modulations (figure 4.5A). In response to monaural modulations, population VS had a band-pass characteristic with a best MF around 64 Hz. The percentage of neurons in each population with significant VS is shown as a function of MF in figure 4.5B. The large majority of neurons in each population exhibited significant VS for MFs up to 64 Hz. For higher MFs, the proportion of neurons locking to the modulation decreased rapidly for the binaural modulations and only slightly for monaural modulation. However, up to a MF of 512 Hz, still above 15 % of the neurons expressed significant VSs to the binaural modulations and 81 % expressed significant VSs to the monaural modulation.

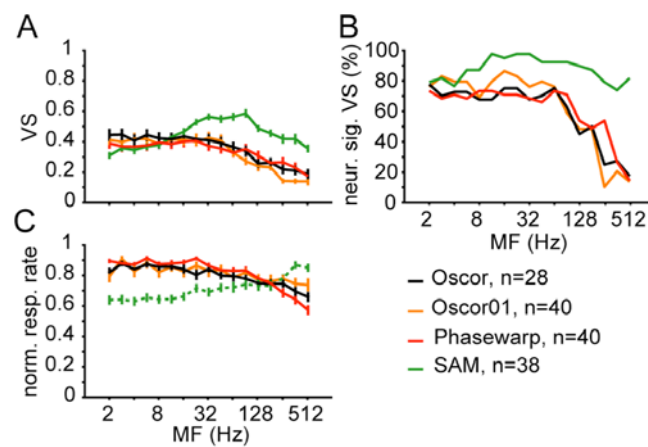


Figure 4.5 Population data of both the temporal (A) and rate analyses (C). Average vector strength (A) and normalized response rate (C) are shown as a function of MF. Error bars represent standard errors of the mean across cells. B shows the percentage of recorded cells meeting a threshold VS for each of the four stimulus types as a function of MF. In the recorded population, most cells could lock very well to the SAM modulation even at the highest tested modulation frequency of 512 Hz. For all three types of binaural modulations, the frequency of occurrence of responses with significant VS decreases with increasing MF for MFs above about 64 Hz.

As it was the case for the single-neuron data in figure 4.4, differences between the monaural and binaural modulations were visible in the population rate response

(figure 4.5C): With increasing MF, the normalized response rate increased in response to monaural modulation, but it decreased in response to binaural modulations.

DNLL neurons typically responded more vigorously to narrowband than to broadband stimulation. This is reflected in the population rate-level function shown in figure 4.6A. Therefore, we tested if the stimulus bandwidth affects the response to the binaural modulations, specifically, the Oscore and Phasewarp stimuli. In general, the VSs for the narrowband stimuli were higher than for the broadband stimuli (figure 4.6B). However, narrowband filtering imposes a low-pass characteristic in the modulation-frequency domain. This low-pass characteristic affected both monaural and binaural modulations in the same way (figure 4.6B). Thus it does not reflect a low-pass characteristic of neuronal processing.

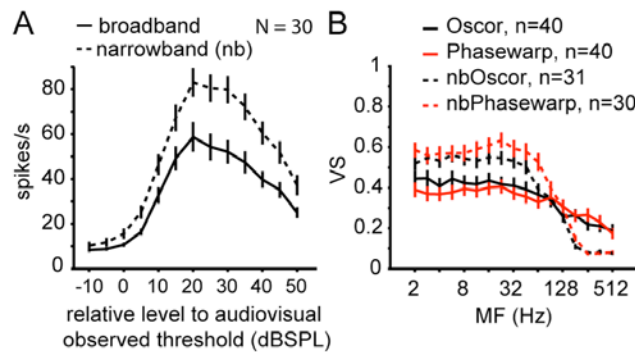


Figure 4.6 effect of narrow-band filtering on neuronal responses. The population rate-level functions (A) show that, in general, cells responses more vigorously to narrow-band filtered stimuli than to broadband stimuli. Error bars represent standard errors of the mean across cells. VSs averaged across the recorded population is shown as a function of MF in B. While for low MFs, VS was generally higher in the narrow-band than in the broadband condition, the narrow-band filtering imposes a strong low-pass characteristic on the temporal response characteristics. This low-pass characteristic reflects a stimulus feature rather than a temporal limit of neuronal processing.

The VS for MFs below 64 Hz was constant for the three binaural modulations in contrast to the monaural modulation. This may be due to the shape of the modulation, which is sinusoidal along a linear amplitude axis. As it is evident from the raster plot in figure 4.4A, the SAM responses had a higher “duty cycle” than the responses to the binaural modulations. This high duty cycle results from the compressive characteristics of the auditory periphery. Peripheral compression can be circumvented by modulating the amplitude sinusoidally along the dB axis (dBSAM). Studying a subgroup of neurons (N = 22) with dBSAM stimuli, it was found that the VS strongly increased compared to SAM

stimulation (figure 4.7A). Nevertheless VS still increased with increasing MF up to 64 Hz. The lower duty cycle of the dB SAM stimulus in contrast to the SAM stimulus is reflected in the lower response rate of low MFs (figure 4.7B).

In summary, both the temporal and rate characteristics of the recorded neurons indicated a difference in sensitivity and precision of the encoding of monaural modulations compared to binaural modulations. Specifically, the analysis in figure 4.5A showed that the VSs in response to monaural modulations at higher MFs were higher than in response to binaural modulations. In consequence, figure 4.5B shows that the proportion of neurons which produced significant VS at high MFs in response to monaural modulations at higher MFs was higher than in response to binaural modulations. These results appear indicative of a neuronal correlate of binaural sluggishness. In contrary to the psychophysical data, all three types of binaural modulations appeared to elicit very similar responses in the DNLL.

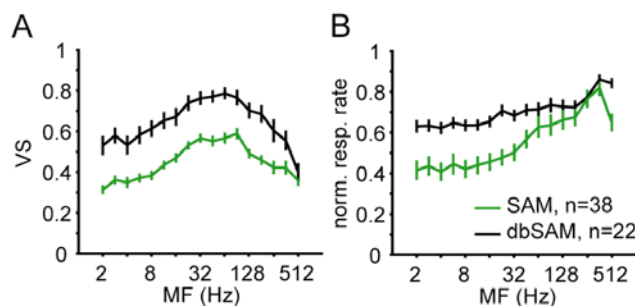


Figure 4.7 Effect of modulator shape on temporal and rate-response characteristics for monaural modulations. VS is shown as a function of MF for two types of monaural modulations, namely a classical SAM and a sinusoidal amplitude modulation imposed on a logarithmic (dB) amplitude scale. The latter modulator is designed to compensate for the peripheral auditory amplitude compression. The Population data show that with the SAM applied to a dB scale produces more accurate temporal firing characteristic expressed as a considerably higher VS. This temporal improvement is accompanied by a stronger increase in the rate response with increasing MF.

4.4.3 Comparison of psychophysical and electrophysiological performance

A crucial difference in the psychophysical and electrophysiological approaches is the way in which sensitivity is tested and expressed. In psychophysics, sensitivity is quantified as the SMR, which is required to detect the modulation. In the electrophysiology, stimuli were always at an infinite SMR and the sensitivity is quantified as VS.

Here, the human psychophysical performance and the electrophysiological sensitivity of gerbil DNLL neurons are directly compared using a ‘receiver operating characteristics’ (ROC) approach. The ROC analysis has been successfully used in a number of studies relating physiology to psychophysics (Britten et al. 1992; Skottun et al. 2001; Firzlafl et al. 2006). The neurometric function reflects the probability of an ideal observer to accurately detect the modulation basing his judgments on neuronal responses.

To generate neurometric functions, additional electrophysiological data were recorded from 19 neurons for the Oscan and the Phasewarp stimuli at MFs and SMRs matching the range of psychophysical data acquisition. Raster plots and period histograms of a single-cell response with Phasewarp stimulation are shown in figure 4.8. Both the precision of spike timing and the response strength increased with increasing SMR.

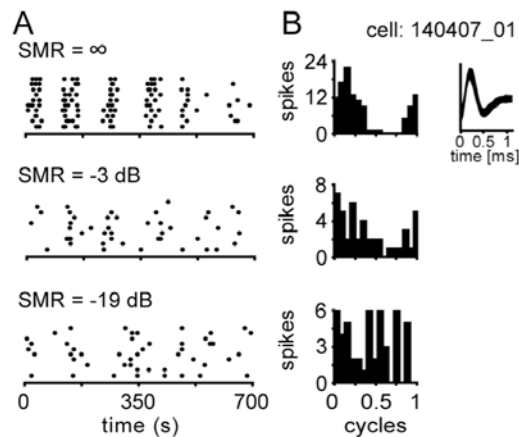


Figure 4.8 Responses of a DNLL cell to Phasewarp stimuli at a fixed MF of 8 Hz and different signal-to-masker ratios (SMRs). Raster plots in response to Phasewarp stimulation are shown in A; period histograms extracted from these responses are shown in B. At a SMR of infinity, the spikes are well locked to binaural modulation but this locking deteriorates with decreasing SMR. Again, this inset in B shows the highly stable spike waveform.

The ROC analysis was then performed by generating a so-called ROC curve for the comparison of each signal condition (SMR > -20 dB) and the standard condition (SMR = -20 dB). The ROC curve shows the probability that both the response in a signal condition and the response in the standard condition exceed a certain threshold. This probability was plotted as a function of the height of the threshold, resulting in so called ‘ROC curves’. From there, the (neuronal) percent correct discrimination for each signal condition was generated by calculating the area under the ROC curve. The ROC analysis

was applied either on the strength or on the timing of the recorded responses (see methods).

Examples of neurometric functions generated from the data in figure 4.8 and neurometric functions averaged across the population of 19 cells are shown in figure 4.9. Neurometric thresholds were extracted using the same threshold criterion (70.7 % correct) as in the psychophysics (dashed lines in figure 4.9).

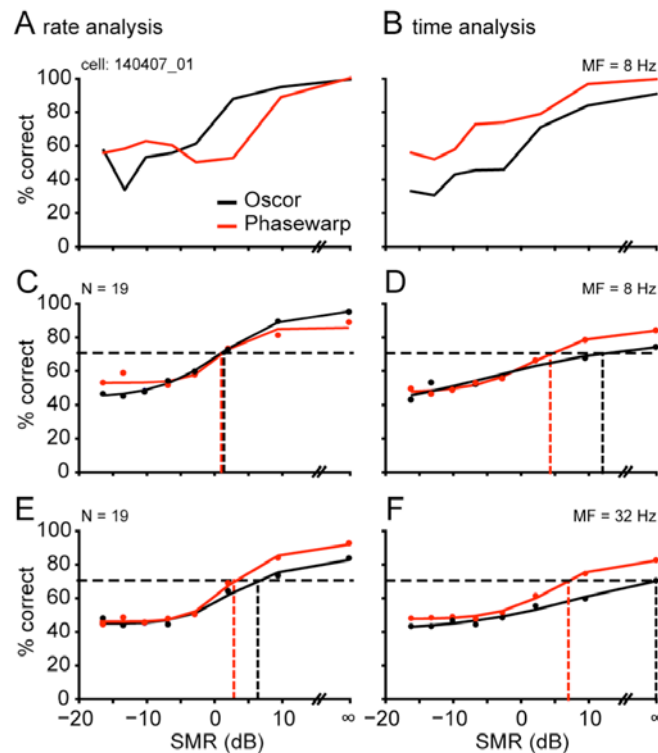


Figure 4.9 Neurometric functions based on a ROC analysis of the neuronal responses recorded as a function of SMR. Neurometric performance based on a rate analysis is shown in the left column; performance based on a temporal analysis is shown in the right column. Single-cell neurometric functions, expressed as percent correct choices of an ideal observer, are plotted as a function of SMR in **A** and **B**. Neurometric functions averaged across the population of cells recorded with this paradigm at a modulation frequency of 8 Hz are shown in **C** and **D**. Average neurometric functions in response to 32-Hz binaural modulations are shown in **E** and **F**. The horizontal dashed lines represent the threshold criterion (70.7 % correct). The vertical dashed lines show threshold SMRs extracted from a sigmoid fit to the averaged psychometric functions. Note that at a modulation frequency of 32 Hz, the averaged psychometric function based on the temporal analysis of the Oscor responses does not reach the threshold criterion (**F**).

A direct comparison of electrophysiological and psychophysical thresholds is shown in figure 4.10. Electrophysiological thresholds in the left column were based on a response-strength analysis, and electrophysiological thresholds in the right column were based on a

response-timing analysis. Overall, electrophysiological thresholds are higher than psychophysical thresholds. However, both with the rate-based and with the timing-based analysis, differences are found between electrophysiological sensitivity to the binaural properties of the Oscor and Phasewarp. In qualitative agreement with the psychophysical data, electrophysiological sensitivity to the Phasewarp is higher and persists to higher modulation frequencies compared to the Oscor. With the spike-timing analysis, no thresholds could be determined for Oscor stimulation at a modulation frequency of 32 Hz because the neurometric function averaged across the cell population just failed to reach the 70.7 % threshold criterion (cf. figure 4.9F).

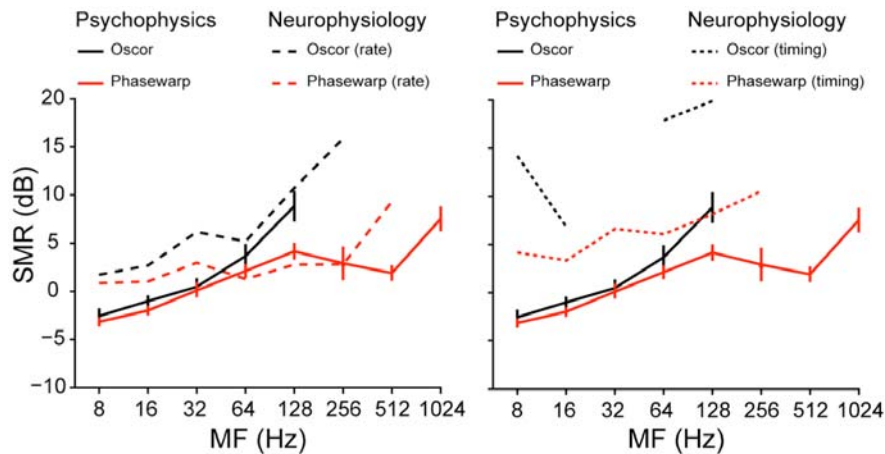


Figure 4.10 Direct comparison of the human psychophysical performance and the animal neurometric performance for the detection of binaural modulations. The psychophysical performance is shown by the solid lines in black for the Oscor and grey for the Phasewarp. Neurometric performance based on the rate analysis is shown in the **A**; neurometric performance based on the temporal analysis is shown in the **B**. Note that while overall neurometric performance is slightly worse than human psychophysical performance, both rate and temporal analyses of neuronal data indicate better thresholds for the Phasewarp than for the Oscor. Thus, the neurometric data reflect the human psychophysical performance qualitatively correct.

4.5 Discussion

This study was designed to directly compare temporal accuracy of the monaural and binaural system in following modulations of amplitude and interaural correlation, respectively. A combination of human psychophysics and gerbil electrophysiology was

used. A set of three different binaural stimuli was created with none of these providing any monaural cues for the modulation. Psychophysical sensitivity to binaural modulations depended strongly on the stimulus type: Sensitivity was worst for the Oscor01 stimulus where the modulation of interaural correlation was limited to the range between zero and one. An interaural correlation of zero produces no focused binaural image, whereas a correlation of one produces a well-focused, centralized binaural image. The psychophysical data show, however, that this modulation can only be detected at very low MFs (8 Hz). In the Oscor stimulus, the correlation is sinusoidally modulated between minus one and one. A correlation of minus one produces a semi-focussed binaural image, typically at a different position in the head than the highly focused image produced by a correlation of plus one. Thus, the Oscor produces a complex pattern of changes in spatial image width and position. The psychophysical sensitivity to the Oscor modulation was much better than to the Oscor01. All listeners could detect modulations up to 128 Hz. The Phasewarp stimulus produces a time-course of interaural correlation, which is most similar to a movement of a sound-source around the head. With the Phasewarp, sensitivity to binaural modulation was again considerably better than with the Oscor. Moreover, the low-pass characteristic of the sensitivity to the binaural modulation of the Phasewarp was well comparable to the low-pass characteristic of the sensitivity to the monaural modulation quantified with SAM noise. This finding suggests that given the optimal stimulation, the binaural system is not more sluggish than the monaural system. Recent electrophysiological evidence and simulations with realistic models of peripheral auditory processing show that the low-pass characteristic of the monaural system is largely determined by temporal integration associated with cochlear band-pass filtering and the time constants of inner-hair cell mechano-electrical transduction. This peripheral monaural 'sluggishness' is inevitable for the binaural system and consequently it is impossible for the binaural system to be faster than the monaural peripheral system. The current results appear to be at variance with the results of previous investigations of binaural temporal processing. Grantham (1982) also used Oscor stimuli to quantify the time constant of ITD extraction and found a considerably lower sensitivity. However, this study was performed with stimuli that were first filtered and then modulated and added. The modulation, applied after the filtering, produces side bands, which become increasingly audible with increasing MF. The author was well aware of this and confined

his analysis to that range of MFs, which were supposedly not contaminated with this spectral effect. Grantham concluded that the time constant of binaural processing was considerably longer than those described for monaural processing (Viemeister 1979; Dau et al. 1999). He also attempted to reconcile his results with previous studies by Pollak (1978) who found that listeners could detect the periodic switching between binaural sound sources with periods as short as 1.5 to 2 ms. More recent quantifications used a masking-period pattern paradigm (Kollmeier and Gilkey 1990) or a binaural probe configuration (Akeroyd and Summerfield 1999; Akeroyd and Bernstein 2001). These studies suggested a considerably longer window of temporal integration for the binaural system than for the monaural system. The apparent discrepancy of our results with those by e.g. Akeroyd and Summerfield (1999) may be related to the fact that these studies did not specifically implement time-variant ITDs as they are generated by, to some degree natural sources, like a moving sound source, but rather an abrupt change in interaural correlation. The binaural system might be more optimized in detecting naturally occurring changes in interaural parameters than in detecting the formation or disintegration of a focused sound source.

The first set of the current electrophysiological results shows that at the level of the gerbil auditory midbrain, the monaural modulations of the SAM noise and the binaural modulations of the Oscore and Phasewarp stimuli are well preserved. First, it is noteworthy that although the BFs of the recorded cells were mostly below 1 kHz, many cells showed significant vector strength to MFs as high as 512 Hz. The recordings with the band-pass filtered stimuli already show that filtering imposes a low-pass characteristic in the modulation domain. It appears that the band-pass filters in the gerbil inner ear are, despite the low BF, wide enough to transmit such high MFs.

Overall, the temporal code for monaural modulation was considerably better than for the binaural modulations. At higher MFs, both the VS averaged across the population and the number of units exhibiting significant VS is higher for SAM noise stimulation than for stimulation with any kind of binaural modulation. This difference could be interpreted as a neuronal correlate of binaural sluggishness.

In the only previous electrophysiological study on the dynamics of the mammalian binaural systems, published by Joris et al. (2006), single cells in the cat inferior colliculus were recorded while stimulating with the Oscore stimulus. Consistent with the present

results, Joris et al. reported a very good temporal encoding of the binaural modulations. The discrepancy of these electrophysiological findings with the strong binaural sluggishness reported in the human-psychophysical work by Grantham (1982) was interpreted in that there is no neuronal substrate at the level of the midbrain or higher to read out this temporal code. The current psychophysical data indicate, however, that the Phasewarp stimulus is capable of producing perceivable modulations of ITDs at MFs up to 1024 Hz. These new results indicate that with optimal stimulation, the central auditory system, at the level of the inferior colliculus and above, is well capable of reading out the temporal code of binaurally sensitive units when the time-course of activation along both the ITD and the time axis is appropriate.

The second electrophysiological data set was recorded to quantitatively compare psychophysical and electrophysiological binaural modulation detection. Here, not only the MF was varied but also the signal-to-masker ratio was varied in a manner consistent with the psychophysics. A ROC analysis based either on the response strength or on spike timing revealed significant differences between the encoding of the binaural modulations of Oscor and Phasewarp. The neurometric thresholds are in at least qualitative agreement with the psychophysical thresholds. Note that these differences are apparently swamped when the stimuli are only presented at full modulation depth, as it is typically done in electrophysiological experiments.

It is remarkable that the ROC analysis based on the response strength provides a better fit to the psychophysical data than the analysis based on spike timing. Nevertheless, it may be critical to associate the psychophysical performance with the response strength: As outlined in the psychophysical control experiment, the degree of interaural correlation in higher frequency channels, where the binaural system is mostly driven by the stimulus envelope, is lower for the Phasewarp than for uncorrelated noise. In consequence, the degree of interaural correlation in at these frequencies decreases with decreasing SMR. A neuron that is sensitive to interaural correlation per se, as described by Shackleton et al. (2005) could pick up these changes. The ROC analysis based on spike-timing using the Kullback-Leibler divergence, however, was specifically designed to be insensitive to changes in response strength. Also with this analysis, neuronal sensitivity to the Phasewarp was better than to the Oscor.

Taken together, the current psychophysical and electrophysiological data show that given appropriate binaural stimulation, the binaural system can process time variant ITDs similarly fast as the monaural system can process time-variant amplitudes. The limits of processing were measured using detection thresholds. At binaural or monaural modulation frequencies above 8 Hz, neither the monaural nor the binaural system is able to “track” the modulation as specific level fluctuation or binaural movement or spatial image width change. Rather, a monaural or binaural flutter or roughness is perceived. If the term binaural sluggishness is used and related to time constants ≥ 10 Hz, the authors claim that this does not describe the temporal resolution of internal binaural information accessible to higher stages of the brain. More likely, an additional binaural sluggishness is task dependent and occurs if the task is to “track” specific interaural changes, as tracking a source in space or to perceive movement. The electrophysiological data show that neuronal encoding at the level of the DNLL is very fast. Our capability to read out these fast modulations, however, appears to depend strongly on the type of ITD change. The read out appears to be much more effective when a focused binaural image is present at all times while the read out appears sluggish when a binaural image emerges and disintegrates periodically. The ROC analysis and resulting neurometric thresholds show that both neuronal response strength and timing transmit information, which substantiates the perceptual differences in the processing of binaural modulations.

5 General discussion and outlook

In the presented thesis, I addressed three novel approaches for the analysis of sound localization. In mammals, localization of sound sources in the horizontal plane is primarily achieved by an extraordinary sensitivity to time differences between the ears. These ITDs are processed by neurons in the brainstem, which are sensitive to ITDs in the microsecond range. However, despite decades of research on this topic, surprisingly little is known about ITD processing in the DNLL and the binaural processing of multiple or moving sound sources. To address these questions I measured the ITD sensitivity of a large population of neurons in the DNLL of anesthetized gerbils.

In the first study I characterized the ITD sensitivity of low-frequency DNLL neurons (chapter 2). It appears that most of the low-frequency DNLL neurons express ITD sensitivities that closely resemble those seen in the MSO and LSO. Furthermore, the data confirmed the hypothesis that the location of low frequency sounds is encoded via a population rate-code.

In the second study I used the DNLL as a model to investigate the localization of tones with concurrent background noise and analyzed how these different sound sources influenced each other (chapter 3). I found that the ITD sensitivity of DNLL neurons strongly depends on the locations, the levels, and the spectral compositions of the concurrent sound sources.

In a third study I compared the speed of binaural and monaural processing (chapter 4). These data show that the binaural system can follow changes of the binaural cues much faster than reported previously, when using plausible auditory motion stimulation. In addition, close correlations between psychophysical findings and the neuronal responses in the DNLL could be shown.

5.1 Sensitivity to interaural time differences in the dorsal nucleus of the lateral lemniscus

In the studies presented I focused on low frequency neurons. The abundance of low frequency DNLL neurons is consistent with the well developed low frequency hearing capabilities in the Mongolian gerbil (Ryan 1976). Besides the existence of low frequency DNLL neurons, the existence of a large number of high-frequency neurons in the gerbil DNLL was described in a complementary study from our laboratory (Pecka et al. 2007).

In the first set of experiments, I found a large number of low-frequency ITD-sensitive neurons, which can synchronize their discharge to a specific phase angle of the low frequency tones. The majority of these DNLL neurons showed either a characteristic peak- or trough-type ITD sensitivity, which is known to originate in the MSO and LSO, respectively (Goldberg and Brown 1969; Yin and Kuwada 1983b; Yin and Chan 1990; Spitzer and Semple 1995; Batra et al. 1997a; Batra et al. 1997b; Tollin and Yin 2005). The finding of this unaltered peak- and trough-type ITD sensitivity in the DNLL indicates no substantial further processing of the ITD sensitivity within the DNLL at least in a large population of cells. I also found intermediate-type ITD sensitivity. It is unclear to what extent such intermediate-type ITD sensitivity in DNLL neurons arises from convergent inputs within the DNLL and to what extent it is derived from SOC inputs. My data exclude the possibility that intermediate-type ITD sensitivity is a feature arising first in the IC, since the DNLL is located between the SOC and IC. However, the origin of intermediate-type ITD sensitivity cannot be answered from this study. A possible approach would be to perform electrophysiological recordings in the SOC or in the DNLL and pharmacologically block one of the inputs. Such experiments could contribute to the open question how binaural properties are modified within the DNLL in general.

Results from many studies over the past decades have shown that binaural properties, ITDs and IIDs, are processed in the SOC (for review: Yin 2002). As shown in several studies, the IID-sensitivity is modified in the ascending pathway by inhibitory inputs of the DNLL (Pecka et al. 2007; for review: Pollak et al. 2003). Furthermore, Pollak and colleagues questioned the hypothesis that IID sensitivity exclusively originates in the SOC, showing that it can also be created *de novo* in the IC (Pollak et al. 2003). Regarding ITD sensitivity little is known about modifications or *de novo* generation of the ITD

sensitivity in the ascending binaural pathway. The processing of ITDs requires very exact temporal inputs. One argument against *de novo* generation of ITD sensitivity is that the timing I observed in the DNLL is less exact than the timing observed for the VCN inputs to the coincidence detectors (Joris et al. 1994; Paolini et al. 2001). A similar decrease in the precise timing within the ascending pathway beyond the SOC has also been described by Kuwada et al. (2006). Therefore, it is unlikely that ITD sensitivity is *de novo* generated in the DNLL or in other binaural nuclei beyond the SOC. However, the ITD sensitivity could be modified in the ascending binaural pathway. Kuwada and colleagues suggest that ITD functions are sharpened along the ascending auditory pathway and that first signs of this sharpening are visible in the DNLL (Kidd and Kelly 1996; Wu 1999; Fitzpatrick and Kuwada 2001; Kuwada et al. 2006). They hypothesize that the sharpening could arise through glycinergic inputs from the LSO or GABAergic inputs from the opposite DNLL. Preliminary data measuring the ITD sensitivity of static tones via a pharmacological block of the inhibitory inputs showed that the ITD tuning was not changed in any way by inhibitory inputs (personal observations). Thus, inhibitory inputs may not modify the basic processing of static pure tones in the DNLL. This may differ if complex stimuli with dynamic ITDs are presented as suggested by recent data (Hamish Meffin; manuscript submitted). He found that in natural environments concurrent sound sources produce various fast fluctuations of ITDs and IIDs. These fast fluctuations do not encode the locations of the concurrent signals, but rather blur the valid interaural cues. Using extracellular recordings he found that fast fluctuations of binaural cues could suppress the neuronal response of DNLL neurons. Using a model circuitry centered on the DNLL as proposed by Pecka et al. (2007), he suggests that the persistent inhibition from the opposite DNLL may selectively suppress signals associated with the fast spurious fluctuations but not those associated with valid binaural cues.

Taken together, it appears that for most of the DNLL neurons the ITD sensitivity to static stimuli is nearly identical to those seen in the MSO and LSO. Hence, the electrophysiological recording from the DNLL appears to be a novel and appropriate way to study the basic neuronal processing of ITDs. However, this may be different if more complex concurrent stimuli are used.

5.2 Processing of concurrent sounds by neurons sensitive to interaural time differences

5.2.1 Localization of concurrent sounds

Psychophysical studies, investigating the localization of tones in background noise, showed a decline of accurate discrimination with increasing noise levels (Stern et al. 1983; Good and Gilkey 1996). These findings are consistent with the single cell responses shown in the study described in Chapter 3. Here I could show that DNLL neurons, which were sensitive to ITDs of tones, lost this sensitivity if white noise as concurrent background was presented. This decrease of the ITD sensitivity mostly resulted from a decrease of the response to tones at favorable ITDs. Interestingly, the concurrent noise only marginally increased the response to tones at unfavorable ITDs. Thus, minimal or no response to tones at unfavorable ITD was achieved, even if concurrent noise alone elicited responses. The tone at unfavorable ITDs suppressed the response to the noise and thereby assured the robustness of ITD sensitivity to tones in background noise (see chapter 3). This finding is of particular interest, since most studies about ITD coding focused so far on the maximal response at favorable ITD. Based on these results, I suggest that neuronal ITD sensitivity is not exclusively encoded by the maximal response to favorable ITD but also by the minimal response to unfavorable ITDs. This hypothesis is in contrast to the place-code model, which suggests, that ITDs are exclusively encoded by a maximal response to a certain ITD

The presented data are insufficient to draw conclusions about the neuronal mechanism. However, they suggest that the suppressive effects of tones at unfavorable ITDs occur at the level of the coincidence-detector. Such suppressive effects of tones at unfavorable ITDs, albeit less pronounced, had already been observed in the MSO years ago by Goldberg and Brown (1969). They found that the binaural responses to tones at unfavorable ITDs could suppress the responses to monaural stimuli. Two different hypotheses exist to explain this suppression. The first hypothesis formulated by Brand et al. (2002) suggested that inhibitory inputs suppress the response at unfavorable ITDs. Inhibition and excitation arriving at the coincidence-detector are phase-locked to the stimulus waveform. At a particular unfavorable ITD, inhibitory and excitatory inputs are

on top of each other and the inhibition suppresses the response (Brand et al. 2002; see chapter 1.3). In contrast, a second hypothesis postulated that a simple coincidence model without inhibition is adequate to describe suppressive effects of tones at unfavorable ITDs (Colburn et al. 1990). Using this model with two excitatory inputs, Colburn et al. explained the suppressive effects with the following three assumptions: (i) coincidence-detector neurons are spontaneously innervated; (ii) acoustic stimulation induces synchronization of the response and (iii) an absolute neuronal refractory time follows after a response. They found that the synchronized response led to a synchronized “no-response”, which was below the spontaneous activity of the neuron. This resulted in a lack of coincidences, or suppressive effects of the binaural response, when the synchronized excitatory inputs were out of phase and the synchronized “no-responses” were in phase (Colburn et al. 1990). Additional evidence comes from *in vitro* patch clamp studies in the MSO equivalent of birds, the nucleus laminaris, by Reyes et al. (1996), showing that two out of phase stimulations evoked less neuronal firing than a single stimulation. The authors suggested that the modulation of the discharge rate, at least in birds, did not critically depend on inhibitory inputs but rather on membrane properties of the coincidence-detector neurons. Subsequent experiments showed that these membrane properties of neurons in the nucleus laminaris are strongly modulated by inhibition (Brückner and Hyson 1998; Monsivais et al. 2000). However, several studies showed that mammals and birds probably developed different mechanisms to encode ITDs (for review: Grothe 2003). Now, both mechanisms described above might contribute to the suppressive effects of tones at unfavorable ITD. On the basis of the experiments presented here, neither hypothesis can be favored. Further studies, e.g. using patch clamp experiments in mammals, are necessary to clarify this issue.

While extra-cellular single cell recordings measure the result of the neuronal processing, the action potentials of a neuron, the underlying cellular mechanisms can only be hypothesized. In contrast to this, patch clamp studies allow a detailed study of the cellular mechanisms. However, most patch clamp studies are performed *in vitro* in acute brain slices or cell cultures and are restricted to “unphysiological” stimulations of the neuronal circuitry within this brain slice. Furthermore, spontaneous activity is mostly absent in neurons in brain slices. This absence of spontaneous activity may influence the synaptic transmission of auditory brain neurons as recently shown by Hermann et al. (2007). They

reintroduced *in vivo*-like spontaneous activity to *in vitro* brainstem synapses and found that the steady-state amplitude of the excitatory postsynaptic currents and, accordingly, the excitability of the neurons were reduced. As spontaneous active inputs are also one of the important features of the coincidence-detector model described by Colburn et al. (1990), a combined approach such as *in vivo* patch clamp studies would be useful as have been performed for example more than 10 years ago by Casseday et al. (1994). This method combines the advantages of both methods and permits *in vivo* investigation of cellular mechanisms, thus enabling a test of the hypothesized sub-threshold excitatory or inhibitory currents.

Investigating the general role of coincidence-detector neurons in the processing of concurrent sounds by using tones and background noise was experimentally challenging. First, the noise activated strong inhibitory interactions across frequency, which most likely did not involve the coincidence-detection. Second, the effective intensities of these two sound sources were not easily comparable (see chapter 3). Based on these two findings, two pure tones instead of noise and tone as concurrent sound sources were used in subsequent experiments. The rationale of such an approach is the possibility to compare the effective levels of the two sound sources and to diminish cross-frequency interactions. Preliminary data using two tones with different frequencies showed that neurons could be sensitive to ITDs of both tones if the difference between the effective levels of the tones was below 20 dB. If this difference is increased, the neurons were only sensitive to ITDs of the tone with the higher intensity. This simple finding opens the field for many further investigations. In the next part I will focus on one possible experiment.

ITDs are encoded by a population of neurons (Jeffress 1948; Fitzpatrick et al. 1997; Hancock and Delgutte 2004; Harper and McAlpine 2004; Stecker et al. 2005). Therefore, an increase in the number of ITD-sensitive neurons could increase the precision of sound localization. How many ITD-sensitive neurons are necessary to achieve the psychophysical precision in detecting just noticeable differences in ITD? As mentioned in the introduction, Skottun and colleagues hypothesized that this precise detection of ITDs could be accomplished by single ITD-sensitive neurons (Skottun et al. 2001; Shackleton et al. 2003). A combined electrophysiological and psychophysical study analyzing the ITD sensitivity to tones with an increasing masking level of another concurrent tone

could test this hypothesis. This experimental approach would take advantage of the finding that the psychophysical accuracy in detecting just noticeable differences in ITD and the ITD sensitivity in the DNLL decrease with masking sounds. Thus, comparing the psychophysical accuracy with the ITD sensitivity in the DNLL could give an estimate how many DNLL neurons are needed for the precise encoding of ITDs.

5.2.2 Detection and grouping of concurrent sounds

It is an ongoing question to what extents the ITDs of concurrent sounds are used to detect, segregate and group auditory signals. The contribution of ITDs to the detection is classically shown by the binaural masking level difference. The binaural masking difference indicates that the perceptual detection of a tone, masked by noise, is improved when the tone and the noise are presented with different ITDs (Moore 2003). Careful studies in the Palmer laboratory could correlate this psychophysical phenomenon with neuronal data of ITD-sensitive neurons in the IC (for review: Palmer and Shackleton 2002). However, as described in chapter 3, the effect of noise on the response of tones depends on spectral and temporal processing. Since Palmer and colleagues neglected the spectral processing and, according to the psychophysical experiments, estimated the detection of tones using two quite unnatural conditions, this data cannot entirely explain the underlying mechanism of how ITDs of the different sound sources influences the detection. Furthermore, the connection between localization and detection of concurrent sounds is unclear. Preliminary psychophysical data, using a tone as signal and a second tone as masker, suggest that with increasing signal-to-masker ratio the accuracy to detect ITDs of the signal decreases. Interestingly, at the signal-to-noise ratio, at which the listeners accuracy to detect ITD decreases, the listeners had no problems to detect the tone. These results indicate that the signal-to-masker threshold for the detection of a tone is much lower than for the localization. Thus, with an increasing signal-to-masker ratio, the tones are first detected and than localized. This finding indicates that ITDs could only influence the detection at low signal-to-masker ratios. For precise localization, the binaural processing of signals requires a higher signal-to-masker ratio than the neuronal detection of the signal. From these findings I hypothesize that ITD-sensitive neurons can

improve the detection, which is possibly processed by a different population of monaural neurons.

In contrast to the detection of auditory signals, only some psychophysical studies investigated the contribution of ITDs to grouping and segregation of different sound sources (Culling and Summerfield 1995; Darwin and Hukin 1997; Drennan et al. 2003). These experiments are based on the fact that human listeners can identify competing vowels, whose first and second formants are represented by a pair of discrete bands of noise. Systematically changing the ITDs of the noise-band pairs, Drennan et al. (2003) could show that listeners are able to segregate concurrent vowels based only on the ITDs. To date, electrophysiological data investigating the grouping of different sound sources using ITDs are missing. The results reported in chapter 3 and my preliminary data from stimulations with two tones indicate that the neuronal response highly depends on the ITD of the two sound sources. Consequently, the neuronal response depends on matched or unmatched ITDs of the concurrent tones. These results strongly suggest some kind of grouping, which requires further investigation.

5.2.3 Pitch detection of concurrent sounds

The results reported in chapter 3 showed that the spectral composition of concurrent sound sources has a strong effect on the response of the ITD-sensitive neurons. This finding leads to the question of whether ITD-sensitive neurons could contribute to the perception of pitches. More than twenty years ago Loeb et al. (1983) hypothesized that the coincidence-detector could be involved in the perception of pitches. In their model a pitch of two tones can be detected by a detection of synchronicity between the two signals. This detection of synchronicity requires neuronal sensitivity to differences in the relative timing of the input signals, a feature described for the coincidence-detectors in the MSO. Unfortunately, this hypothesis was not further investigated and electrophysiological data investigating the response of ITD-sensitive neurons to concurrent tones by changing the pitch are missing. My preliminary data using two concurrent tones raise several questions regarding this issue. For all neurons observed, the low-frequency tone had to be more intense to have the same effect on the high-frequency tone as the high-frequency tone had on the low-frequency tone. However, the

average response to the two tones was quite similar. This effect could be explained by an increased temporal precision for high-frequency tones (Koppl 1997; Paolini et al. 2001). Yet, an interesting future study would be to investigate the dependency of the pitch on the response of the ITD-sensitive neurons to two tones. In addition, related human psychophysical masking experiments using two tones would be beneficial. As mentioned above (5.2.2), preliminary psychophysical data suggest that the masking thresholds for detection and localization of tones differ. What is the masking threshold for the pitch perception? Is it similar to the masking threshold for detection or to the threshold for the localization of tones? If both pitch perception and localization, were computed within the same neuronal circuitry, would the pitch detection threshold be at the same level as the threshold for localization? These questions will need to be addressed in future studies requiring electrophysiological and psychophysical experiments.

5.2.4 Adaptation to noisy background

Background noise can change the ITD sensitivity to tones as shown in Chapter 3. But what happens if animals are constantly exposed to noise? Do they adapt to the background noise? During development, the physiological features of ITD-sensitive neurons of young animals are changed by a noisy environment (Kapfer et al. 2002; Seidl and Grothe 2005). These findings suggest that the neuronal network around the MSO is plastic. During my diploma thesis and in studies together with Evelyn Schiller I showed that a noisy background has a high impact on the binaural response of DNLL neurons in adult stages as well (Kollmar 2003; Schiller 2007; manuscript in preparation). The exposure to omnidirectional noise changed the ITD and IID coding of the neurons. More simply, the noise exposure resulted in alterations of both the ITD and the IID sensitivity. The effects disappeared when animals were allowed to recover for more than 14 days after the exposure to the noise. The experiments indicate a quantifiable, reversible adaptation in sound localization mechanisms, which can be used as a model system to investigate adult plasticity in the auditory brainstem without damaging or invasive treatment.

These changes of the ITD and IID coding most likely resulted from changes of the complex binaural interactions in the SOC and can be explained by an increase of the

inhibitory input. The inhibitory input to the LSO and MSO is known to be glycinergic. Recent studies by Magnusson et al. (2005b) showed that the glycinergic and glutamatergic currents in the LSO are regulated by a dendritic GABA release. Furthermore, the authors found substantial GABAergic effects on the responses of LSO neurons recorded *in vivo*. In conclusion, they hypothesize that the GABA release in the LSO depends on the spiking activity and thereby GABA controls the gain of the inputs in the LSO. Preliminary *in vitro* data from MSO neurons suggest that GABA might also influence the glycinergic currents in the MSO (Ursula Koch, personal communications). However, if the GABAergic system controls the gain in the SOC, it is likely that the continuous noise exposure changes this GABAergic control system. However, to investigate the underlying cellular physiological mechanisms, the best experiments would be comparative *in vitro* patch clamp studies of animals with or without noise exposure. A cellular understanding of the adaptation to background noise and the potential mechanisms would help to understand the general problem of processing concurrent noise.

5.3 Processing of binaurally modulated auditory signal

The sensitivity to ITDs shows remarkable acuity. However, in contrast to the monaural system, the binaural system has been hypothesized to be sluggish in following binaural modulations (for review: Moore 2003). The origin of binaural sluggishness is unclear, but has been hypothesized to arise between a general binaural processor and a more centrally located detection mechanism (Grantham 1982). However, recent electrophysiological data suggest that binaural sluggishness is not caused by a sluggish temporal processing at the level of the first binaural processor (Joris et al. 2006). This finding was also confirmed by my electrophysiological data (chapter 4). In addition, the psychophysical data from chapter 4 challenge the view of binaural sluggishness. Using a new stimulation of binaural modulation, the binaural perception was significantly better than reported previously. These data show that the binaural system can process fast binaural modulations. The perception and the neuronal DNLL response depend on the type of binaural modulation used. This finding, in conjunction with the results from Hamish

Meffin (mentioned above in chapter 5.1), suggests that the neuronal discharge of DNLL neurons depends on the changes of the binaural cues. Similar findings are reported for IC neurons. Spitzer and Semple (Spitzer and Semple 1991; Spitzer and Semple 1993) showed that IC neurons in the gerbil and cat are responsive to different types of IPD changes. The authors concluded that the discharge of IC neurons reflects the recent history of stimulation. Extending these findings, McAlpine et al. (2000) could show that the response of IC neurons to interaurally modulated stimuli does not depend on the history of the stimulation but on the history of their response to stimulation. These results suggest an adaptation mechanism at or above the level of binaural integration. Hence, I hypothesize that the different responses recorded in the DNLL are part of an adaptation mechanism, which may improve the auditory localization performance to stimuli. This adaptation could be driven by GABAergic regulated mechanism as suggested above (Magnusson et al. 2005b, chapter 5.3.4). Interestingly, the most naturalistic stimulus (chapter 4) achieved the best psychophysical and neuronal performance. To test the hypothesis that features of a naturalistic stimulus may in general trigger adaptive mechanisms and thus improve the psychophysical and neuronal performances, further studies will be required.

Taken together, the DNLL serves as a novel and effective model system to further study binaural processing. In the presented thesis, I investigated several points of binaural processing, focusing on the processing of ITDs. The usage of more complex and naturalistic stimuli turned out to be a promising and also necessary approach for further analysis and will hopefully help to shed light on the mechanisms of sound localization in natural environments. In a larger perspective, my findings could also be of clinical interest, since the processing of concurrent naturalistic signals is one of the major problems of the aging hearing deficits and of its medical treatment devices, such as hearing aids and cochlear implants.

References

Adams JC and Mugnaini E. Dorsal nucleus of the lateral lemniscus: a nucleus of GABAergic projection neurons. *Brain Res Bull* 13:585-590, 1984.

Adams JC and Mugnaini E. Immunocytochemical evidence for inhibitory and disinhibitory circuits in the superior olive. *Hear Res* 49: 281-298, 1990.

Adelson EH and Bergen JR. Spatiotemporal energy models for the perception of motion. *J Opt Soc Am A* 2: 284-299, 1985.

Aitkin LM, Anderson DJ and Brugge JF. Frequency Organization and Response Characteristics of Single Neurons in Nuclei of Lateral Lemniscus of Cat. *J Acoust Soc Am* 47: 59, 1970.

Akeroyd MA and Bernstein LR. The variation across time of sensitivity to interaural disparities: behavioral measurements and quantitative analyses. *J Acoust Soc Am* 110: 2516-2526, 2001.

Akeroyd MA and Summerfield AQ. A binaural analog of gap detection. *J Acoust Soc Am* 105: 2807-2820, 1999.

Bajo VM, Villa AE, de Ribaupierre F and Rouiller EM. Discharge properties of single neurons in the dorsal nucleus of the lateral lemniscus of the rat. *Brain Res Bull* 47: 595-610, 1998.

Batra R, Kuwada S and Fitzpatrick DC. Sensitivity to interaural temporal disparities of low- and high- frequency neurons in the superior olivary complex. i. heterogeneity of responses. *J Neurophysiol* 78: 1222-1236, 1997a.

Batra R, Kuwada S and Fitzpatrick DC. Sensitivity to interaural temporal disparities of low- and high- frequency neurons in the superior olivary complex. ii. coincidence detection. *J Neurophysiol* 78: 1237-1247, 1997b.

Batra R and Yin TC. Cross correlation by neurons of the medial superior olive: a reexamination. *J Assoc Res Otolaryngol* 5: 238-252, 2004.

Batschelet E. *Circular statistics in Biology*. London: Academic Press, 1981.

Beckius GE, Batra R and Oliver DL. Axons from anteroventral cochlear nucleus that terminate in medial superior olive of cat: observations related to delay lines. *J Neurosci* 19: 3146-3161, 1999.

Bernstein LR and Trahiotis C. Lateralization of low-frequency, complex waveforms: the use of envelope-based temporal disparities. *J Acoust Soc Am* 77: 1868-1880, 1985.

Blauert J. Spatial hearing: The psychophysics of human sound localization. Cambridge, Massachusetts: MIT Press, 1997.

Boudreau JC and Tsuchitani C. Binaural interaction in the cat superior olive S segment. *Journal of Neurophysiology* 31: 442-454, 1968.

Brand A, Behrend O, Marquardt T, McAlpine D and Grothe B. Precise inhibition is essential for microsecond interaural time difference coding. *Nature* 417: 543-547, 2002.

Britten KH, Shadlen MN, Newsome WT and Movshon JA. The analysis of visual motion: a comparison of neuronal and psychophysical performance. *J Neurosci* 12: 4745-4765, 1992.

Brown AM. Acoustic distortion from rodent ears: a comparison of responses from rats, guinea pigs and gerbils. *Hear Res* 31: 25-37, 1987.

Brückner S and Hyson RL. Effect of GABA on the processing of interaural time differences in nucleus laminaris neurons in the chick. *Eur J Neurosci* 10:3438-3450, 1998.

Brugge JF, Anderson DJ and Aitkin LM. Responses of neurons in the dorsal nucleus of the lateral lemniscus of cat to binaural tonal stimulation. *J Neurophysiol* 33: 441-458, 1970.

Burger RM and Pollak GD. Reversible inactivation of the dorsal nucleus of the lateral lemniscus reveals its role in the processing of multiple sound sources in the inferior colliculus of bats. *J Neurosci* 21: 4830-4843, 2001.

Cai H, Carney LH and Colburn HS. A model for binaural response properties of inferior colliculus neurons. I. A model with interaural time difference-sensitive excitatory and inhibitory inputs. *J Acoust Soc Am* 103: 475-493, 1998a.

Cai H, Carney LH and Colburn HS. A model for binaural response properties of inferior colliculus neurons. II. A model with interaural time difference-sensitive excitatory and inhibitory inputs and an adaptation mechanism. *J Acoust Soc Am* 103: 494-506, 1998b.

Caird D and Klinke R. Processing of binaural stimuli by cat superior olivary complex neurons. *Exp Brain Res* 52: 385-399, 1983.

Caird D and Klinke R. Processing of interaural time and intensity differences in the cat inferior colliculus. *Exp Brain Res* 68: 379-392, 1987.

Caird DM, Palmer AR and Rees A. Binaural masking level difference effects in single units of the guinea pig inferior colliculus. *Hear Res* 57: 91-106, 1991.

Cant NB and Casseday JH. Projections from the anteroventral cochlear nucleus to the lateral and medial superior olivary nuclei. *J Comp Neurol* 247: 457-476, 1986.

Cant NB and Hyson RL. Projections from the lateral nucleus of the trapezoid body to the medial superior olivary nucleus in the gerbil. *Hear Res* 58: 26-34, 1992.

Carney LH and Yin TC. Responses of low-frequency cells in the inferior colliculus to interaural time differences of clicks: excitatory and inhibitory components. *J Neurophysiol* 62: 144-161, 1989.

Carr CE and Konishi M. Axonal delay lines for time measurement in the owl's brainstem. *Proc Natl Acad Sci U S A* 85: 8311-8315, 1988.

Carr CE and Soares D. Evolutionary convergence and shared computational principles in the auditory system. *Brain Behavior and Evolution* 59: 294-311, 2002.

Casseday JH, Ehrlich D and Covey E. Neural tuning for sound duration: role of inhibitory mechanisms in the inferior colliculus. *Science* 264: 847-850, 1994.

Chen L, Kelly JB and Wu SH. The commissure of probst as a source of GABAergic inhibition. *Hear Res* 138:106-14, 1999.

Clark GM and Dunlop CW. Field potentials in the cat medial superior olivary nucleus. *Exp Neurol* 20:31-42, 1968.

Clark GM. The ultrastructure of nerve endings in the medial superior olive of the cat. *Brain Res* 14: 293-305, 1969.

Cohen MF. Interaural time discrimination in noise. *J Acoust Soc Am* 70: 1289-1293, 1981.

Cohen MF and Koehnke J. Detection and interaural time discrimination of a sinusoid masked by interaurally delayed white noise. *J Acoust Soc Am* 72: 1418-1420, 1982.

Colburn HS, Han YA and Culotta CP. Coincidence model of MSO responses. *Hear Res* 49: 335-346, 1990.

Covey E. Response properties of single units in the dorsal nucleus of the lateral lemniscus and paralemniscal zone of an echolocating bat. *J Neurophysiol* 69: 842-859, 1993.

Crow G, Rupert AL and Moushegian G. Phase locking in monaural and binaural medullary neurons: implications for binaural phenomena. *J Acoust Soc Am* 64: 493-501, 1978.

Culling JF and Summerfield Q. Perceptual separation of concurrent speech sounds: absence of across- frequency grouping by common interaural delay. *J Acoust Soc Am* 98: 785-797, 1995.

D'Angelo WR, Sterbing SJ, Ostapoff EM and Kuwada S. Role of GABAergic inhibition in the coding of interaural time differences of low-frequency sounds in the inferior colliculus. *J Neurophysiol* 93: 3390-3400, 2005.

Darwin CJ and Hukin RW. Perceptual segregation of a harmonic from a vowel by interaural time difference and frequency proximity. *J Acoust Soc Am* 102: 2316-2324, 1997.

Dau T, Verhey J and Kohlrausch A. Intrinsic envelope fluctuations and modulation-detection thresholds for narrow-band noise carriers. *J Acoust Soc Am* 106: 2752-2760, 1999.

Drennan WR, Gatehouse S and Lever C. Perceptual segregation of competing speech sounds: the role of spatial location. *J Acoust Soc Am* 114: 2178-2189, 2003.

Ewert SD and Dau T. Characterizing frequency selectivity for envelope fluctuations. *J Acoust Soc Am* 108: 1181-1196, 2000.

Field KJ and Siebold AL. *Hamster and Gerbil*. London, UK: CRC: 1999.

Firzlaff U, Schornich S, Hoffmann S, Schuller G and Wiegrebe L. A neural correlate of stochastic echo imaging. *J Neurosci* 26: 785-791, 2006.

Fitzpatrick DC, Batra R, Stanford TR and Kuwada S. A neuronal population code for sound localization. *Nature* 388: 871-874, 1997.

Fitzpatrick DC and Kuwada S. Tuning to interaural time differences across frequency. *J Neurosci* 21: 4844-4851, 2001.

Fitzpatrick DC, Kuwada S and Batra R. Transformations in processing interaural time differences between the superior olivary complex and inferior colliculus: beyond the Jeffress model. *Hear Res* 168: 79-89, 2002.

Gai Y and Carney LH. Temporal measures and neural strategies for detection of tones in noise based on responses in anteroventral cochlear nucleus. *J Neurophysiol* 96: 2451-2464, 2006.

Gerstner W and van Hemmen JL. Coding and information processing in neuronal networks. In: Models of neuronal networks II, edited by Domany E, van Hemmen JL and Schulten K. New York: Springer-Verlag, 1994.

Glendenning KK, Brunso-Bechtold JK, Thompson GC and Masterton RB. Ascending auditory afferents to the nuclei of the lateral lemniscus. *J Comp Neurol* 197: 673-703, 1981.

Goldberg JM and Brown PB. Functional organization of the dog superior olivary complex: an anatomical and electrophysiological study. *J Neurophysiol* 31: 639-656, 1968.

Goldberg JM and Brown PB. Response of binaural neurons of dog superior olivary complex to dichotic tonal stimuli: some physiological mechanisms of sound localization. *J Neurophysiol* 32: 613-636, 1969.

Goldberg JM and Greenwood DD. Response of neurons of the dorsal and posteroventral cochlear nuclei of the cat to acoustic stimuli of long duration. *J Neurophysiol* 29: 72-93, 1966.

Gollisch T. Estimating receptive fields in the presence of spike-time jitter. *Network* 17: 103-129, 2006.

Good MD and Gilkey RH. Sound localization in noise: the effect of signal-to-noise ratio. *J Acoust Soc Am* 99: 1108-1117, 1996.

Grantham DW. Detectability of time-varying interaural correlation in narrow-band noise stimuli. *J Acoust Soc Am* 72: 1178-1184, 1982.

Grantham DW and Wightman FL. Detectability of varying interaural temporal differences. *J Acoust Soc Am* 63: 511-523, 1978.

Grantham DW and Wightman FL. Detectability of a pulsed tone in the presence of a masker with time-varying interaural correlation. *J Acoust Soc Am* 65: 1509-1517, 1979.

Green DM and Swets JA. Signal detection theory and psychophysics. 1966.

Greenwood DD and Maruyama N. Excitatory and inhibitory response areas of auditory neurons in the cochlear nucleus. *J Neurophysiol* 28: 863-892, 1965.

Grothe B. The evolution of temporal processing in the medial superior olive, an auditory brainstem structure. *Prog Neurobiol* 61: 581-610, 2000.

Grothe B. New roles for synaptic inhibition in sound localization. *Nat Rev Neurosci* 4: 540-550, 2003.

Grothe B and Park TJ. Sensitivity to interaural time differences in the medial superior olive of a small mammal, the Mexican free-tailed bat. *J Neurosci* 18: 6608-6622, 1998.

Grothe B and Sanes DH. Bilateral inhibition by glycinergic afferents in the medial superior olive. *J Neurophysiol* 69: 1192-1196, 1993.

Grothe B and Sanes DH. Synaptic inhibition influences the temporal coding properties of medial superior olivary neurons: an in vitro study. *J Neurosci* 14: 1701-1709, 1994.

Grothe B, Schweizer H, Pollak GD, Schuller G and Rosemann C. Anatomy and projection patterns of the superior olivary complex in the Mexican free-tailed bat, *Tadarida brasiliensis mexicana*. *J Comp Neurol* 343: 630-646, 1994.

Guinan JJ, Jr., Guinan SS and Norris BE. Single Auditory Units in the Superior Olivary Complex I: Responses to Sounds and Classifications Based on Physiological Properties. *Intern J Neuroscience* 4: 101-120, 1972.

Haftner ER, De Maio J and Hellman WS. Difference thresholds for interaural delay. *J Acoust Soc Am* 57: 181-187, 1975.

Han Y and Colburn HS. Point-neuron model for binaural interaction in MSO. *Hear Res* 68: 115-130, 1993.

Hancock KE and Delgutte B. A physiologically based model of interaural time difference discrimination. *J Neurosci* 24: 7110-7117, 2004.

Harper NS and McAlpine D. Optimal neural population coding of an auditory spatial cue. *Nature* 430: 682-686, 2004.

Heffner RS and Heffner HE. Sound localization and use of binaural cues by the gerbil (*Meriones unguiculatus*). *Behav Neurosci* 102: 422-428, 1988.

Held H. Die zentrale Gehörleitung. *Arch Anat Physiol* 17: 201-248, 1893.

Hermann J, Pecka M, von Gersdorff H, Grothe B and Klug A. Synaptic transmission at the calyx of held under in vivo like activity levels. *J Neurophysiol* 98: 807-820, 2007.

Huang GT, Rosowski JJ, Ravicz ME and Peake WT. Mammalian ear specializations in arid habitats: structural and functional evidence from sand cat (*Felis margarita*). *J Comp Physiol A Neuroethol Sens Neural Behav Physiol* 188: 663-681, 2002.

Irvine DR. Physiology of the auditory brainstem. In: *The Mammalian auditory pathway: Neurophysiology*, edited by Popper AN and Fay RR. New York: Springer, 1992, p. 153-231.

Irvine DR, Park VN and McCormick L. Mechanisms underlying the sensitivity of neurons in the lateral superior olive to interaural intensity differences. *J Neurophysiol* 86: 2647-2666, 2001.

Ito Y, Colburn HS and Thompson CL. Masked discrimination of interaural time delays with narrow-band signal. *J Acoust Soc Am* 72: 1821-1826, 1982.

Jeffress LA. A place theory of sound localization. *J Comp Physiol Psychol* 41: 35-39, 1948.

Jiang D, McAlpine D and Palmer AR. Detectability index measures of binaural masking level difference across populations of inferior colliculus neurons. *J Neurosci* 17: 9331-9339, 1997a.

Jiang D, McAlpine D and Palmer AR. Responses of neurons in the inferior colliculus to binaural masking level difference stimuli measured by rate-versus-level functions. *J Neurophysiol* 77: 3085-3106, 1997b.

Joris P and Yin TC. A matter of time: internal delays in binaural processing. *Trends Neurosci* 30: 70-78, 2007.

Joris PX. Interaural time sensitivity dominated by cochlea-induced envelope patterns. *J Neurosci* 23: 6345-6350, 2003.

Joris PX, Carney LH, Smith PH and Yin TC. Enhancement of neural synchronization in the anteroventral cochlear nucleus. I. Responses to tones at the characteristic frequency. *J Neurophysiol* 71: 1022-1036, 1994.

Joris PX, Van de SB, Recio-Spinoso A and van der HM. Auditory midbrain and nerve responses to sinusoidal variations in interaural correlation. *J Neurosci* 26: 279-289, 2006.

Joris PX and Yin TC. Envelope coding in the lateral superior olive. I. Sensitivity to interaural time differences. *J Neurophysiol* 73: 1043-1062, 1995.

Joris PX and Yin TC. Envelope coding in the lateral superior olive. III. Comparison with afferent pathways. *J Neurophysiol* 79: 253-269, 1998.

Kapfer C, Seidl AH, Schweizer H and Grothe B. Experience-dependent refinement of inhibitory inputs to auditory coincidence-detector neurons. *Nat Neurosci* 5: 247-253, 2002.

Kelly JB, Buckthought AD and Kidd SA. Monaural and binaural response properties of single neurons in the rat's dorsal nucleus of the lateral lemniscus. *Hear Res* 122: 25-40, 1998.

Kiang NY and Moxon EC. Tails of tuning curves of auditory-nerve fibers. *J Acoust Soc Am* 55: 620-630, 1974.

Kidd SA and Kelly JB. Contribution of the dorsal nucleus of the lateral lemniscus to binaural responses in the inferior colliculus of the rat: interaural time delays. *J Neurosci* 16: 7390-7397, 1996.

Kil J, Kageyama GH, Semple MN and Kitzes LM. Development of ventral cochlear nucleus projections to the superior olivary complex in gerbil. *J Comp Neurol* 353: 317-340, 1995.

Klumpp R and Eady H. Some measurements of interaural time difference thresholds. *J Acoust Soc Am* 28: 215-232, 1956.

Koch U and Grothe B. Interdependence of spatial and temporal coding in the auditory midbrain. *J Neurophysiol* 83: 2300-2314, 2000.

Kollmar I. Plastizität im auditorischen Hirnstamm der mongolischen Wüstenrennmaus induziert durch akustisches Rauschen (Diplomarbeit). Ludwig-Maximilians-Universität München, 2003.

Kollmeier B and Gilkey RH. Binaural forward and backward masking: evidence for sluggishness in binaural detection. *J Acoust Soc Am* 87: 1709-1719, 1990.

Koppl C. Phase locking to high frequencies in the auditory nerve and cochlear nucleus magnocellularis of the barn owl, *Tyto alba*. *J Neurosci* 17: 3312-3321, 1997.

Kudo M, Nakamura Y, Moriizumi T, Tokuno H and Kitao Y. Bilateral projections from the medial superior olivary nucleus to the inferior colliculus in the mole (*Mogera robusta*). *Brain Res* 463: 352-356, 1988.

Kuwabara N and Zook JM. Projections to the medial superior olive from the medial and lateral nuclei of the trapezoid body in rodents and bats. *J Comp Neurol* 324: 522-538, 1992.

Kuwada S, Fitzpatrick DC, Batra R and Ostapoff EM. Sensitivity to interaural time differences in the dorsal nucleus of the lateral lemniscus of the unanesthetized rabbit: comparison with other structures. *J Neurophysiol* 95: 1309-1322, 2006.

Kuwada S, Stanford TR and Batra R. Interaural phase-sensitive units in the inferior colliculus of the unanesthetized rabbit: effects of changing frequency. *J Neurophysiol* 57: 1338-1360, 1987.

Kuwada S and Yin TC. Binaural interaction in low-frequency neurons in inferior colliculus of the cat. I. Effects of long interaural delays, intensity, and repetition rate on interaural delay function. *J Neurophysiol* 50: 981-999, 1983.

Lane CC and Delgutte B. Neural correlates and mechanisms of spatial release from masking: single-unit and population responses in the inferior colliculus. *J Neurophysiol* 94: 1180-1198, 2005.

Langford TL. Responses elicited from medial superior olivary neurons by stimuli associated with binaural masking and unmasking. *Hear Res* 15: 39-50, 1984.

Leibold C and van Hemmen JL. Spiking neurons learning phase delays: how mammals may develop auditory time-difference sensitivity. *Phys Rev Lett* 94: 168102, 2005.

Loeb GE, White MW and Merzenich MM. Spatial cross-correlation. A proposed mechanism for acoustic pitch perception. *Biol Cybern* 47: 149-163, 1983.

Loskota WJ, Lomax P and Verity MA. *A Stereotaxic Atlas of the Mongolian Gerbil Brain*. Ann Arbor: Ann Arbor Science Publishers, Inc., 1974.

Magnusson AK, Kapfer C, Grothe B and Koch U. Maturation of glycinergic inhibition in the gerbil medial superior olive after hearing onset. *J Physiol* 568: 497-512, 2005a.

Magnusson, AK, Koch, U, Brand, A, Heise, I, Grothe, B, and Park, TJ. GABA(B) receptor modulate binaural response properties in LSO neurons. *Soc Neurosci*. Abst.44.8, 2005b.

Maier JK and Klump GM. Resolution in azimuth sound localization in the Mongolian gerbil (*Meriones unguiculatus*). *J Acoust Soc Am* 119: 1029-1036, 2006.

Maki K and Furukawa S. Acoustical cues for sound localization by the Mongolian gerbil, *Meriones unguiculatus*. *J Acoust Soc Am* 118: 872-886, 2005.

Makous JC and Middlebrooks JC. Two-dimensional sound localization by human listeners. *J Acoust Soc Am* 87: 2188-2200, 1990.

Malmierca MS, Merchan MA, Henkel CK, Oliver DL. Direct projections from cochlear nuclear complex to auditory thalamus in the rat. *J Neurosci* 22:10891-10897, 2002.

Markowitz NS and Pollak GD. The dorsal nucleus of the lateral lemniscus in the mustache bat: monaural properties. *Hear Res* 71: 51-63, 1993.

Markowitz NS and Pollak GD. Binaural processing in the dorsal nucleus of the lateral lemniscus. *Hear Res* 73: 121-140, 1994.

Masterton RB and Diamond IT. Medial superior olive and sound localization. *Science* 155: 1696-1697, 1967.

McAlpine D and Grothe B. Sound localization and delay lines--do mammals fit the model? *Trends Neurosci* 26: 347-350, 2003.

McAlpine D, Jiang D and Palmer AR. Binaural masking level differences in the inferior colliculus of the guinea pig. *J Acoust Soc Am* 100: 490-503, 1996.

McAlpine D, Jiang D and Palmer AR. A neural code for low-frequency sound localization in mammals. *Nat Neurosci* 4: 396-401, 2001.

McAlpine D, Jiang D, Shackleton TM and Palmer AR. Convergent input from brainstem coincidence detectors onto delay-sensitive neurons in the inferior colliculus. *J Neurosci* 18: 6026-6039, 1998.

McAlpine D, Jiang D, Shackleton TM and Palmer AR. Responses of neurons in the inferior colliculus to dynamic interaural phase cues: evidence for a mechanism of binaural adaptation. *J Neurophysiol* 83: 1356-1365, 2000.

McAlpine D and Palmer AR. Blocking GABAergic inhibition increases sensitivity to sound motion cues in the inferior colliculus. *J Neurosci* 22: 1443-1453, 2002.

Middlebrooks JC, Clock AE, Xu L and Green DM. A panoramic code for sound location by cortical neurons. *Science* 264: 842-844, 1994.

Monsivais P, Yang L, Rubel EW. GABAergic inhibition in nucleus magnocellularis: implications for phase locking in the avian auditory brainstem. *J Neurosci* 20:2954-2963, 2000.

Moore BCJ. An Introduction to the Psychology of Hearing. London: Academic press, 2003.

Moushegian G, Rupert A and Whitcomb MA. Brain-stem neuronal response patterns to monaural and binaural tones. *J Neurophysiol* 27: 1174-1191, 1964.

Moushegian G, Rupert AL, Langford TL. Stimulus coding by medial superior olivary neurons. *J Neurophysiol* 30:1239-1261, 1967.

Oliver DL. Ascending efferent projections of the superior olivary complex. *Microsc Res Tech* 51: 355-363, 2000.

Oliver DL, Beckius GE, Bishop DC, Kuwada S. Simultaneous anterograde labeling of axonal layers from lateral superior olive and dorsal cochlear nucleus in the inferior colliculus of cat. *J Comp Neurol* 382:215-29, 1997.

Oliver DL and Huerta MF. Inferior and superior colliculi. In: The mammalian auditory pathway: Neuroanatomy, edited by Webster DB, Popper AN and Fay RR. New York: Springer-Verlag, 1992, p. 168-221.

Palmer AR, Jiang D and McAlpine D. Desynchronizing responses to correlated noise: A mechanism for binaural masking level differences at the inferior colliculus. *J Neurophysiol* 81: 722-734, 1999.

Palmer AR and Shackleton TM. The physiological basis for the binaural masking level difference. *Acta Acoust unit Acust* 88: 312-319, 2002.

Paolini AG, FitzGerald JV, Burkitt AN and Clark GM. Temporal processing from the auditory nerve to the medial nucleus of the trapezoid body in the rat. *Hear Res* 159: 101-116, 2001.

Park TJ. IID sensitivity differs between two principal centers in the interaural intensity difference pathway: the LSO and the IC. *J Neurophysiol* 79: 2416-2431, 1998.

Park TJ, Grothe B, Pollak GD, Schuller G and Koch U. Neural delays shape selectivity to interaural intensity differences in the lateral superior olive. *J Neurosci* 16: 6554-6566, 1996.

Patterson RD. The sound of a sinusoid: Time-interval models. *J Acoust Soc Am* 96: 1419-1428, 1994.

Pecka M, Zahn TP, Saunier-Rebori B, Siveke I, Felmy F, Wiegrebe L, Klug A, Pollak GD and Grothe B. Inhibiting the inhibition: a neuronal network for sound localization in reverberant environments. *J Neurosci* 27: 1782-1790, 2007.

Perkins RE. An electron microscopic study of synaptic organization in the medial superior olive of normal and experimental chinchillas. *J Comp Neurol* 148: 387-415, 1973.

Pollack I. Temporal switching between binaural information sources. *J Acoust Soc Am* 63: 550-558, 1978.

Pollak GD, Burger RM and Klug A. Dissecting the circuitry of the auditory system. *Trends Neurosci* 26: 33-39, 2003.

Ramon y Cajal S. Histologie du systeme nerveux de l'homme et des vertebrates. Paris: Malonie, 1907.

Rayleigh LJ. On our perception of sound direction. *Philos Mag* 13: 214-232, 1907.

Reyes AD, Rubel EW and Spain WJ. In vitro analysis of optimal stimuli for phase-locking and time-delayed modulation of firing in avian nucleus laminaris neurons. *J Neurosci* 16: 993-1007, 1996.

Rhode WS, Geisler CD and Kennedy DT. Auditory nerve fiber response to wide-band noise and tone combinations. *J Neurophysiol* 41: 692-704, 1978.

Rhode WS and Greenberg S. Physiology of the cochlear nuclei. In: The mammalian auditory pathway: Neurophysiology, edited by Webster DB, Popper AN and Fay RR. New-York: Springer, 1992, p. 94-152.

Rose JE, Gross NB, Geisler CD and Hind JE. Some neural mechanisms in the inferior colliculus of the cat which may be relevant to localization of a sound source. *J Neurophysiol* 29: 288-314, 1966.

Rosowski JJ, Ravicz ME, Teoh SW and Flandermeyer D. Measurements of middle-ear function in the Mongolian gerbil, a specialized mammalian ear. *Audiology & Neuro-Otology* 4: 129-136, 1999.

Ruggero MA, Robles L and Rich NC. Two-tone suppression in the basilar membrane of the cochlea: mechanical basis of auditory-nerve rate suppression. *J Neurophysiol* 68: 1087-1099, 1992.

Rouiller EM, Cronin-Schreiber R, Fekete DM, Ryugo DK. The central projections of intracellularly labeled auditory nerve fibers in cats: an analysis of terminal morphology. *J Comp Neurol* 249:261-278, 1986.

Ryan A. Hearing sensitivity of the mongolian gerbil, *Meriones unguiculatus*. *J Acoust Soc Am* 59: 1222-1226, 1976.

Ryugo DK and Sento S. Synaptic connections of the auditory nerve in cats: relationship between endbulbs of held and spherical bushy cells. *J Comp Neurol* 305:35-48, 1991.

Sakitt B. Indices of discriminability. *Nature* 241: 133-134, 1973.

Schiller E. Reversible Plastizität von binauralen Neuronen im auditorischen Hirnstamm der mongolischen Wüstenrennmaus (*Meriones unguiculatus*) (Diplomarbeit). Ludwig-Maximilians-Universität München, 2007.

Schuller G, Radtke Schuller S and Betz M. A stereotaxic method for small animals using experimentally determined reference profiles. *J Neurosci Methods* 18: 339-350, 1986.

Schwartz IR. The superior olivary complex and lateral lemniscal nuclei. In: The mammalian auditory pathway: Neuroanatomy, edited by Webster DB, Popper AN and Fay RR. New York: Springer, 1992, p. 117-167.

Scott LL, Mathews PJ and Golding NL. Posthearing developmental refinement of temporal processing in principal neurons of the medial superior olive. *J Neurosci* 25: 7887-7895, 2005.

Seidl AH and Grothe B. Development of sound localization mechanisms in the mongolian gerbil is shaped by early acoustic experience. *J Neurophysiol* 94: 1028-1036, 2005.

Shackleton TM, Arnott RH and Palmer AR. Sensitivity to interaural correlation of single neurons in the inferior colliculus of guinea pigs. *J Assoc Res Otolaryngol* 6: 244-259, 2005.

Shackleton TM, McAlpine D and Palmer AR. Modelling convergent input onto interaural-delay-sensitive inferior colliculus neurones. *Hear Res* 149: 199-215, 2000.

Shackleton TM, Skottun BC, Arnott RH and Palmer AR. Interaural time difference discrimination thresholds for single neurons in the inferior colliculus of Guinea pigs. *J Neurosci* 23: 716-724, 2003.

Shamma SA, Shen Nm and Gopaldaswamy P. Stereausis: binaural processing without neural delays. *J Acoust Soc Am* 86: 989-1006, 1989.

Shinn-Cunningham BG, Santarelli S and Kopco N. Tori of confusion: binaural localization cues for sources within reach of a listener. *J Acoust Soc Am* 107: 1627-1636, 2000.

Shneiderman A, Oliver DL and Henkel CK. Connections of the dorsal nucleus of the lateral lemniscus: an inhibitory parallel pathway in the ascending auditory system? *J Comp Neurol* 276: 188-208, 1988.

Shneiderman A, Stanforth DA, Henkel CK and Saint-Marie RL. Input-output relationships of the dorsal nucleus of the lateral lemniscus: Possible substrate for the processing of dynamic spatial cues. *Journal of Comparative Neurology* 410: 265-276, 1999.

Siveke I, Pecka M, Seidl AH, Baudoux S and Grothe B. Binaural response properties of low-frequency neurons in the gerbil dorsal nucleus of the lateral lemniscus. *J Neurophysiol* 96: 1425-1440, 2006.

Skottun BC, Shackleton TM, Arnott RH and Palmer AR. The ability of inferior colliculus neurons to signal differences in interaural delay. *Proc Natl Acad Sci U S A* 98: 14050-14054, 2001.

Smith PH, Joris PX, Carney LH, Yin TC. Projections of physiologically characterized globular bushy cell axons from the cochlear nucleus of the cat. *J Comp Neurol* 304: 387-407, 1991.

Smith PH, Joris PX and Yin TC. Projections of physiologically characterized spherical bushy cell axons from the cochlear nucleus of the cat: evidence for delay lines to the medial superior olive. *J Comp Neurol* 331: 245-260, 1993.

Smith PH, Joris PX and Yin TC. Anatomy and physiology of principal cells of the medial nucleus of the trapezoid body (MNTB) of the cat. *J Neurophysiol* 79: 3127-3142, 1998.

Sommer I, Lingenhohl K and Friauf E. Principal cells of the rat medial nucleus of the trapezoid body: an intracellular in vivo study of their physiology and morphology. *Exp Brain Res* 95: 223-239, 1993.

Spangler Km, Warr WB and Henkel CK. The projections of principal cells of the medial nucleus of the trapezoid body in the cat. *J Comp Neurol* 238: 249-262, 1985.

Spitzer MW and Semple MN. Interaural phase coding in auditory midbrain: influence of dynamic stimulus features. *Science* 254: 721-724, 1991.

Spitzer MW and Semple MN. Responses of inferior colliculus neurons to time-varying interaural phase disparity: effects of shifting the locus of virtual motion. *J Neurophysiol* 69: 1245-1263, 1993.

Spitzer MW and Semple MN. Neurons sensitive to interaural phase disparity in gerbil superior olive: diverse monaural and temporal response properties. *J Neurophysiol* 73: 1668-1690, 1995.

Stecker GC, Harrington IA and Middlebrooks JC. Location coding by opponent neural populations in the auditory cortex. *PLoS Biol* 3: e78, 2005.

Stern RM, Jr., Slocum JE and Phillips MS. Interaural time and amplitude discrimination in noise. *J Acoust Soc Am* 73: 1714-1722, 1983.

Stotler WA. An experimental study of the cells and connections of the superior olivary complex of the cat. *Journal of Comparative Neurology* 98: 401-432, 1953.

Sutter ML, Schreiner CE, McLean M, O'Connor KN and Loftus WC. Organization of inhibitory frequency receptive fields in cat primary auditory cortex. *J Neurophysiol* 82: 2358-2371, 1999.

Svirskis G, Dodla R and Rinzel J. Subthreshold outward currents enhance temporal integration in auditory neurons. *Biol Cybern* 89: 333-340, 2003.

Tan Q and Carney LH. A phenomenological model for the responses of auditory-nerve fibers. II. Nonlinear tuning with a frequency glide. *J Acoust Soc Am* 114: 2007-2020, 2003.

Thompson SP. On the function of the two ears in the perception of space. *Philos Mag* 13: 406-416, 1882.

Thompson AM and Schofield BR. Afferent projections of the superior olivary complex. *Microsc Res Tech* 51:330-54, 2000.

Tollin DJ and Yin TC. Interaural phase and level difference sensitivity in low-frequency neurons in the lateral superior olive. *J Neurosci* 25: 10648-10657, 2005.

Viemeister NF. Temporal modulation transfer functions based upon modulation thresholds. *J Acoust Soc Am* 66: 1364-1380, 1979.

von Gersdorff H and Borst JG. Short-term plasticity at the calyx of held. *Nat Rev Neurosci* 3: 53-64, 2002.

Watanabe T, Liao TT, Katsuki Y. Neuronal response patterns in the superior olivary complex of the cat to sound stimulation. *Jpn J Physiol* 18:267-287, 1968.

Webster DB and Plassmann W. Parallel evolution of low-frequency sensitivity in old world and new world desert rodents. In: *The evolutionary biology of hearing*, edited by Webster DB, Fay RR and Popper AN. New York: Springer-Verlag, 1992, p. 633-636.

Webster DB and Webster M. Auditory systems of Heteromyidae: functional morphology and evolution of the middle ear. *J Morphol* 146: 343-376, 1975.

Wenthold RJ, Huie D, Altschuler RA and Reeks KA. Glycine immunoreactivity localized in the cochlear nucleus and superior olivary complex. *Neuroscience* 22: 897-912, 1987.

Willard FH and Martin GF. Collateral innervation of the inferior colliculus in the North American opossum: a study using fluorescent markers in a double-labeling paradigm. *Brain Res* 303: 171-182, 1984.

Wu SH and Kelly JB. In vitro brain slice studies of the rat's dorsal nucleus of the lateral lemniscus. III. synaptic pharmacology. *J Neurophysiol* 75:1271-82, 1996.

Wu SH. Synaptic excitation in the dorsal nucleus of the lateral lemniscus. *Prog Neurobiol* 57: 357-375, 1999.

Xie R, Meitzen J and Pollak GD. Differing roles of inhibition in hierarchical processing of species-specific calls in auditory brainstem nuclei. *J Neurophysiol* 94: 4019-4037, 2005.

Yin TC. Neural mechanisms of encoding binaural localization cues. In: *Integrative functions in the mammalian auditory pathway*, edited by Oertel D, Fay RR and Popper AN. New York: Springer-Verlag, 2002, p. 99-159.

Yin TC and Chan JC. Interaural time sensitivity in medial superior olive of cat. *J Neurophysiol* 64: 465-488, 1990.

Yin TC and Kuwada S. Binaural interaction in low-frequency neurons in inferior colliculus of the cat. II. Effects of changing rate and direction of interaural phase. *J Neurophysiol* 50: 1000-1019, 1983a.

Yin TC and Kuwada S. Binaural interaction in low-frequency neurons in inferior colliculus of the cat. III. Effects of changing frequency. *J Neurophysiol* 50: 1020-1042, 1983b.

Young ED and Barta PE. Rate responses of auditory nerve fibers to tones in noise near masked threshold. *J Acoust Soc Am* 79: 426-442, 1986.

Zhou Y, Carney LH and Colburn HS. A model for interaural time difference sensitivity in the medial superior olive: interaction of excitatory and inhibitory synaptic inputs, channel dynamics, and cellular morphology. *J Neurosci* 25: 3046-3058, 2005.

Contributions to the manuscripts

Binaural Response Properties of Low-Frequency Neurons in the Gerbil Dorsal Nucleus of the Lateral Lemniscus (Chapter 2)

Michael Pecka, Armin Seidl, Sylvia Bourdoux, and I recorded the *in vivo* data dealing with ITD processing, whereas I recorded and analyzed the majority of data. Michael Pecka recorded the *in vivo* data dealing with IID processing. Prof. Benedikt Grothe, Michael Pecka and I designed the experiments. The immunocytochemical experiments were carried out by me. Ignacio Plaza and Manolo Malmierca (head of department: Prof. Dr. Miguel Merchan, Salamanca, Spain) introduced me to the technique of immunodouble-labelling. I wrote most of the manuscript, while Michael Pecka wrote the IID processing part. Michael Pecka and Benedikt Grothe modified the manuscript.

Spectral composition of concurrent noise affects neuronal sensitivity to interaural time differences of tones in the dorsal nucleus of the lateral lemniscus (Chapter 3)

I designed, implemented and analyzed all *in vivo* experiments. Christian Leibold performed the modelling part. I wrote the manuscript, except for the part dealing with the model. The manuscript was modified by Christian Leibold and finally corrected by Benedikt Grothe.

Perceptual and Physiological Characteristics of Binaural Sluggishness (Chapter 4)

All *in vivo* data were recorded and analyzed by me. The *in vivo* experiments were designed together with Lutz Wiegrebe. The psychophysical experiments were designed, coordinated and analyzed by Stefan Ewert and Lutz Wiegrebe. Lutz Wiegrebe and I wrote the manuscript in close collaboration.

Curriculum Vitae



Personal details

name: Ida Siveke nee Kollmar
title: diploma in biological sciences (“Diplom-Biologin”)
priv.-address: Danklstrasse 13, D-81371 Munich
work-address: Dep. Neurobiology, Biocenter of the LMU, Ludwig-Maximilians-Universität of Munich, Großhadernerstr. 2, D-82152 Martinsried,
phone +49 89 2180-74-316
nationality: german
data of birth: 6th of June 1978
place of birth: Kassel (Germany)

Scientific education

06/97 High-School Diploma (“Abitur”) at the Friedrichsgymnasium Kassel
09/97 - 02/00 Biological studies at the Eberhart-Karls-Universität of Tuebingen with intermediate examination
02/00 - 12/00 Biological studies at the Universidade de São Paulo in Riberão Preto (Brazil)
04/01 - 09/01 Biological studies at the Ruprecht-Karls-Universität of Heidelberg
09/01 - 09/03 Biological studies at the Ludwig-Maximilians-Universität of Munich; Final examination (final grade 1.0 – “with distinction”)
02/02 - 10/03 Diploma Thesis in the junior research group of Prof. Dr. B. Grothe, Max-Planck-Institute of Neurobiology: “Plastizitaet im auditorischen Hirnstamm der mongolischen Wuestenrennmaus induziert durch

akustisches Rauschen” (Noise Induced Plasticity in the Gerbil Auditory Brainstem)

since 01/04 PhD under supervision of Prof. Dr. B. Grothe, Max-Planck-Institute of Neurobiology and Ludwig-Maximilians-Universität of Munich: “Novel approaches for the analysis of study sound localization”

3. Professional & research experience

01/99 – 02/00 Research Assistant for animal (monkey) treatment (Prof. Dr. H.G. Erkert)

02/00 - 12/00 Project work in the laboratory of Dr. W. Ferreira dos Santos, Universidade de Sao Paulo in Riberao Preto (Brazil): “Evaluation of the biological role of the epidermic secretion from *A.g. clamitans* and the relationship of this secretion with its behavior and environment”

02/01 Project work at the Max-Planck-Institute for Brain Research Frankfurt with Dr. M.H.J. Munk

04/01 – 09/01 Teaching Assistant of the Neurophysiological Practicum (Dr. H.-H. Gerdes)

11/03 - 12/03 Research period at the Universidad de Salamanca (Spain) (Dr. M. Malmierca)

Grants

02/00 - 12/00 DAAD scholarship

01/05 - 06/07 PhD scholarship of the “Studienstiftung des deutschen Volkes”

03/06 Travel grant (“Studienstiftung des deutschen Volkes”)

List of publications

Siveke I, Ewert SD, Lutz Wiegrebe L. Perceptual and Physiological Characteristics of Binaural Sluggishness (prepared for submission to the *Journal of Neuroscience*)

Siveke I, Leibold C, Grothe B. Spectral composition of concurrent noise affects neuronal sensitivity to interaural time differences of tones in the dorsal nucleus of the lateral lemniscus. *Journal of Neurophysiology* doi:10.1152/jn.00275.2007, 2007

Pecka M, Zahn TP, Saunier-Rebori B, **Siveke I**, Felmy F, Wiegrebe L, Klug A, Pollak GD, Grothe B. Inhibiting the inhibition: a neuronal network for sound localization in reverberant environments. *Journal of Neuroscience* 27(7):1782-90, 2007.

Siveke I, Pecka M, Seidl AH, Baudoux S, Grothe B. Binaural response properties of low-frequency neurons in the gerbil dorsal nucleus of the lateral lemniscus. *Journal of Neurophysiology* 96(3):1425-40, 2006.

List of presentations

Siveke I, Schiller E, and Grothe B. Reversible Plasticity in the Auditory Brainstem Induced by Noise Exposure: 30th Midwinter Research Meeting, Association for Research in Otolaryngology, Abstr. 417, 2006 (Poster)

Siveke I, Leibold C, and Grothe B. Interaural Time Sensitivity to tones in noise: 31th Neurobiology Conference, Abstr. TS19-4C, 2007 (Poster)

Siveke I, Ewert SD, and Lutz Wiegrebe L. Perceptual and Physiological Characteristics of Binaural Sluggishness, 14th International Symposium on Hearing, 2006 (Talk)

Siveke I, Leibold C, and Grothe B. Interaural Time Sensitivity to Tones in Noise: 29th Midwinter Research Meeting, Association for Research in Otolaryngology, Abstr. 171, 2006 (Poster)

Kollmar I, Tripathi P, and Grothe B. Adult Plasticity of Interaural Time Differences Processing is Regulated by Glycinergic Inhibition. 30th Neurobiology Conference, Abstr. 151A, 2005 (Poster)

Kollmar I and Grothe B. Plasticity in the Auditory Brainstem of Adult Mongolian Gerbils Induced by Acoustic Noise. 28th Midwinter Research Meeting, Association for Research in Otolaryngology, Abstr. 171, 2004 (Poster)

Acknowledgments

First and foremost I wish to thank Prof. Dr. Benedikt Grothe for giving me the opportunity to accomplish my PhD thesis in his laboratory. I continuously felt warmly and excellently guided in an atmosphere of freedom and personal responsibility. Knowing his busy schedule it sounds incredible, but whenever I asked for it he found the time for personal support and valuable scientific discussion! Thank you.

Thanks to all former and active members of the Grothe Lab for the downright nice time, especially to Michael Pecka (“How often did we scare someone because of endless discussions about CP and CD?”), Jochen Hermann (“Thanks for teaching me, that a bear bottle in the hand keeps from sleeping!”), and Felix Felmy (“Habisch he macht?”) for taking much pleasure in deep scientific and global discussions. Thanks to Nick Lesica for being my Matlab and English master.

For instructive and witty team work I thank Prof. Dr. Christan Leibold and Prof. Dr. Lutz Wiegrebe, who helped me enjoying Matlab and auditory filters.

I thank Prof. Dr. George Pollak for showing me quite plainly the importance of every single action potential.

Thanks to Claudia Schulte, the Queen of the Histolab.

My deep gratitude goes to the best Tinni and Utz, Martin, Fritz, Otto, Nina, Tina, and Silvi.

Danke Jens.

Ehrenwörtliche Versicherung und Erklärung

Ich, Ida Siveke, versichere hiermit ehrenwörtlich, dass die vorgelegte Dissertation von mir selbstständig und ohne unerlaubte Beihilfe angefertigt wurde.

Hiermit erkläre ich, dass ich mich nicht anderweitig einer Doktorarbeit ohne Erfolg unterzogen habe und die vorliegende Arbeit nicht bei einer anderen Hochschule eingereicht habe.

Ida Siveke